

140
X-765-72-205

PREPRINT

NASA TM X-65945

ULTRAVIOLET AND CHARGED PARTICLE IRRADIATION OF PROPOSED SOLAR CELL COVERSIDE MATERIALS AND CONDUCTIVE COATINGS FOR THE HELIOS SPACECRAFT

J. FRY
C. A. NICOLETTA

(NASA-TM-X-65945) - ULTRAVIOLET AND CHARGED
PARTICLE IRRADIATION OF PROPOSED SOLAR
CELL COVERSIDE MATERIALS AND CONDUCTIVE
COATINGS FOR THE HELIOS SPACECRAFT (NASA)
112 p HC \$7.75

N73-18571

Unclassified
63944

CSCL 11C

G3/18

JUNE 1972



GSFC

— GODDARD SPACE FLIGHT CENTER —
GREENBELT, MARYLAND

X-765-72-205

ULTRAVIOLET AND CHARGED PARTICLE
IRRADIATION OF PROPOSED SOLAR CELL
COVERSLIDE MATERIALS AND CONDUCTIVE
COATINGS FOR THE HELIOS SPACECRAFT

J. Fry
and
C. A. Nicoletta

June 1972

Goddard Space Flight Center
Greenbelt, Maryland

ULTRAVIOLET AND CHARGED PARTICLE
IRRADIATION OF PROPOSED SOLAR CELL
COVERSLIDE MATERIALS AND CONDUCTIVE
COATINGS FOR THE HELIOS SPACECRAFT

J. Fry
and
C. A. Nicoletta

ABSTRACT

Coverslide materials consisting of Corning 7940 fused silica, multi-layers of titanium and manganese oxides (blue reflector), and indium oxide (conductive-coating) were exposed to 16 UVSC up to 800 EUVSH in vacuum. Slight changes in optical transmittance and optical absorptance were found in the (200-360) m μ regions of the fused silica and conductive coating respectively. Exposure to 4 KeV protons and 4.5 KeV electrons in vacuum, produced decreases of several percent in transmittance, (200-360) m μ region in the fused silicas after total fluxes $\geq 10^{14}$ particles/cm 2 . Sheet resistance of the conductive coating increased above 1.0 k Ω /square after a total flux $\geq 10^{14}$ particles/cm 2 .

Solar cells with coverglasses utilizing the indium oxide conductive coating were exposed to 1 Mev electrons and 1 Mev protons in air and in vacuum. Total fluxes ranged from 10^{11} particles/cm 2 to 10^{15} particle/cm 2 . There was no appreciable degradation in the resistance of the conductive coating during or after these tests.

PRECEDING PAGES BLANK NOT FILMED

CONTENTS

	<u>Page</u>
I. Introduction	1
II. Test Description	1
1. Measurements and Samples	2
2. Ultraviolet Irradiation and Results	3
3. Charged Particle Irradiation of Individual Coverglasses and Results	4
III. Summary and Conclusions	5
IV. Acknowledgments	9
V. References	9

Preceding page blank

ULTRAVIOLET AND CHARGED PARTICLE IRRADIATION OF PROPOSED SOLAR CELL COVERSLIDE MATERIALS AND CONDUCTIVE COATINGS FOR THE HELIOS SPACECRAFT

I. Introduction

In essence this was a testing or scoping study of the solar cell coverslide materials' resistance to ultraviolet and charged particle radiation seen by the Helios spacecraft.

The Helios project is a joint U.S.-West German effort to put a satellite in an eccentric solar orbit which will approach to within 0.3 A.U. of the sun. The first launch is tentatively scheduled for mid 1974. The package is composed of seven German and three U.S. experiments. Some of the experimental objectives are: Measurement of the solar wind velocity, mapping of the interplanetary magnetic field, measurement of plasma and radio waves, and determining the masses and energies of interplanetary dust.

The spacecraft is essentially spool-shaped, with the experiments and electronics housed in the middle cylindrical section. Due to the proximity of the spacecraft to the sun, charge buildup on an essentially non-conductive surface would cause electric fields outside the spacecraft, which would severely affect the sensitive instrumentation on board. It is therefore essential that the spacecraft have an equipotential or conducting surface. Indium oxide was chosen as a suitable coating for the outer surfaces of the solar cell coverslides in that it allows good transmittance and also suitable conductance to match the rest of the spacecraft's metallic skin. It remained to test the materials resistance to radiation comparable to that seen in the spacecraft's orbit, which led to the test plan that follows.

II. Test Description

The irradiation of the coverslides and solar cells/cover slides was divided into three phases:

1. A scoping study to give preliminary results and therefore indications of the scope of the materials resistance to ultraviolet, low energy and high energy charged particle irradiation.

2. Extension of (1) to include higher energy particles (200-300) KeV, with the same total fluxes, and also to determine temperature effects.
3. To determine specific values of energy, total flux of the predominant degradation species, along with an array of temperatures to obtain some correlation of energy, total flux and temperature on the degradation of the material.

Phases (2) and (3), it can be seen were dependent on the results of (1) which is the subject of this report.

Measurements and Samples

The following parameters were measured before and after irradiation. The instrument and its accuracy is also given.

- %T Optical Transmittance $(0.2 - 3.4)\mu$ Beckman Model DK-1A spectrophotometer, $\pm 2.0\%$
- $\% \alpha$, Optical Absorptance $(0.2 - 2.5)\mu$ Beckman Model DK-2A spectrophotometer and integrating sphere, $\pm 2.0\%$
- ϵ_n , Normal emittance, Gier-Dunkle emissometer, $\pm 4.0\%$
- R_{\square} , Sheet Resistance, Cambridge Four Point Probe, $\pm 2.0\%$.
- Resistance of the coating on the solar cell/coverglass module, General Radio Resistance Bridge, Model GR 1650 A, $\pm 1\%$

The above measurements took several days to complete after each irradiation.

A number of coverslide samples were obtained from Optical Coatings Laboratory, Inc., Santa Rosa, California. The samples were all the same size, 25.4 mm by 21.5 mm and about 0.15 mm thick. The coverslides were divided into three groups.

1. Type A consisting only of the Corning 7940 fused silica substrate.
2. Type B consisting of the Corning 7940 substrate with a blue reflector coating on one side. The coating consists of multi-layers of titanium and manganese oxides to a thickness of about 8000 \AA .

3. Type C consisting of the Corning 7940 substrate with the blue reflector coating (8000 \AA°) on the backside and the conductive coating (indium oxide, 1000 \AA° thick) on the front side.

AEG Telefunken supplied a solar cell/coverglass module. This module consisted of two strings of six cover glasses and two strings of six solar cells/cover glasses, all with a conductive coating. Each string was connected in series. The cover glasses with conductive coating were supplied to AEG Telefunken by OCLI and bounded to the solar cell by AEG.

Ultraviolet Irradiation and Results

The ultraviolet exposure was carried out in vacuum using a General Electric A H-6 mercury arc lamp. The lamp was positioned to supply 16 ultraviolet solar constants. The exposure was run for several days to obtain a total of 800 Equivalent Ultraviolet Sun Hours (EUVSH). Temperature of the sample holder was monitored throughout the test and was found to be $145^\circ\text{C} \pm 10\%$. This is well below the critical 180°C specified by OCLI as causing possible degradation of the indium oxide coating. Figures 1-12 give the percentage transmittance vs. wavelength, while figures 13-24 give percentage transmittance vs. wavelength plus reflectance, from which absorptance is obtained, ($1 - T + R = A$).

The type B and C samples did not transmit at all in the near ultraviolet region ($200\text{-}360\text{ m}\mu$), due to the blue reflector coating on both these types which cuts-off at $\sim 415\text{ m}\mu$. See figure 5. This is a transmittance curve for Type B, Type C is similar. A decrease of several percent in transmittance was observed in the near ultraviolet region for Type A samples. See Figure 7. This was found comparable to that observed for Corning 7940 in recent studies of Optical Materials for the Earth Radiation Budget aboard NIMBUS (Reference 1).

A decrease of several percent in absorptance was noted for Type B from (200 to $360\text{ m}\mu$). See Figure 16. Type C exhibited an increase in absorptance over the same region as seen in Figure 22.

Type A material, fused silica, shows an increase in absorptance over the same region, although to a lesser extent. See Figure 19. Comparing Figures 16 and 22, some absorptance can be attributed to the conductive coating. No significant changes were observed for absorptance in the visible and near infra-red regions.

Normal emittance measurements at room temperature showed no changes from the initial values which were: Type A 0.80, Type B 0.79, Type C 0.79.

Sheet resistance for the Type C samples decreased slightly from about 0.9 k Ω /square to about 0.8 k Ω /square.

Scanning electron microscope studies of the samples at 400 X, 2000 X, and 4000 X showed no changes.

Charged Particle Irradiation of Individual Coverglasses and Results

The second part of this scoping phase involved charged particle irradiation at low energies. Specifically these were 4.0 KeV protons and 4.5 KeV electrons to fluences of 10^{12} , 10^{14} , and 10^{16} particles/cm 2 . All samples were exposed in vacuum at approximately 10^{-6} torr. A 300 KeV Texas Nuclear accelerator was used for the two lower fluences, and an ORTEC RF source supplied the radiation for the 10^{16} particle/cm 2 run.

As in the case of the ultraviolet tests, the same before and after measurements were made. Figures 25-66 give percent transmittance, and figures 67-95 give % (transmittance + reflectance). No significant losses in transmittance occurred except for the Type A samples after 10^{16} electrons/cm 2 at 4.5 KeV. (See Figure 64.)

No changes at all were observed in the normal emittance and absorptance measurements.

In the sheet resistance, changes did occur. Table 1 gives the values before and after radiation.

Table 1

Φ particles/cm 2	4 KeV Protons			4.5 KeV Electrons		
	10^{12}	10^{14}	10^{16}	10^{12}	10^{14}	10^{16}
R _□ k Ω /square initial	0.9	1.0	0.8	0.8	1.0	1.0
R _□ k Ω /square after	1.1	1.2	1.3	1.0	1.7	3.6

Note that a large jump in the sheet resistance occurs due to the 10^{16} electrons/cm 2 exposure. The value of 3.6 k Ω /square is still well under the 20 k Ω /square limitation placed on the indium oxide coating.

Charged Particle Irradiation of AEG Telefunken Module (Solar Cell/Coverglass/Conductive Coating) and Results

Two strings, one with solar cells and cover glasses and one with cover glasses only, were shielded and used as a control. The other two strings were irradiated under the following conditions:

1. 1 MeV electrons in air, 10^{11} e/cm² to 10^{15} e/cm². Sample removed from machine for each resistance measurement.
2. 1 MeV protons in vacuum, 10^{11} p/cm² to 10^{15} p/cm². Samples removed from machine for each resistance measurement.
3. 1 MeV electrons in vacuum, 10^{12} e/cm² to 10^{15} e/cm². Samples removed from machine for each resistance measurement.
4. 1 MeV electrons in vacuum, 10^{11} e/cm² to 10^{15} e/cm². Resistance measured simultaneously with irradiation.
5. 1 MeV protons in vacuum, 10^{11} p/cm² to 10^{15} p/cm². Resistance measured simultaneously with irradiation.

Tables 2 and 3 give a summary of the data obtained before and during the irradiation. Figures 96, 97 and 98 show plots of the data against particles/cm². There was no appreciable degradation of the conductive coating during or after any of the tests.

III. Summary and Conclusions

Table 4 gives a summary of changes that occurred due to the ultraviolet and charged particle irradiations.

Essentially no significant changes occur due to radiation which would prohibit use of the conductive coating, blue reflector and Corning 7940 fused silica substrate combined to form a suitable solar cell coverslip. The increase in sheet resistance due to the charged particle irradiation appears to be dependent on the fluence acquired. A high enough accumulation of charged particle radiation produces enough defect structure in the coating to cause resistivity changes. From comparison calculations for germanium taken from tables (Reference 2), the electrons most probably penetrate the conductive coating while the protons do not. Even though all their energy is not expended in the conductive coating, the electrons account for a somewhat greater change in the sheet resistance than do the protons.

Table 2
AEG Telefunken Conductive Coating Irradiation Test

1 MeV Electrons in Air - 10/6/71 - 10/7/71

Resistance in K⁽¹⁾

String	Initial	10^{11} e/cm ²	10^{12} e/cm ²	10^{13} e/cm ²	10^{14} e/cm ²	*	**	10^{15} e/cm ²	*	**
A	11.8	12.2	12.3	12.4	12.0	11.8	11.9	11.2	10.9	10.8
B	8.7	8.9	9.1	9.4	9.2	9.2	9.2	9.2	8.8	8.8
C (control)	12.8	12.8	12.8	12.8	12.5	12.5	12.5	12.6	12.6	12.7
D (control)	8.3	8.3	8.3	8.3	8.3	8.3	8.3	8.2	8.2	8.2

1 MeV Protons in Vacuum - 11/19/71

A	11.5	10.2	10.0	10.2	10.2			11.0		
B	8.2	7.4	7.1	7.1	6.8			8.3		
C (control)	12.4	11.1	10.8	10.7	10.4			12.5		
D (control)	8.2	7.4	7.1	7.1	6.8			7.4		

1 MeV Electrons in Vacuum - 11/22/71

A	11.0		10.1	10.3	10.4			10.4		
B	8.3		8.6	8.6	8.5			8.3		
C (control)	12.5		12.3	12.1	12.0			11.8		
D (control)	7.4		8.1	8.1	8.0			7.6		

*2 hours after exposure

**16 hours after exposure

Table 3

Resistance in K Ω -

1 MeV Electrons in Vacuum, Simultaneous Measurement (12/21/71)										
String	Initial	1.4×10^{14} e/cm ²	2.7×10^{14} e/cm ²	4×10^{14} e/cm ²	5.4×10^{14} e/cm ²	6.7×10^{14} e/cm ²	8×10^{14} e/cm ²	9.5×10^{14} e/cm ²	1×10^{15} e/cm ²	10^{13} e/cm ²
A	11.4	11.6	11.6	11.6	11.7	11.7	11.5	11.6	11.6	11.4
B	9.2	9.6	9.6	9.6	9.7	9.7	9.7	9.7	9.6	9.2
C	13.6	13.6	13.6	13.6	13.6	13.5	13.4	13.4	13.4	13.6
D	8.7	8.7	8.7	8.6	8.6	8.5	8.5	8.5	8.5	8.7

(110 minutes to reach 1×10^{15} e/cm²)

1 MeV Protons in Vacuum Simultaneous Measurement (2/25/72)										
String	Initial	10^{12} p/cm ²	10^{13} p/cm ²	10^{14} p/cm ²	2.5×10^{14} p/cm ²	5×10^{14} p/cm ²	7.5×10^{14} p/cm ²	10^{15} p/cm ²		
A	10.5	10.5	10.4	10.4	10.4	10.3	10.3	10.4		
B	8.2	8.2	8.0	7.9	7.9	7.9	7.9	7.9		
C	9.8	9.8	9.8	9.8	9.8	9.8	9.8	9.8		
D	7.1	7.1	7.1	7.1	7.1	7.1	7.1	7.1		

(167 minutes to reach 1×10^{15} p/cm²)

Table 4

Measurements	U.V.	Protons			Electrons		
	800 EVVSH	10^{12} p/cm ²	10^{14} p/cm ²	10^{16} p/cm ²	10^{12} e/cm ²	10^{14} e/cm ²	10^{16} e/cm ²
% T	Decrease in fused silica (200-360) m μ	Slight decrease in fused silica (200-360) m μ	Slight decrease in fused silica (200-360) m μ	Slight decrease in fused silica (200-360) m μ	No change	Slight decrease in fused silica (200-360) m μ	Decrease in fused silica (200-360) m μ
% α	Slight increase in conductive coating (200-360) m μ	No change	No change	No change	No change	No change	No change
n	No change	No change	No change	No change	No change	No change	No change
R ₁₁	Slight decrease in conductive coating	Slight increase in conductive coating	Slight increase in conductive coating	Increase in conductive coating	Slight increase in conductive coating	Increase in conductive coating	Increase in conductive coating

Due to the favorable results obtained in this first Phase of the coverslip and module tests, phases two and three will not have to be considered.

IV. Acknowledgements

Thanks for irradiation of the samples go to Jules Hirschfield, Arthur Dufault, John Stuart and Ronald Hunkeler. John Henninger, Walter Viehmann and Jane Jellison conducted various measurements on the samples.

V. References

1. C. A. Nicoletta and A. G. Eubanks, "Effect of Simulated Space Radiation on Selected Optical Materials." Upcoming paper in Journal of Applied Optics, June 1972.
2. M. Berger and S. Seltzer, "Additional Stopping Power and Range Tables for Protons, Mesons, and Electrons," NASA SP-3036.

PRECEDING PAGE BLANK NOT FILMED

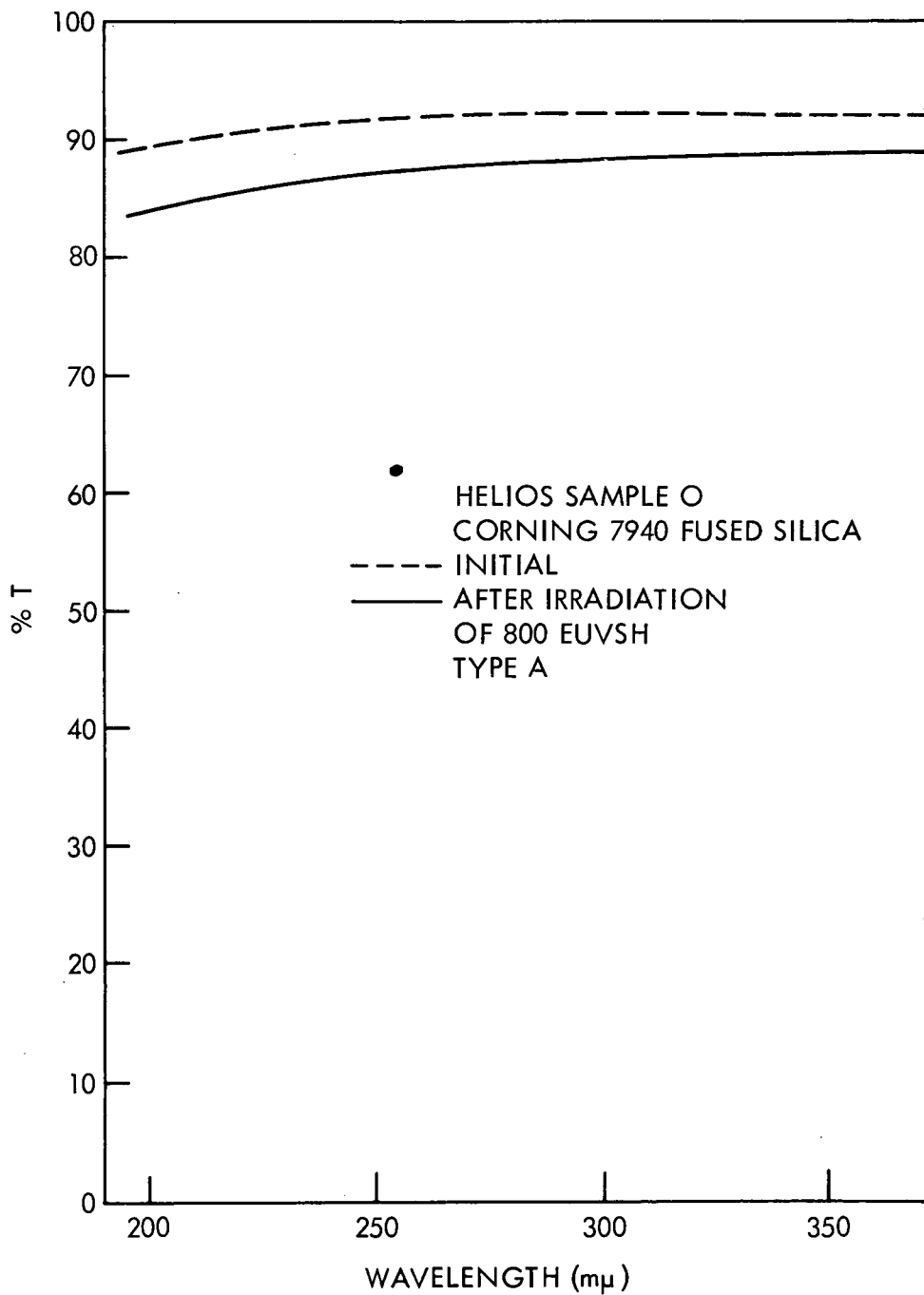


Figure 1.

Preceding page blank

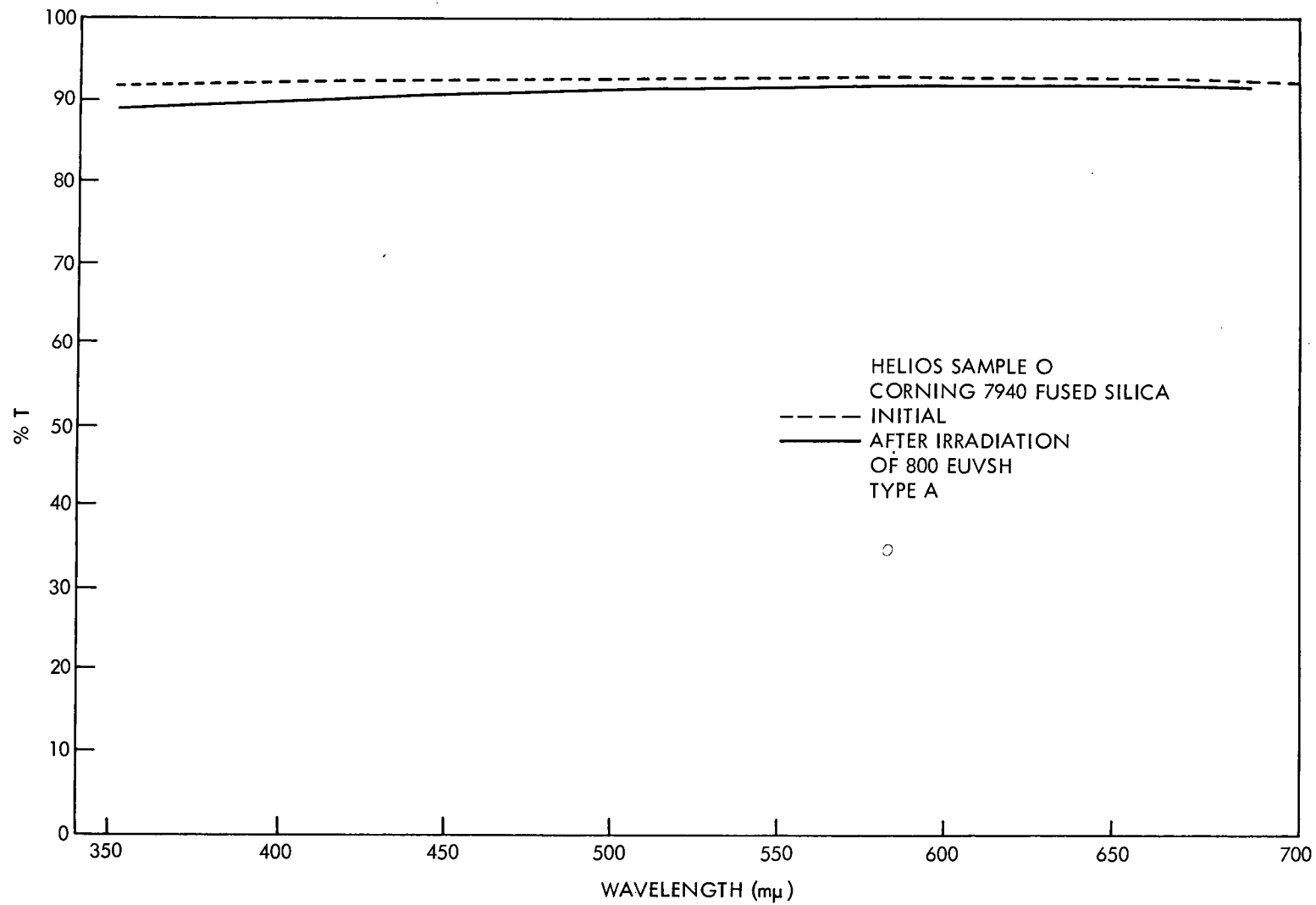


Figure 2.

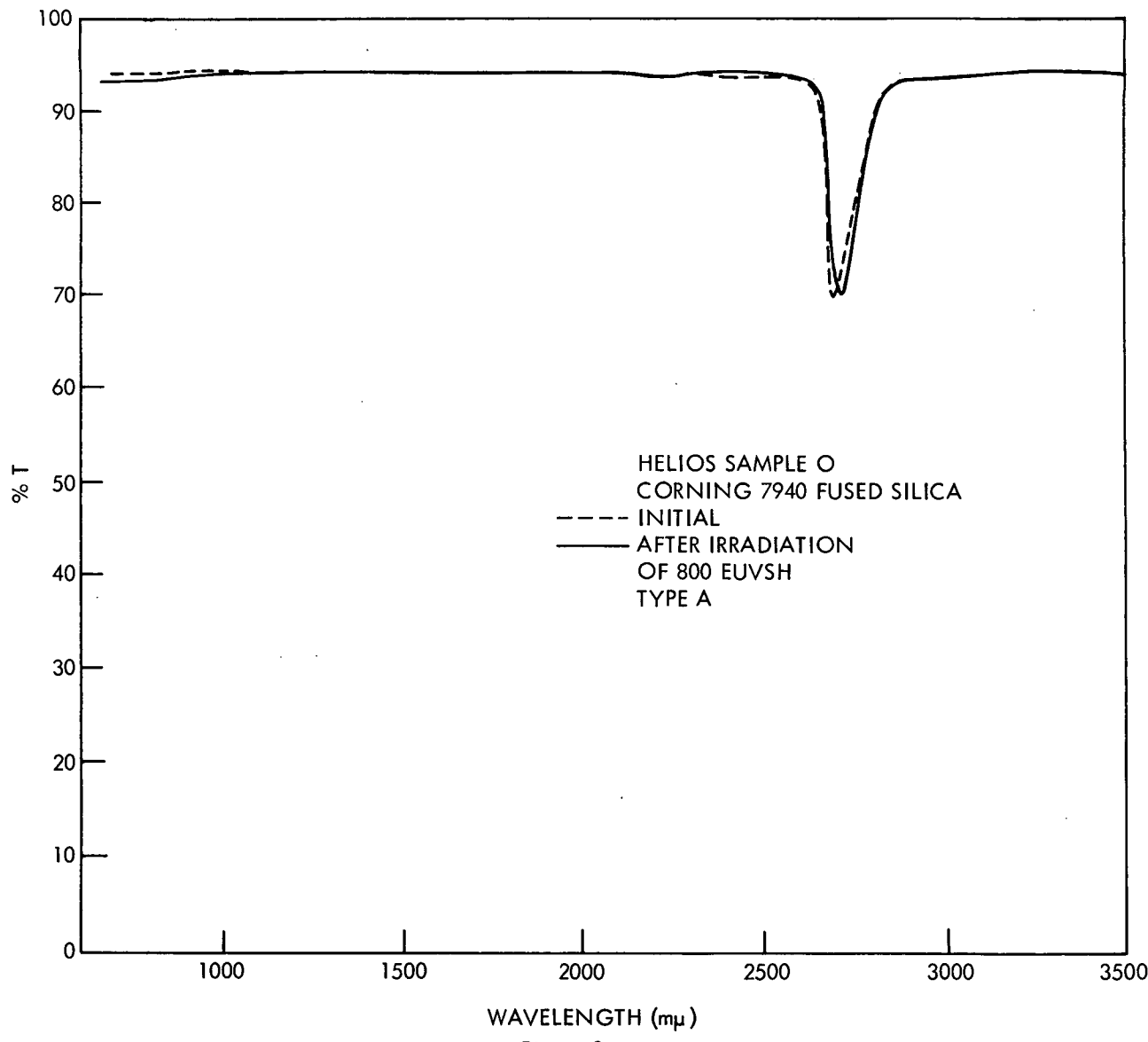


Figure 3.

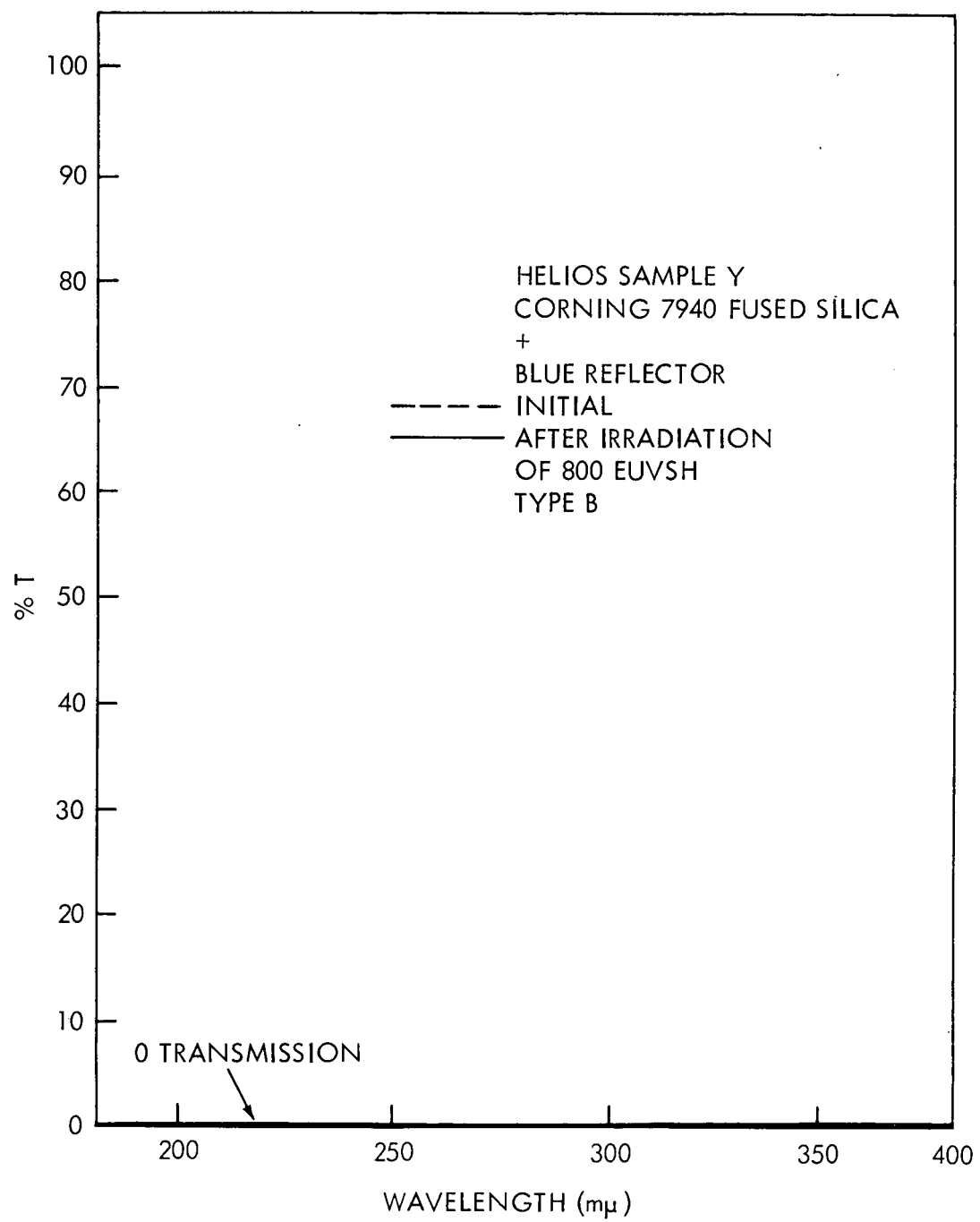


Figure 4.

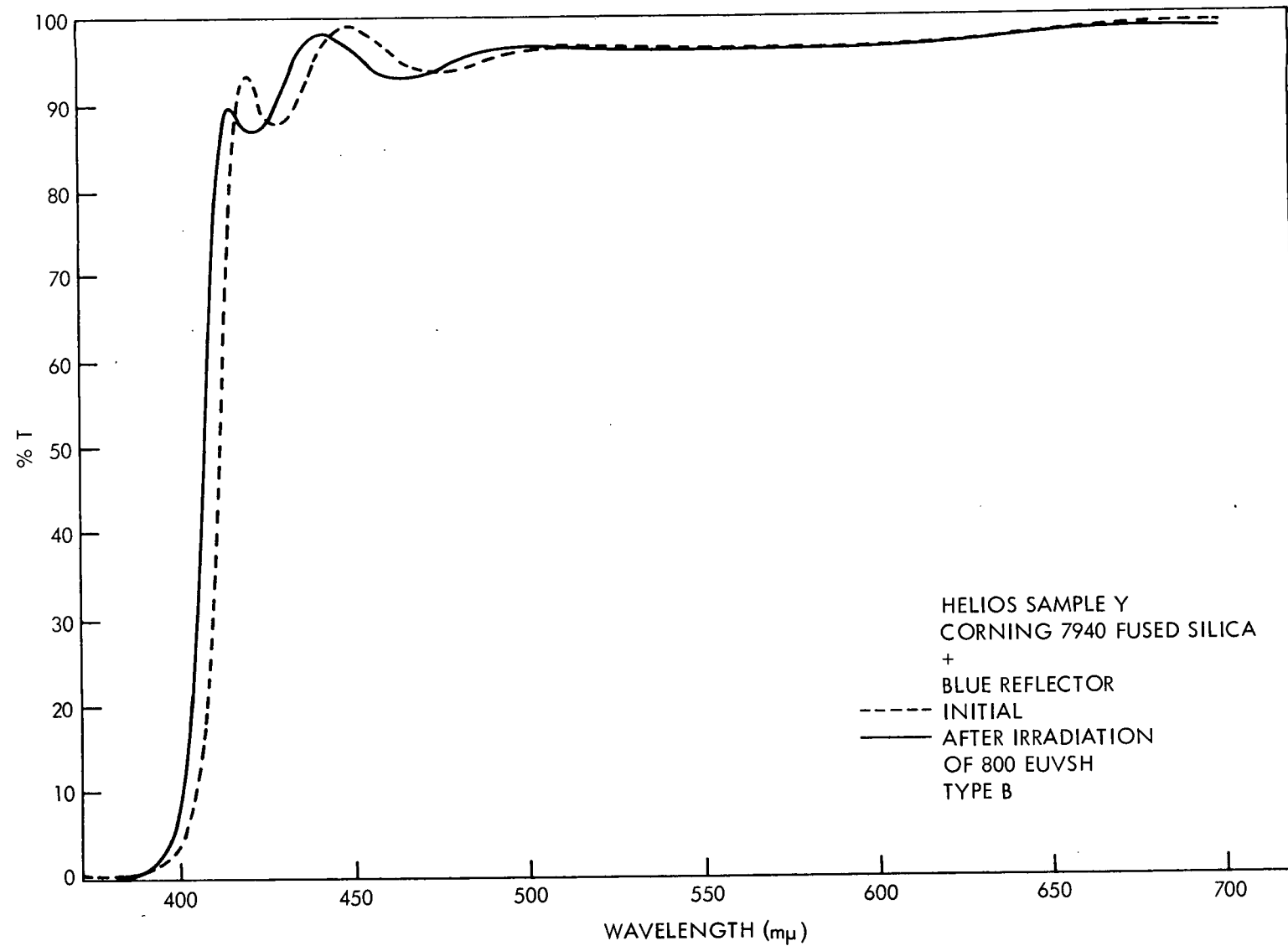


Figure 5.

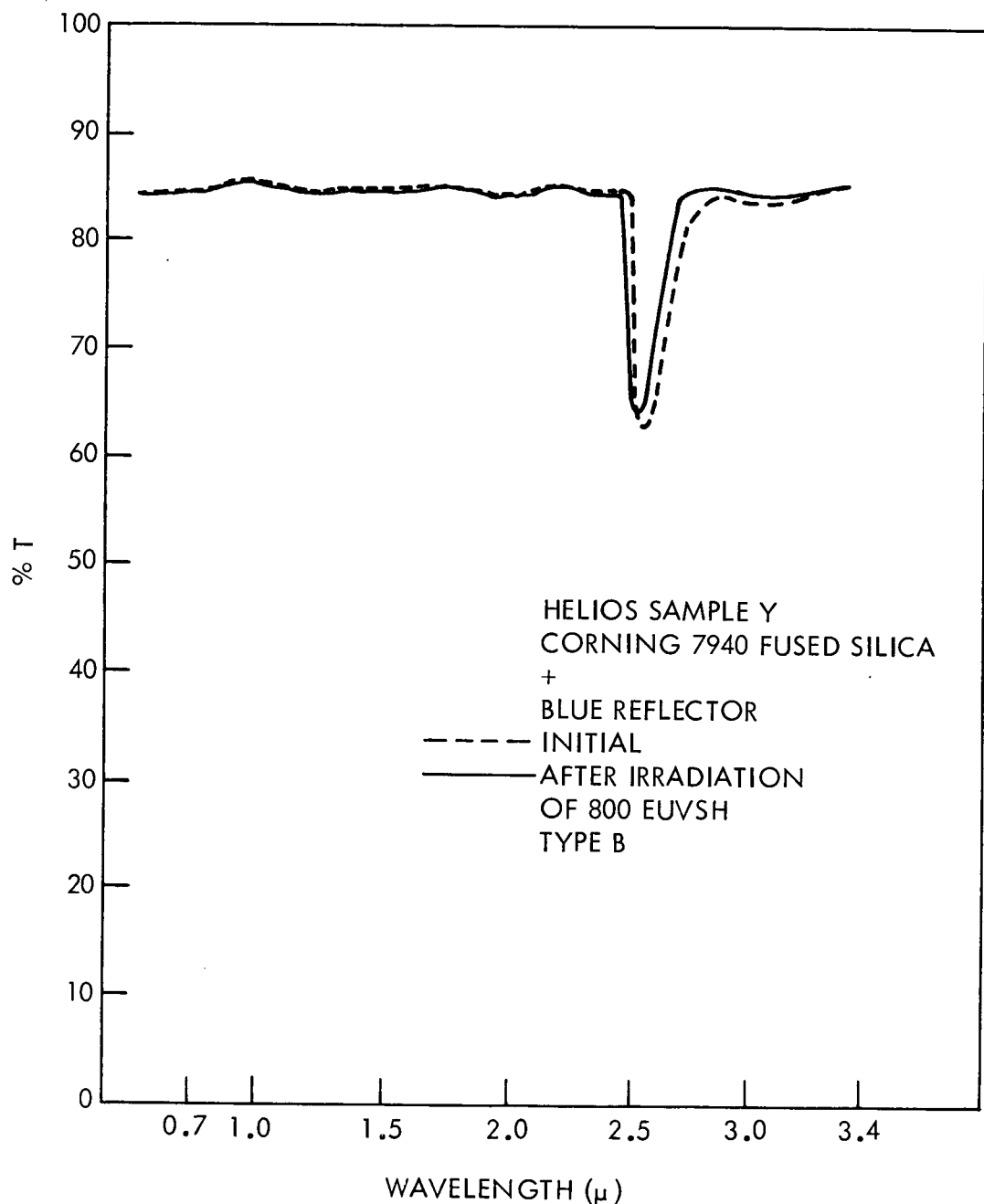


Figure 6.

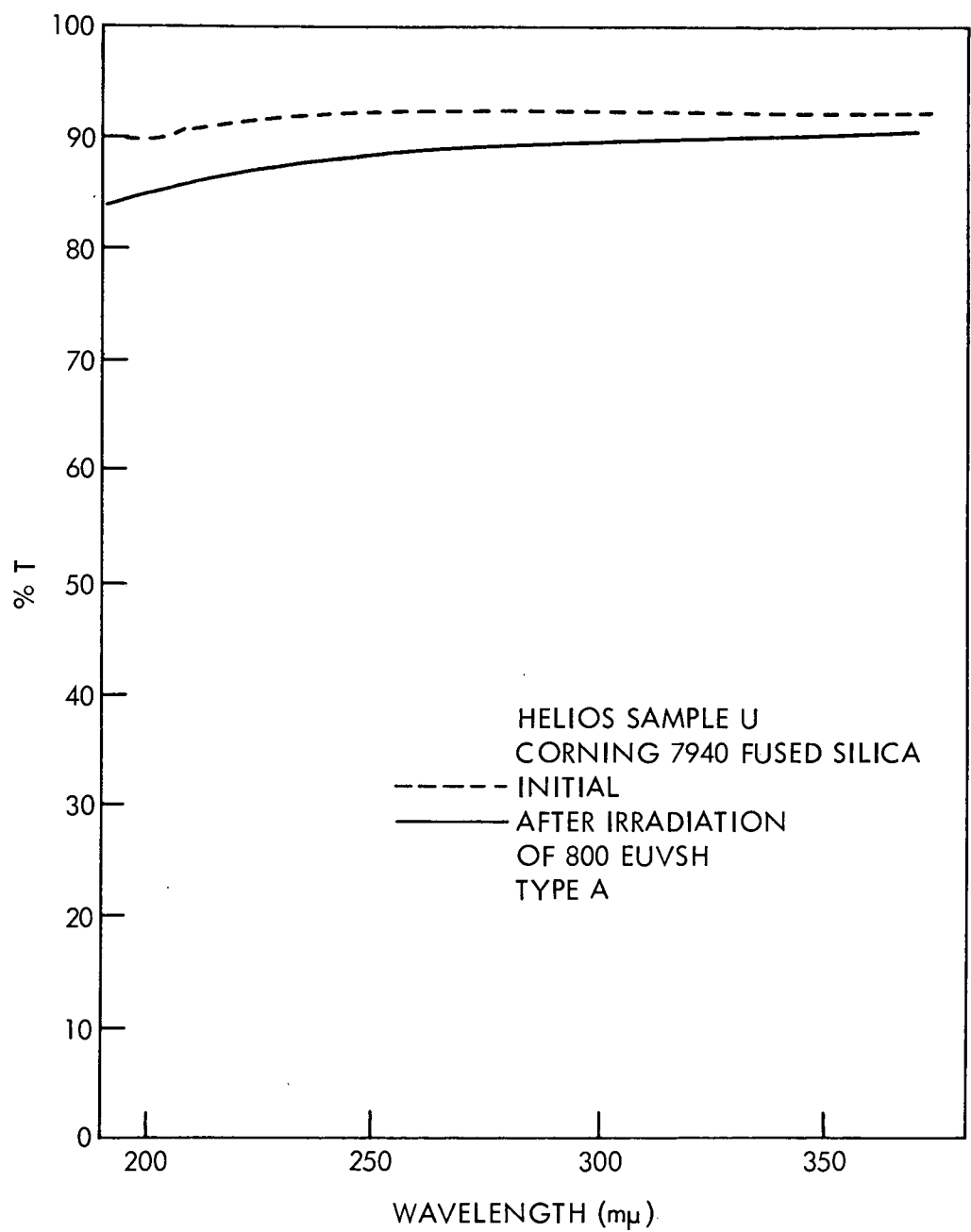


Figure 7.

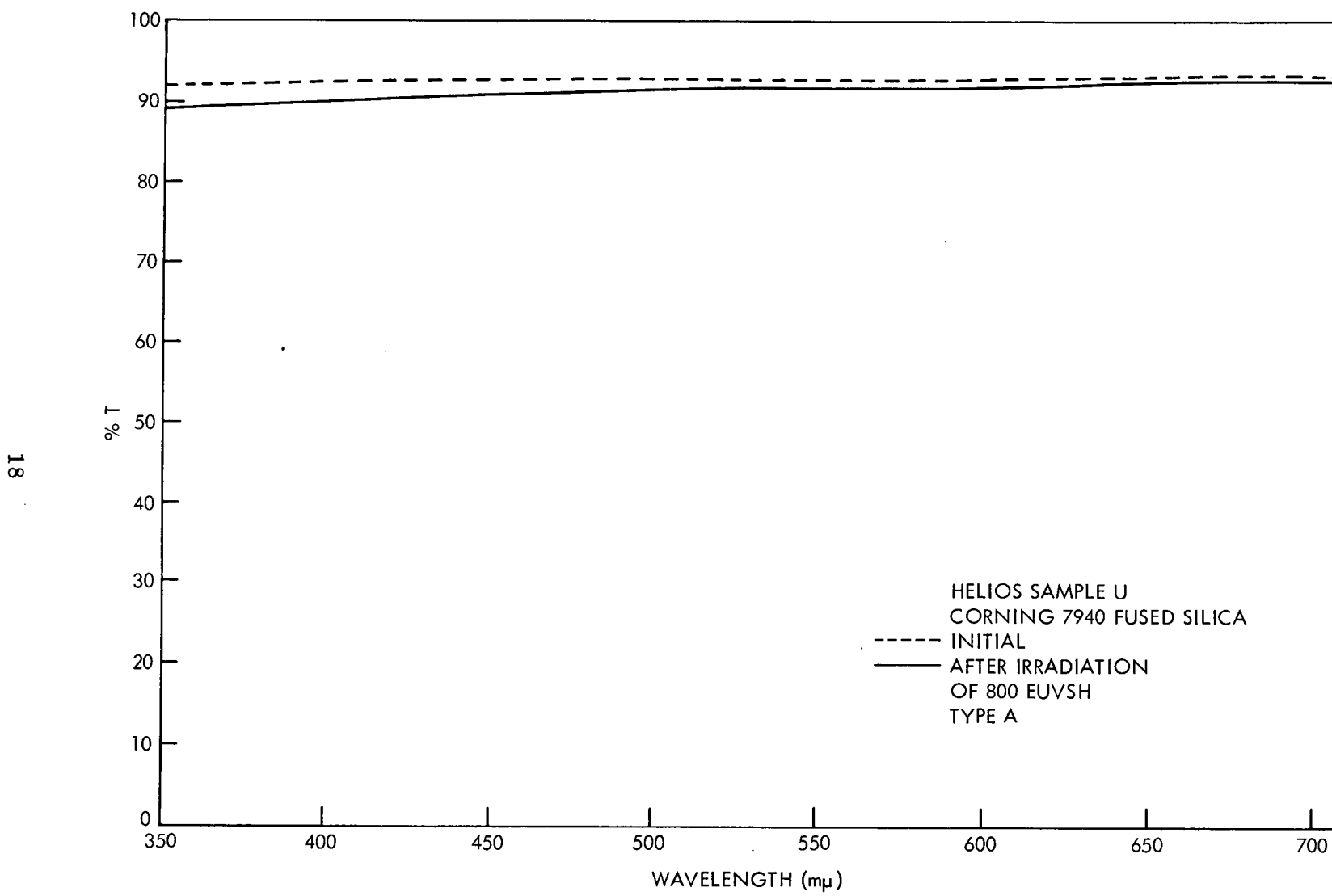


Figure 8.

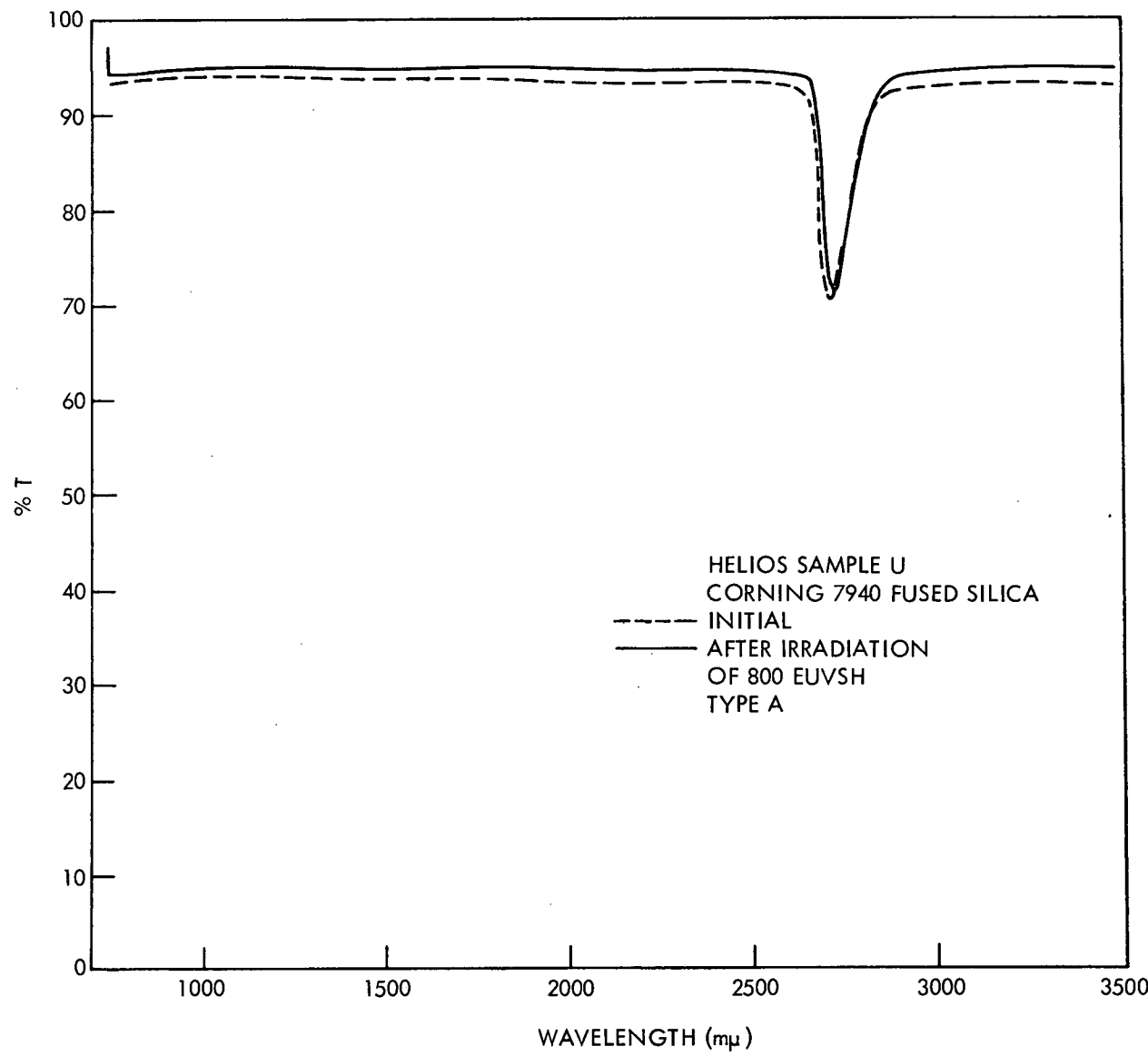


Figure 9.

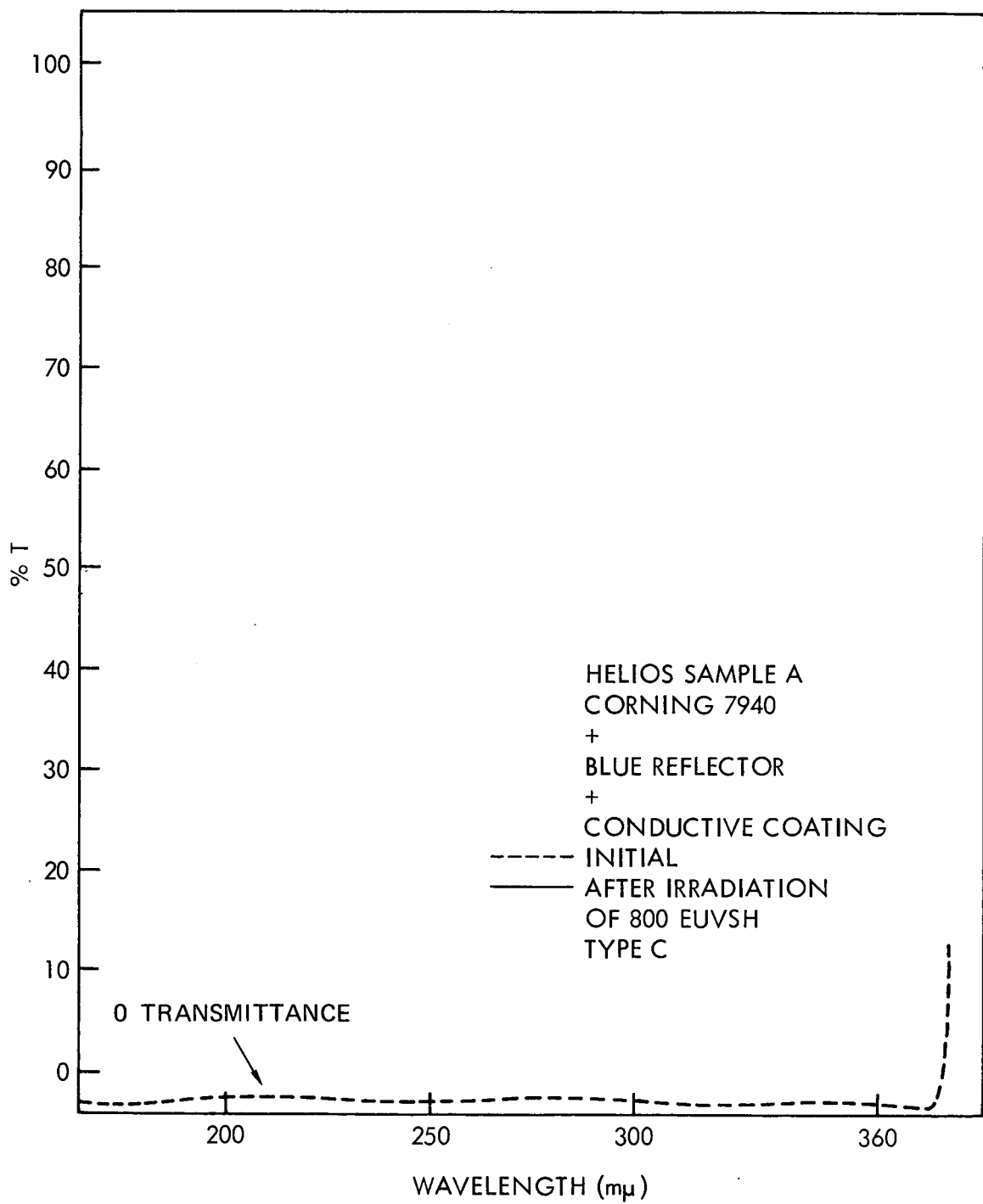


Figure 10.

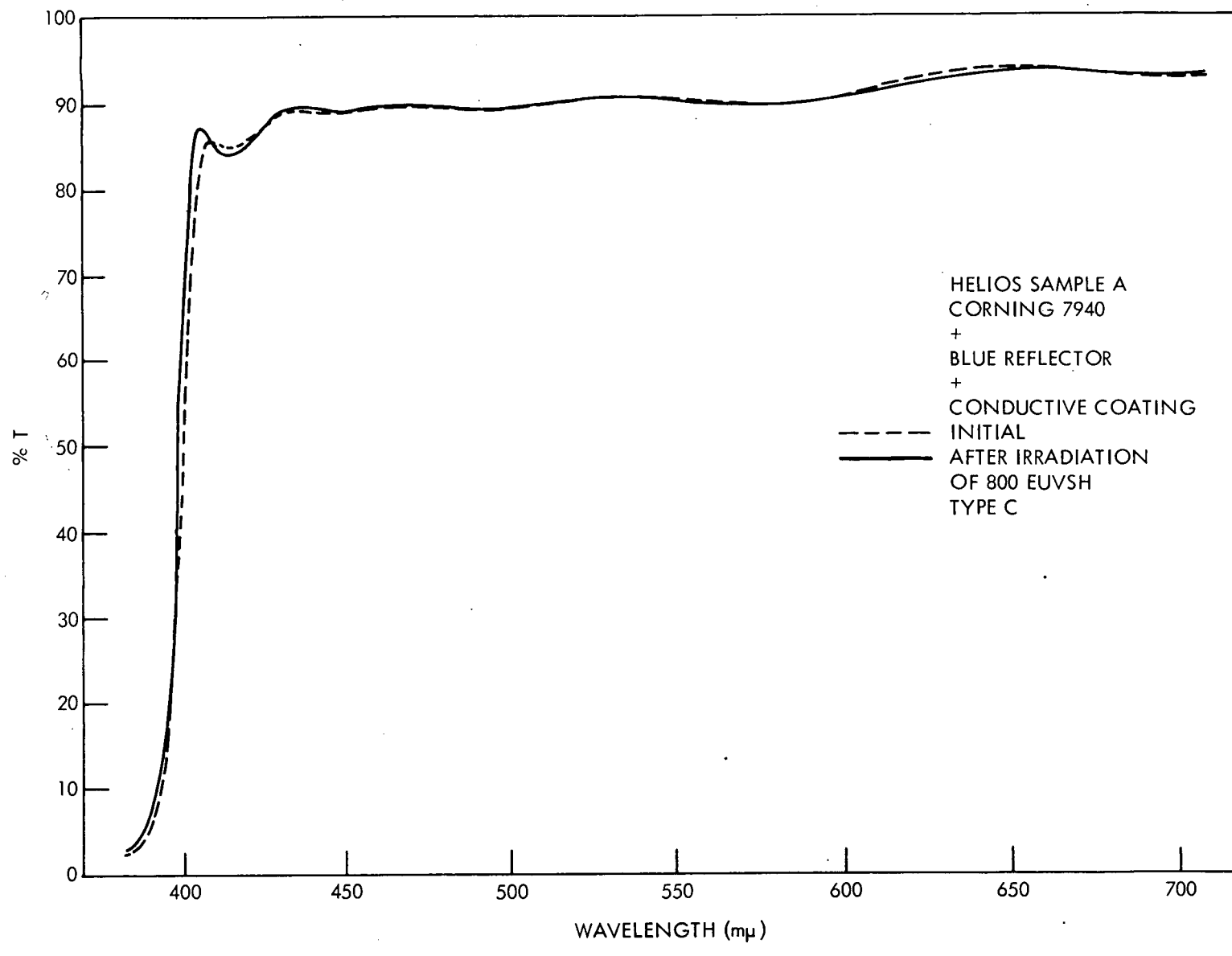


Figure 11.

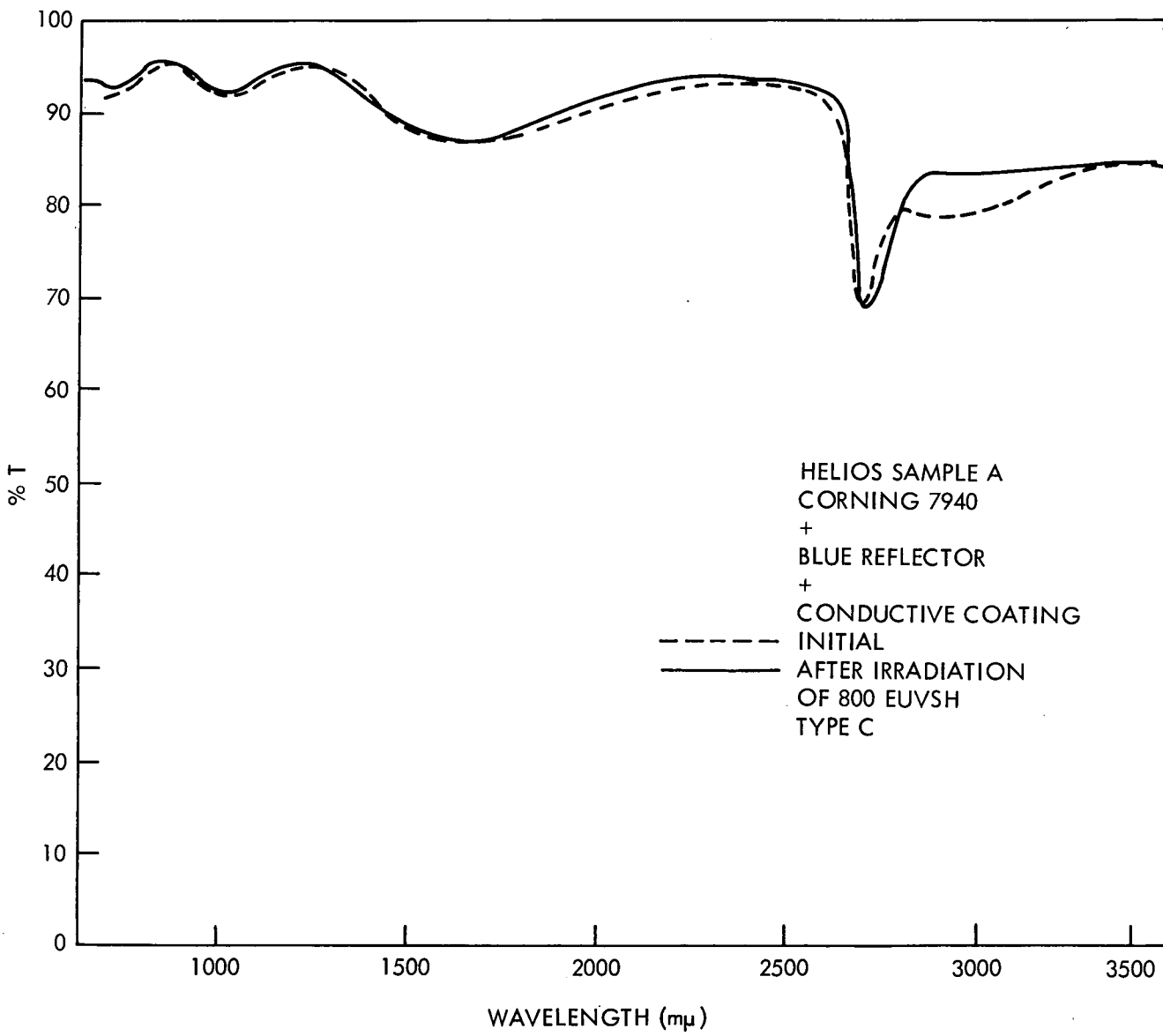


Figure 12.

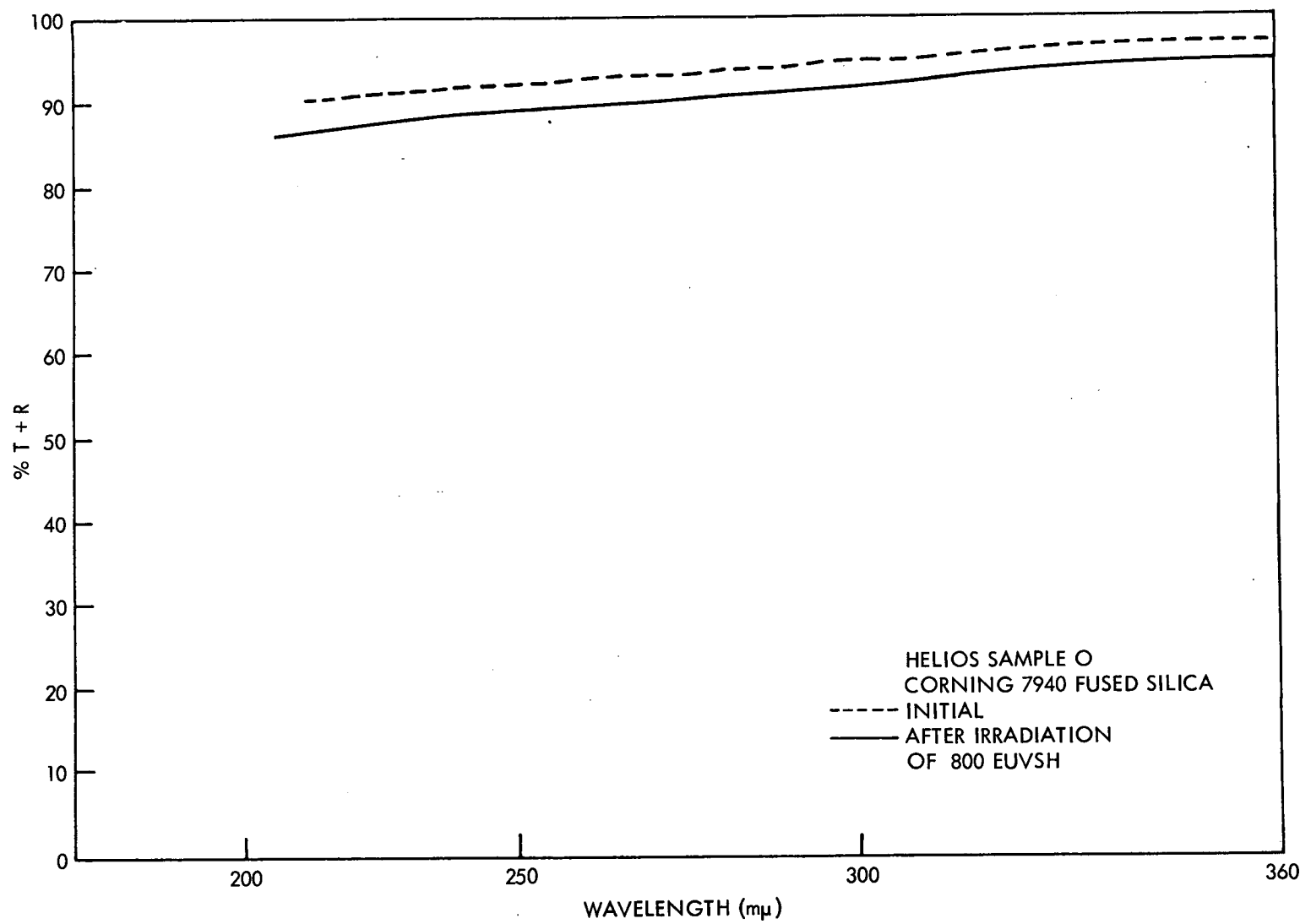


Figure 13.

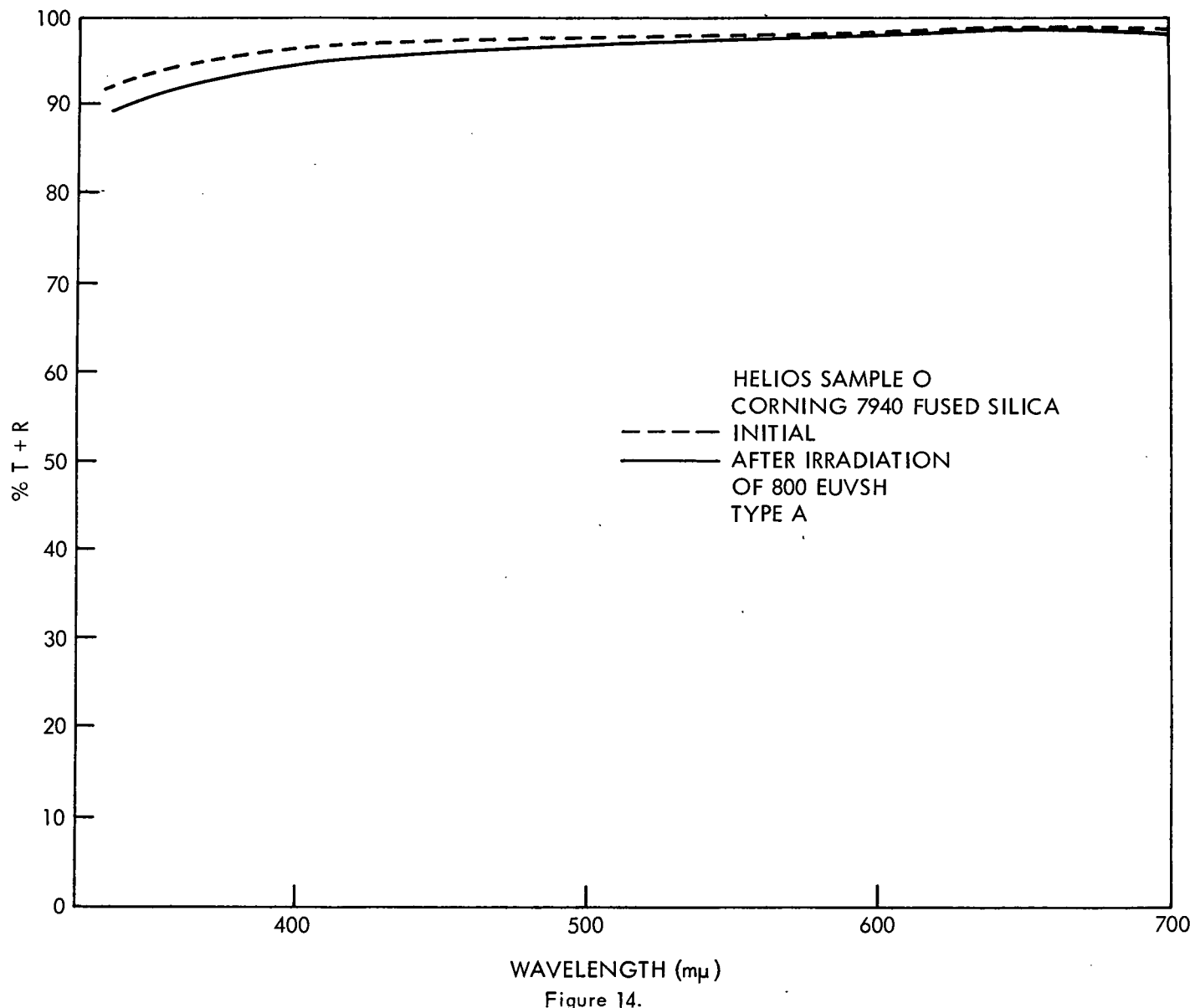


Figure 14.

25

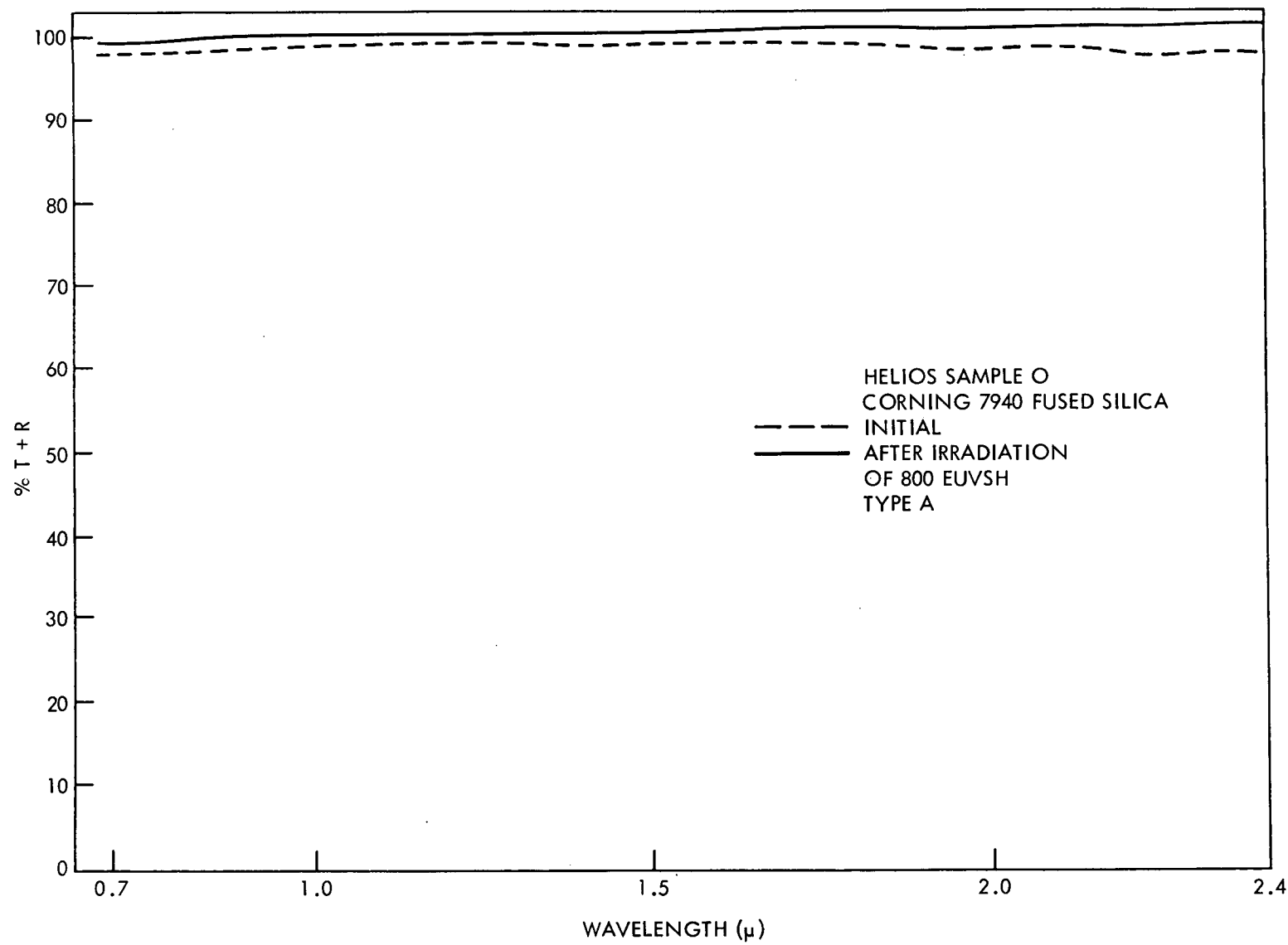


Figure 15.

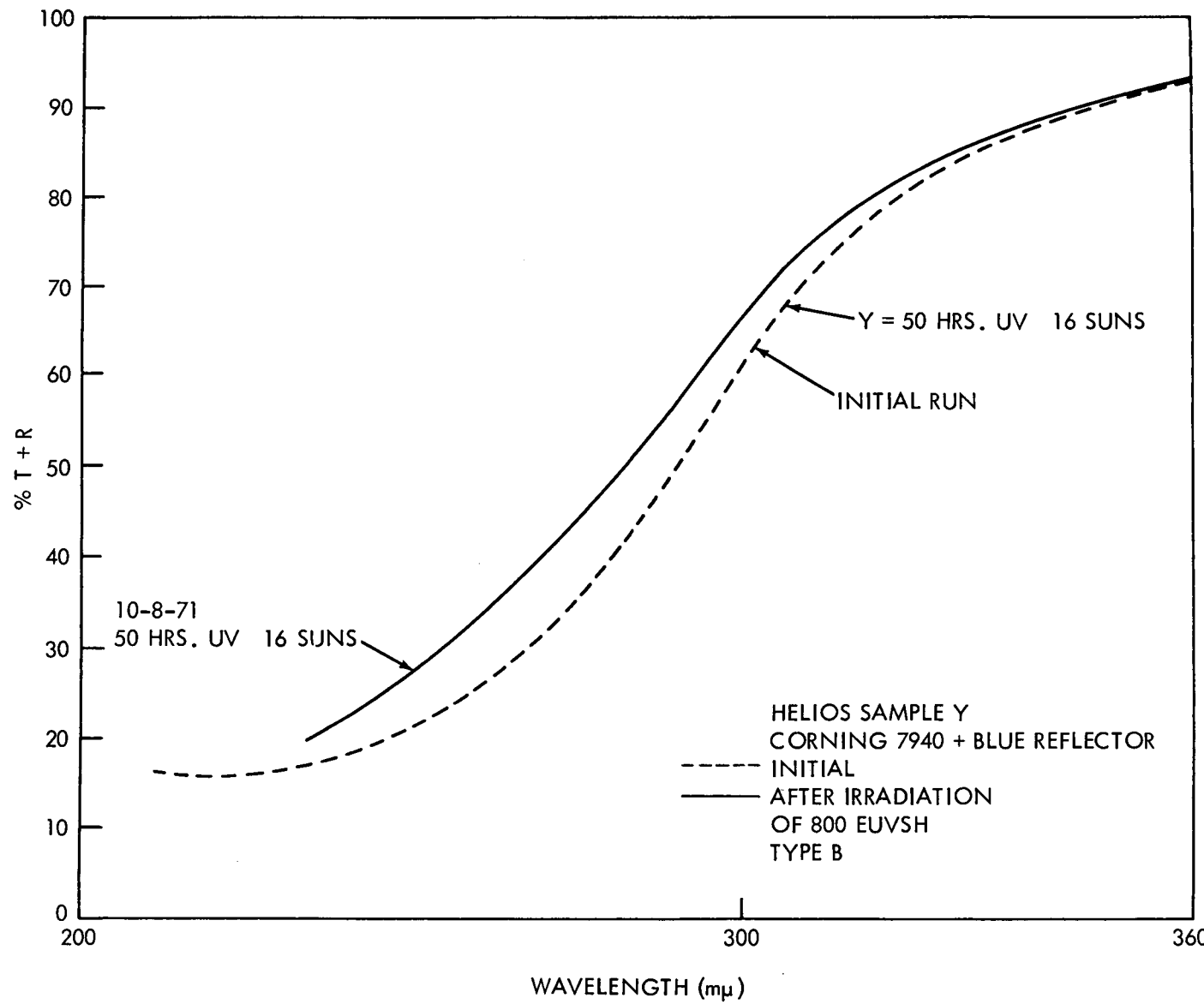


Figure 16.

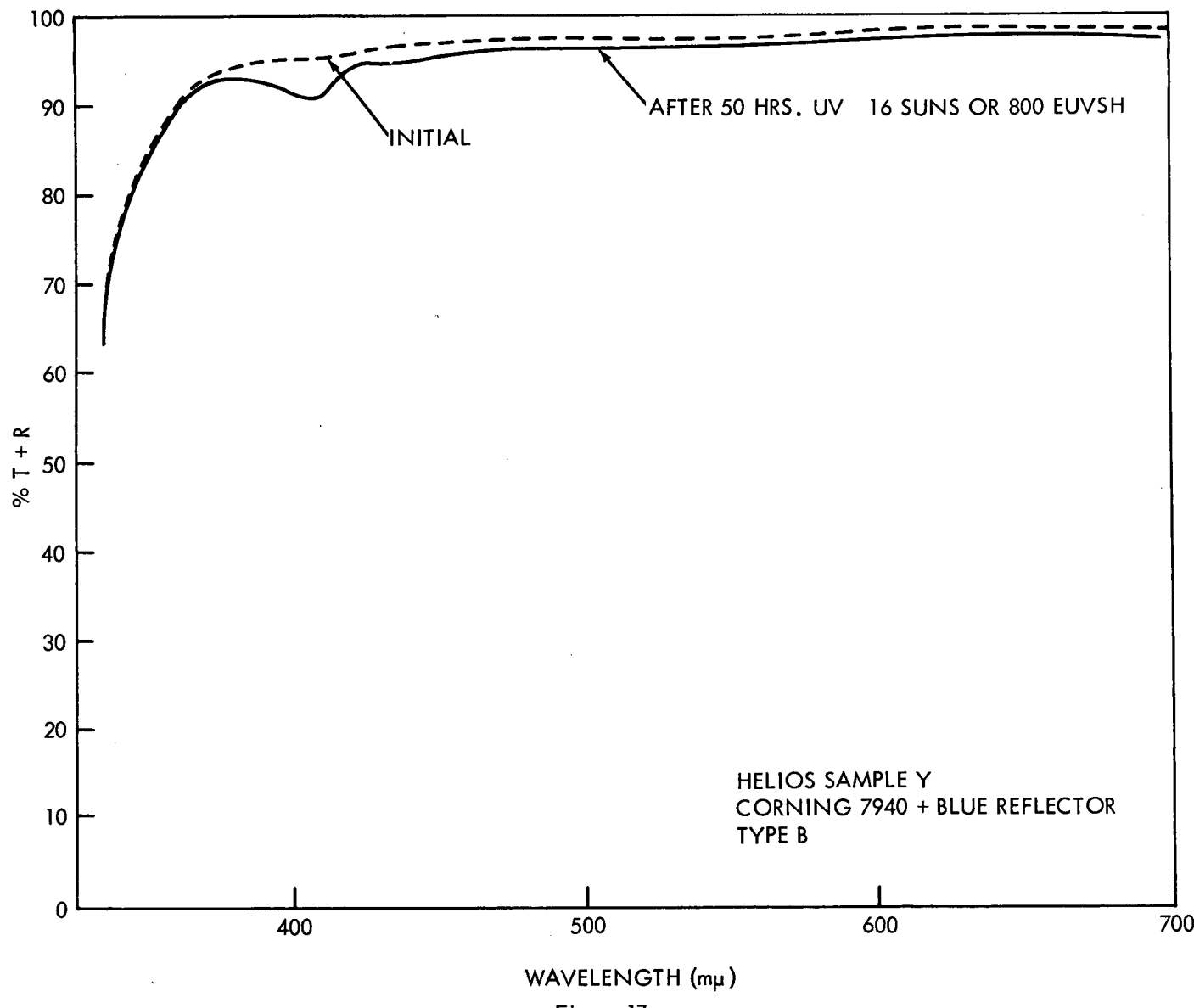


Figure 17.

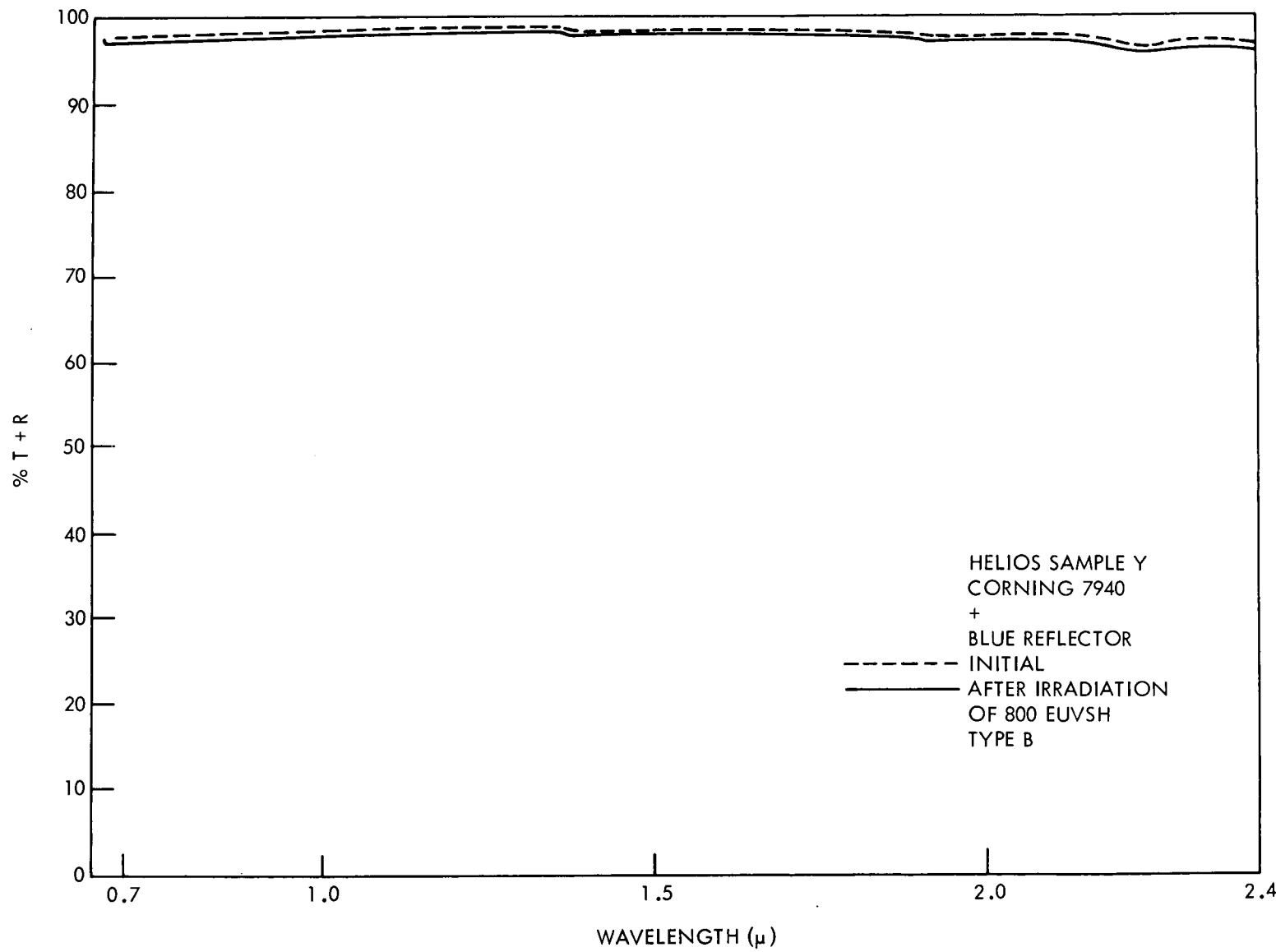


Figure 18.

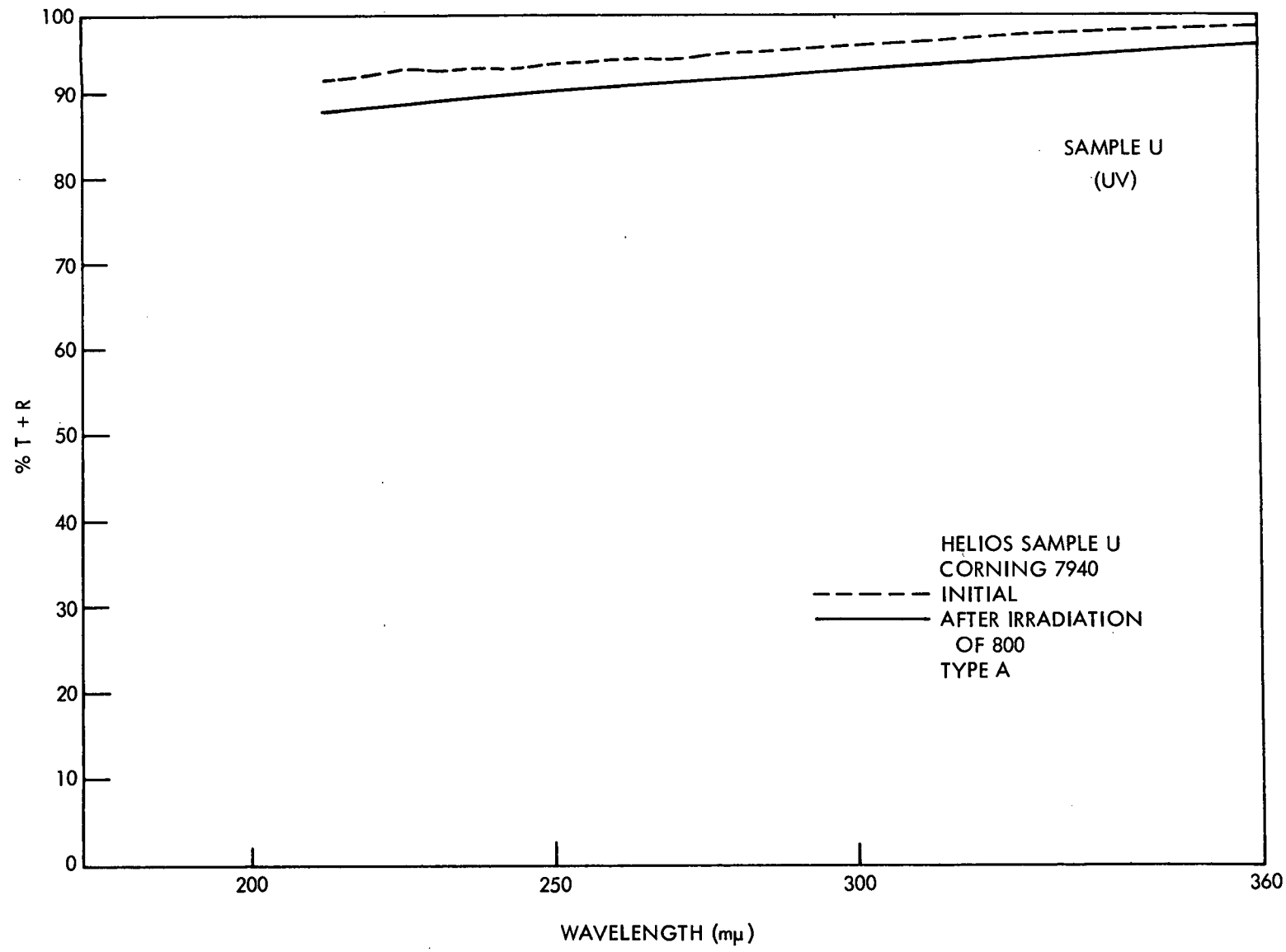


Figure 19.

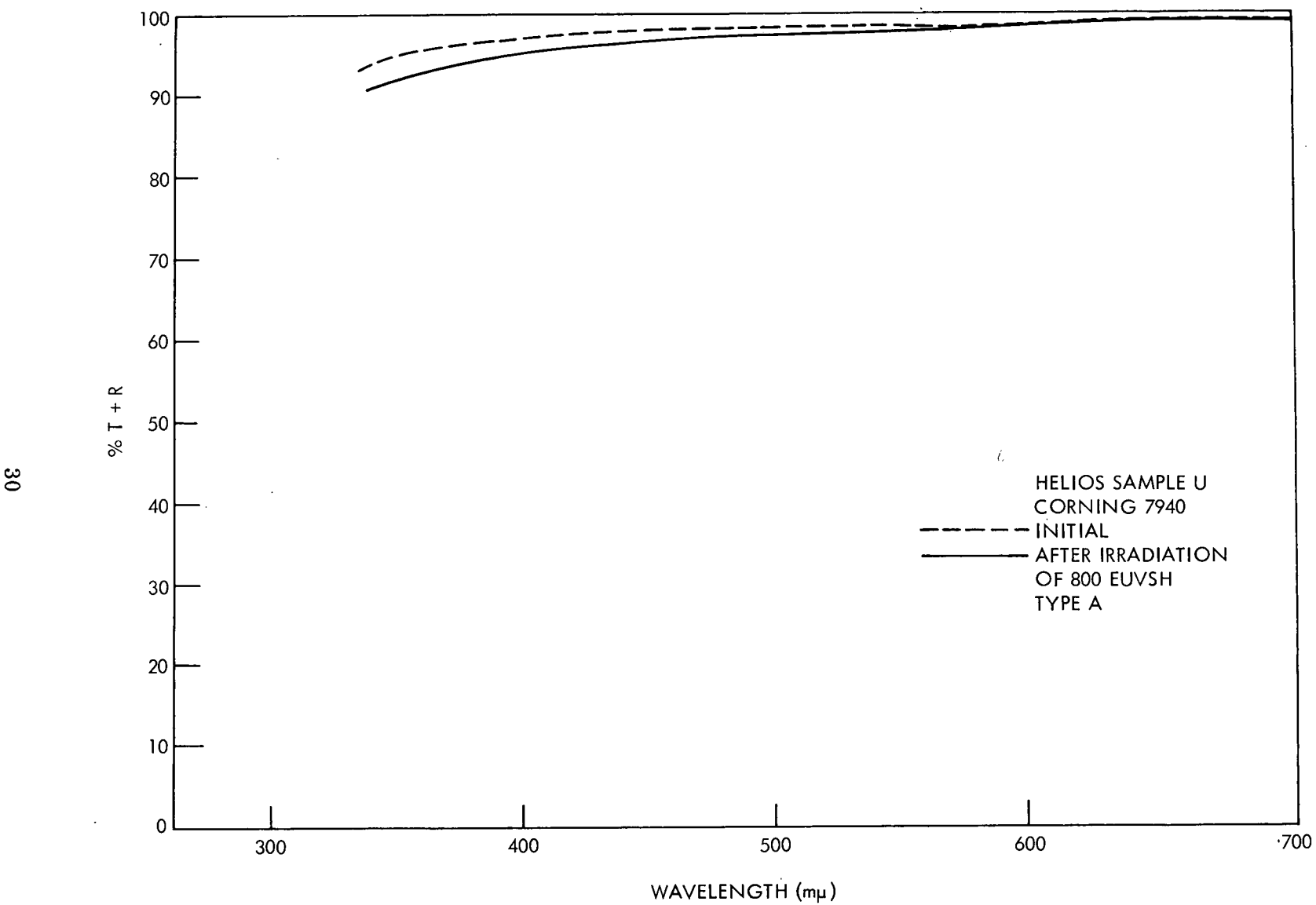


Figure 20.

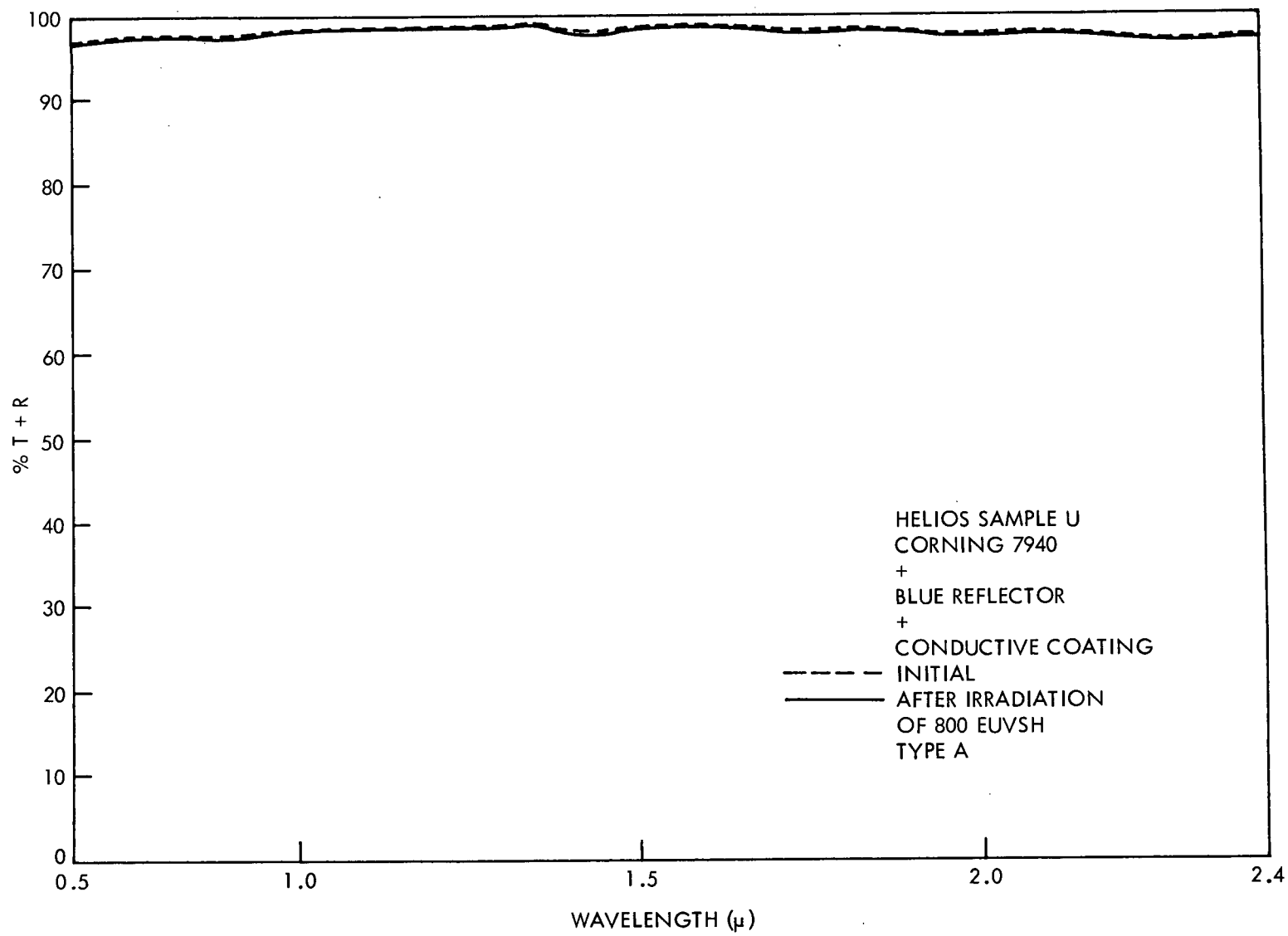


Figure 21.

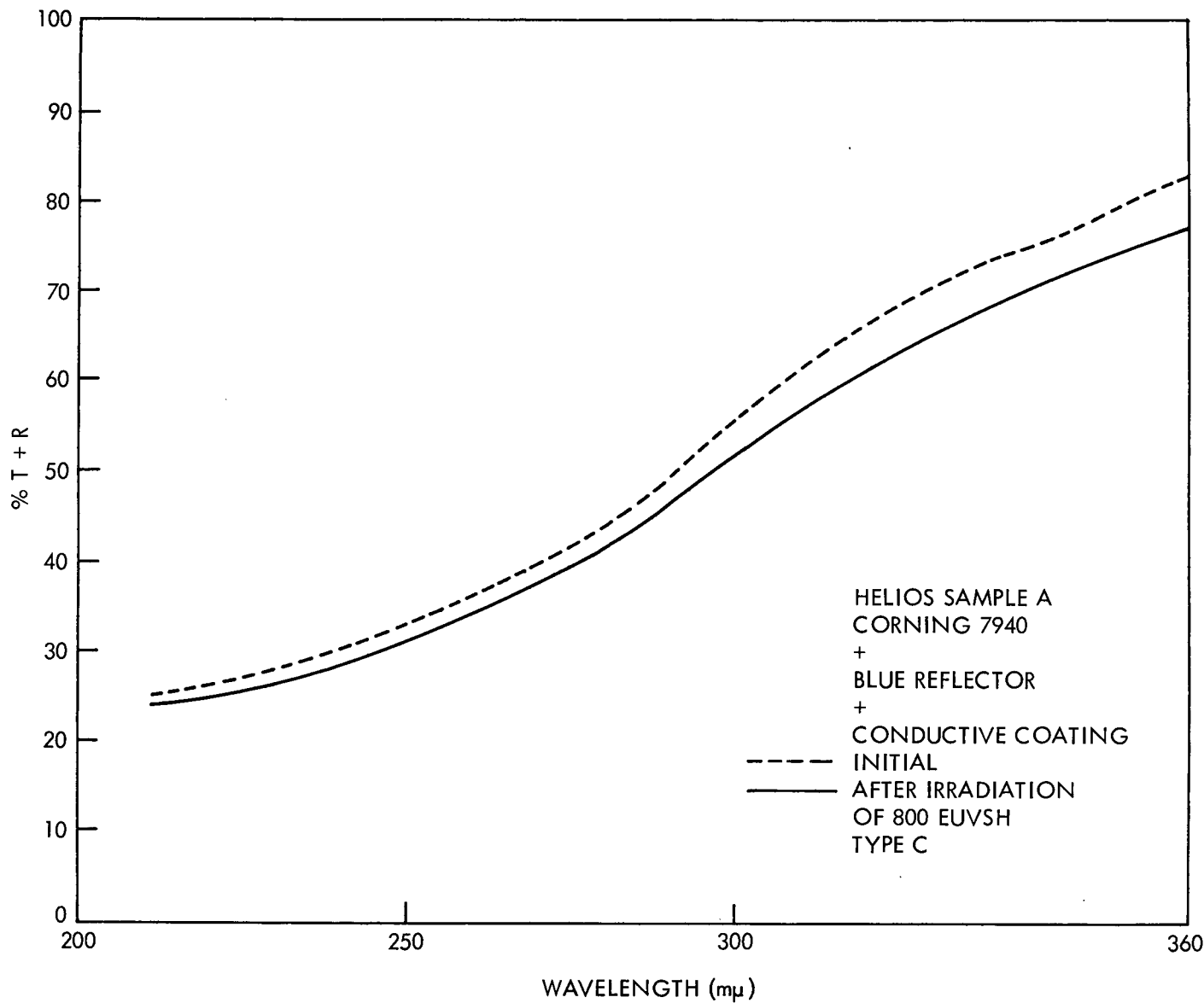


Figure 22.

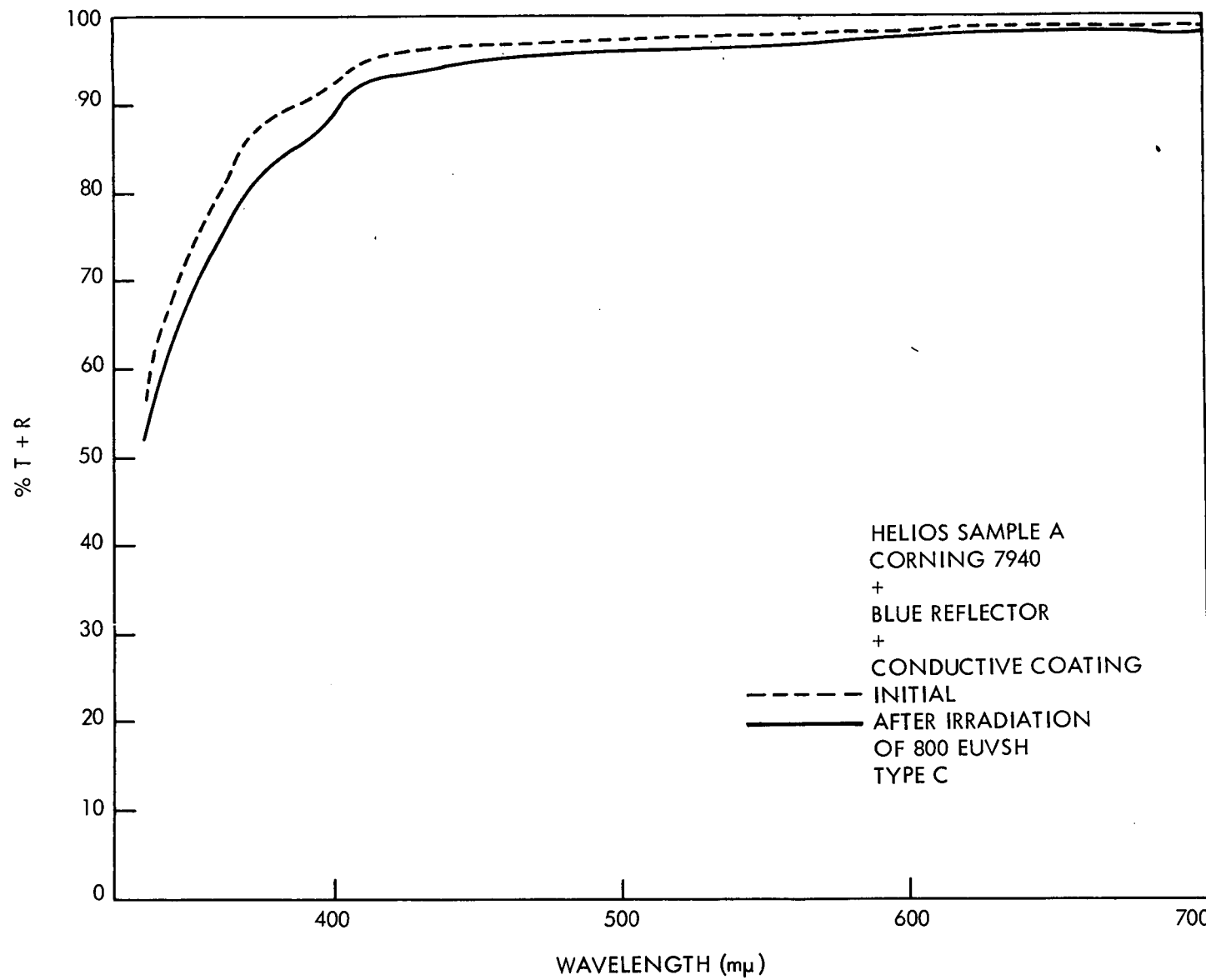


Figure 23.

Fig

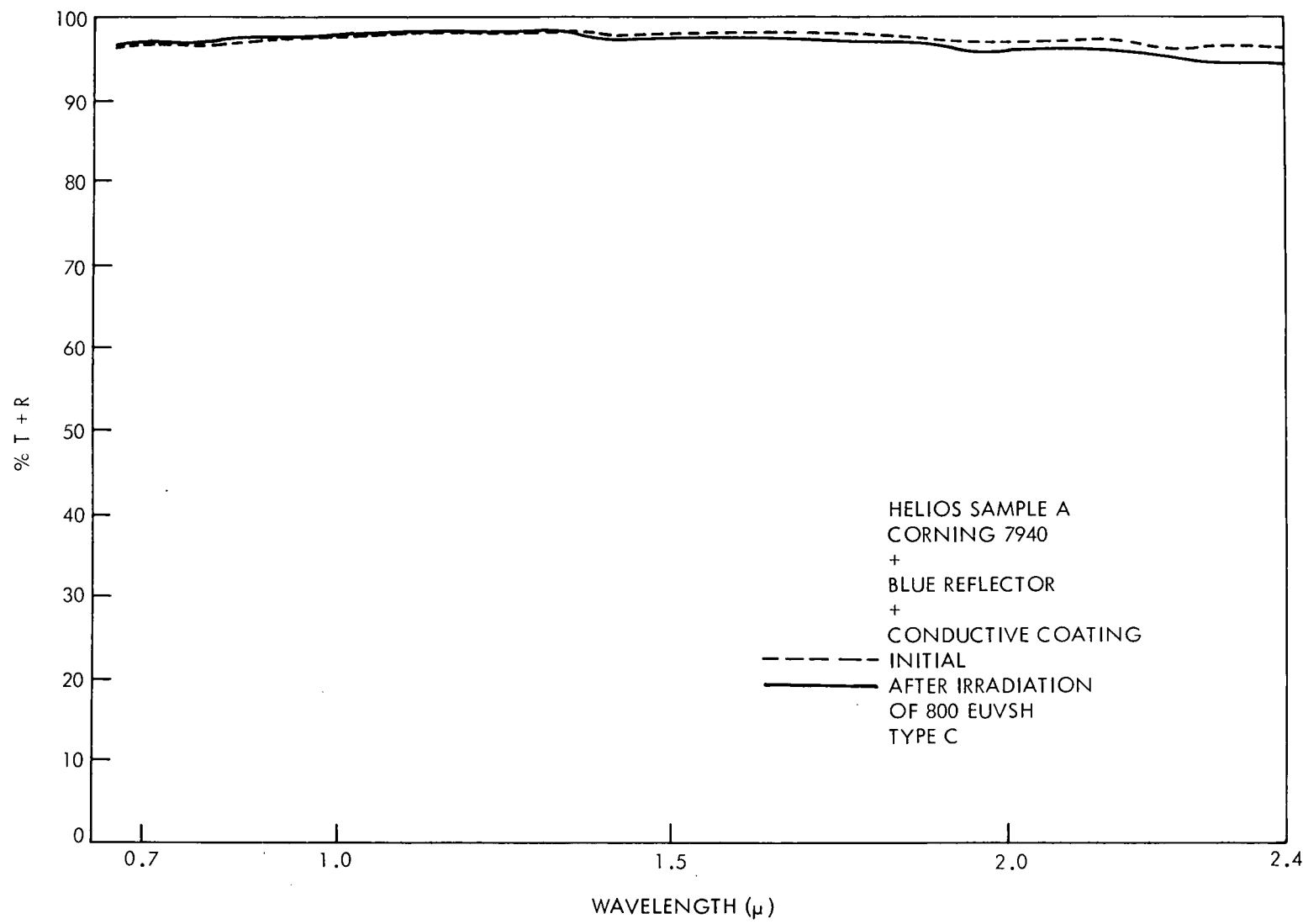


Figure 24.

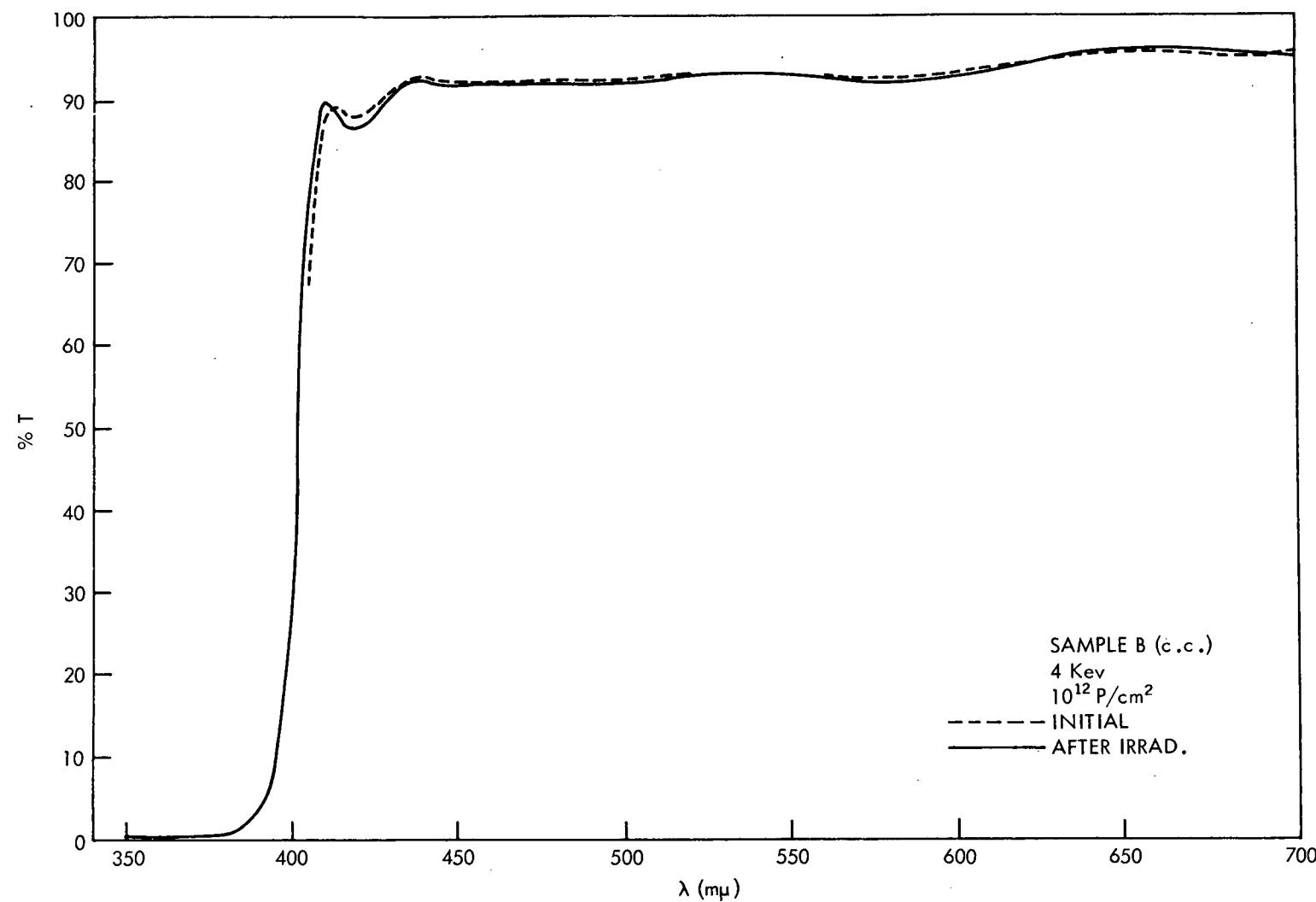


Figure 25.

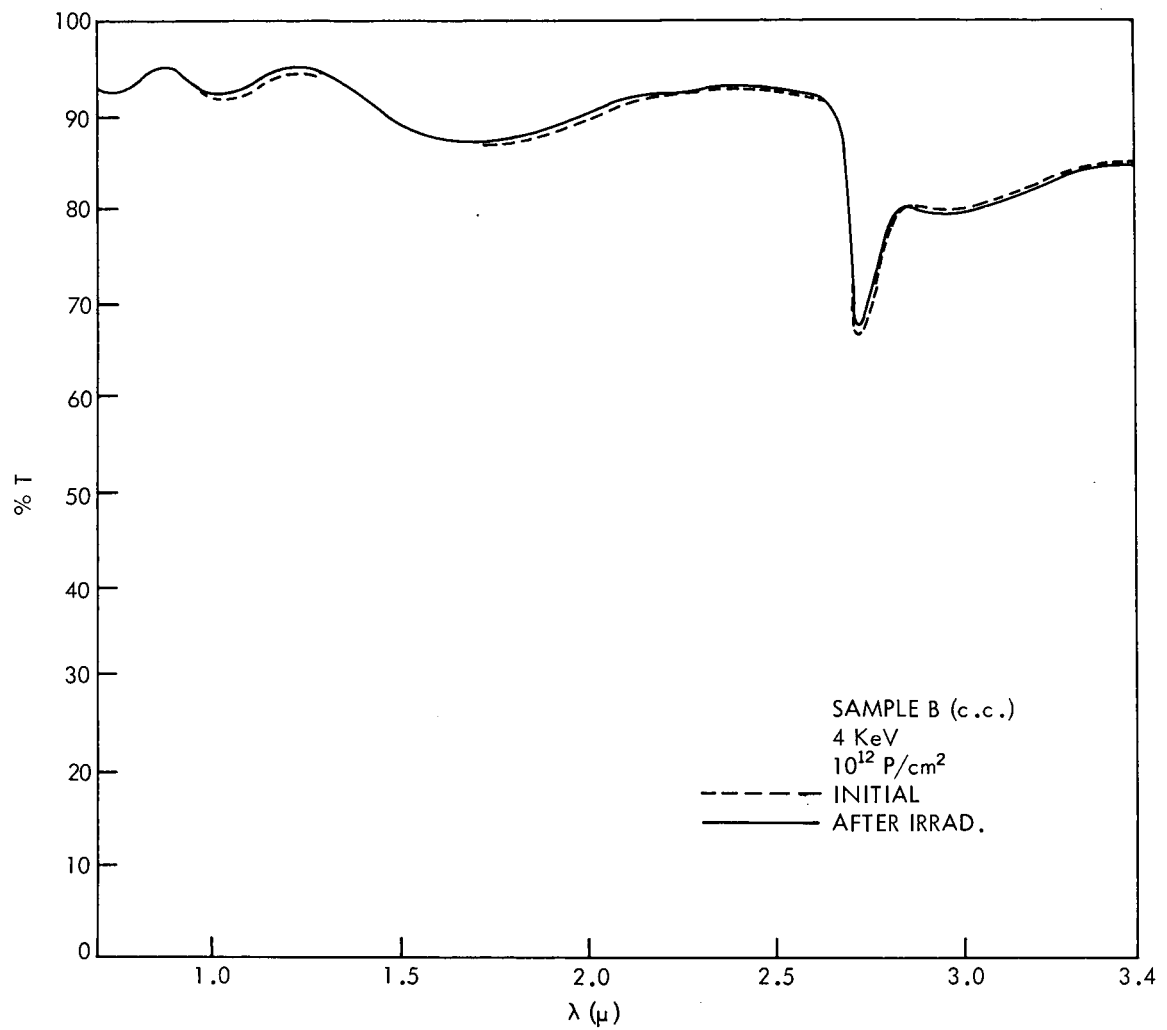


Figure 26.

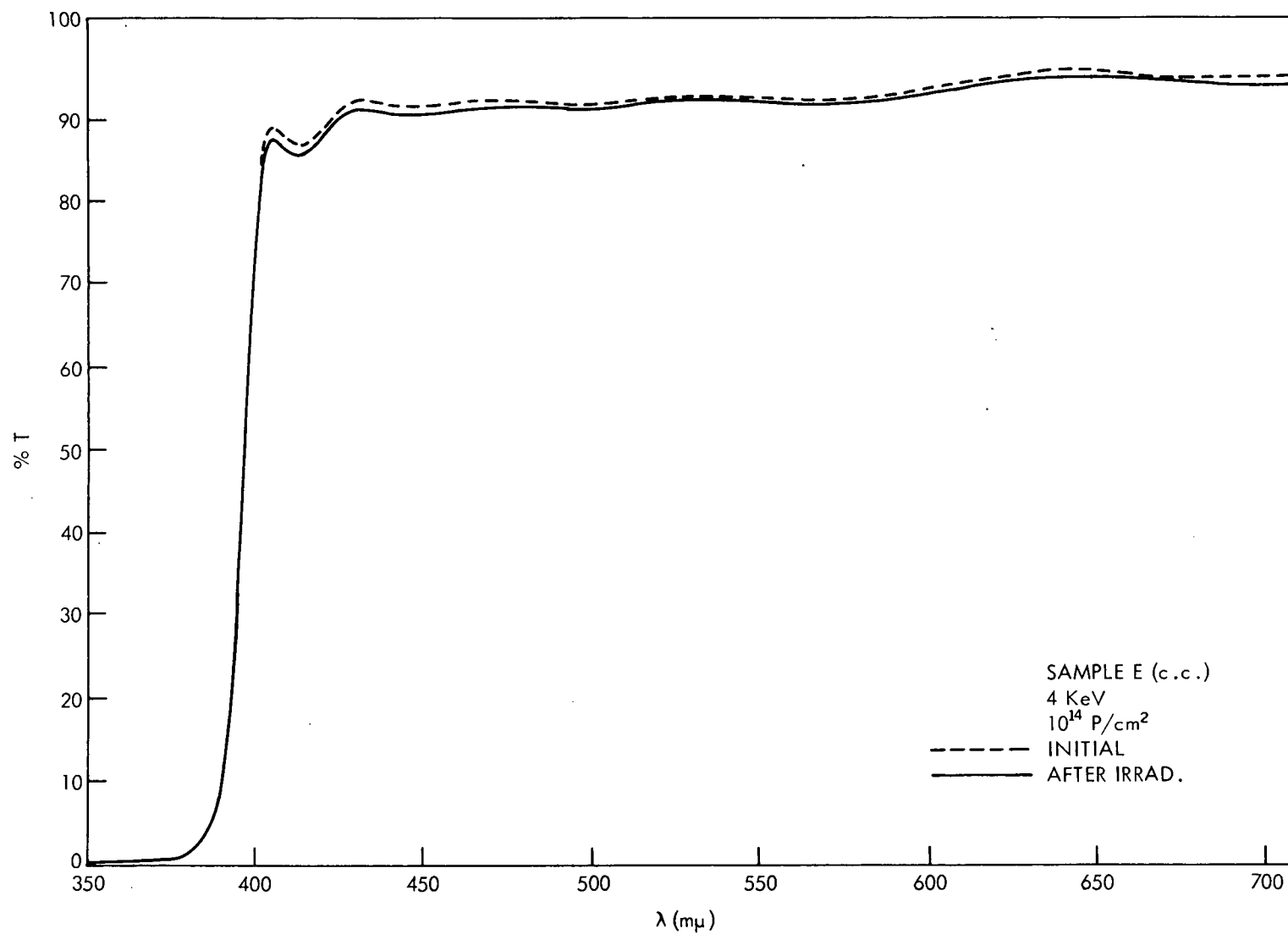


Figure 27.

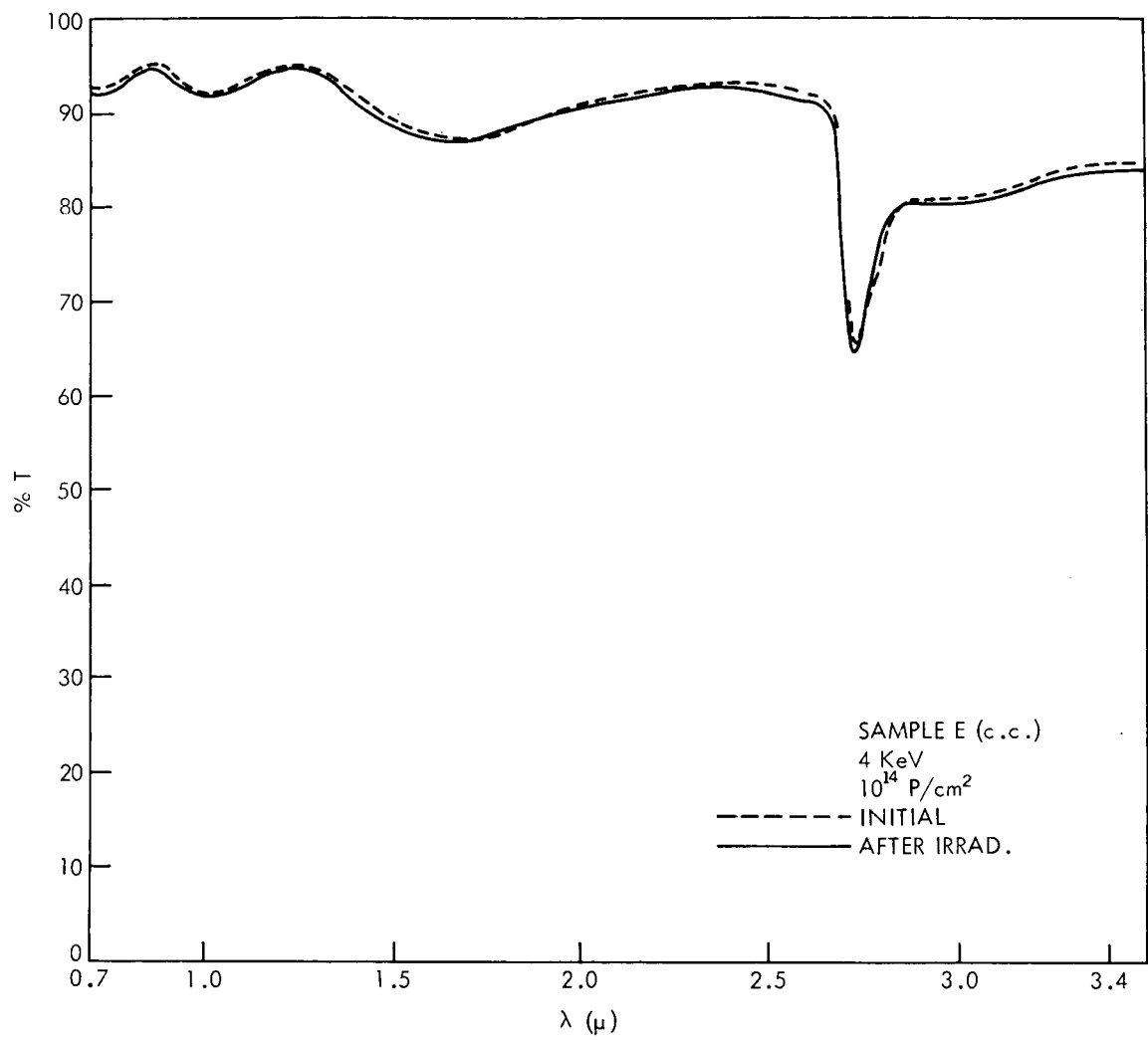


Figure 28.

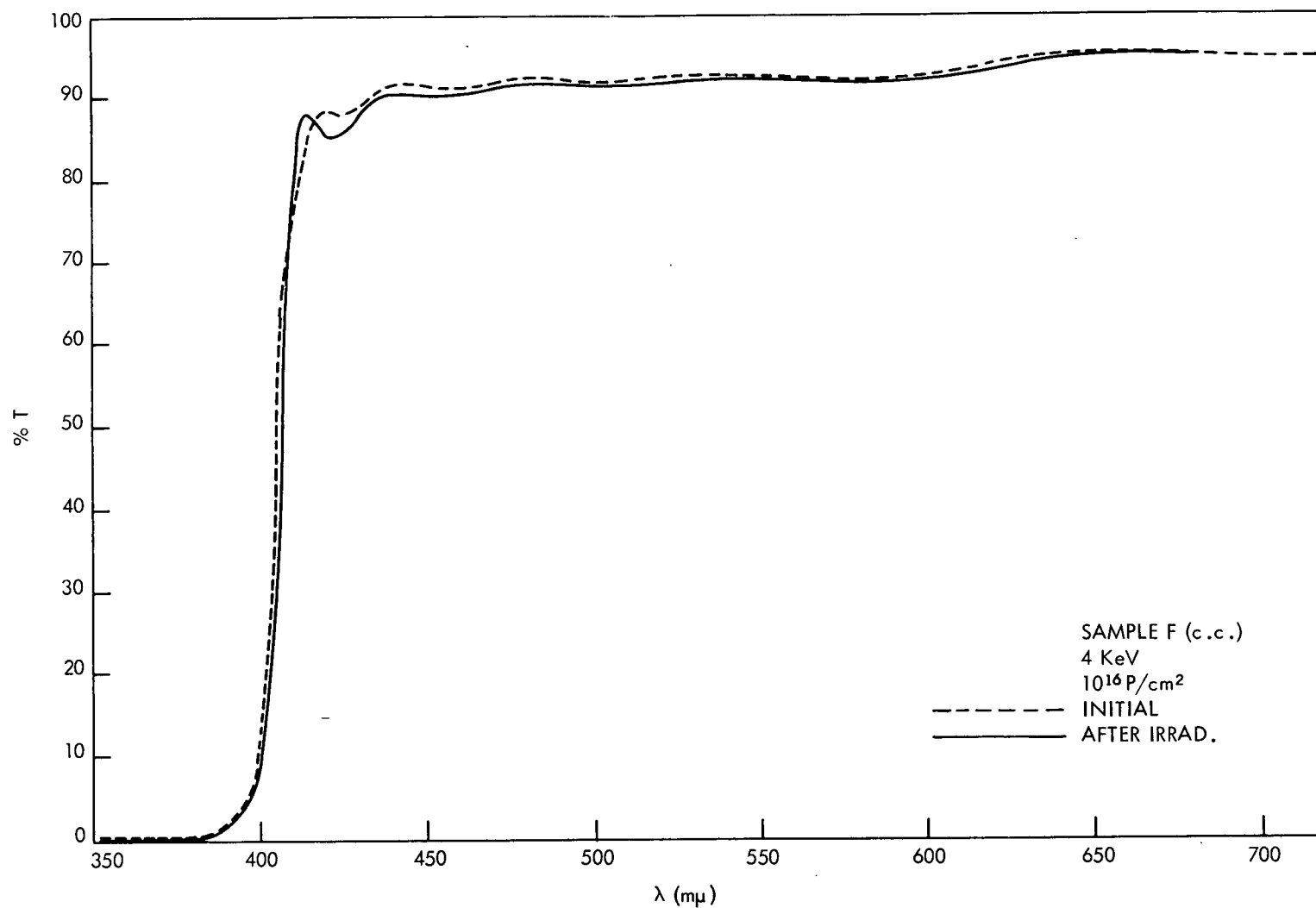


Figure 29.

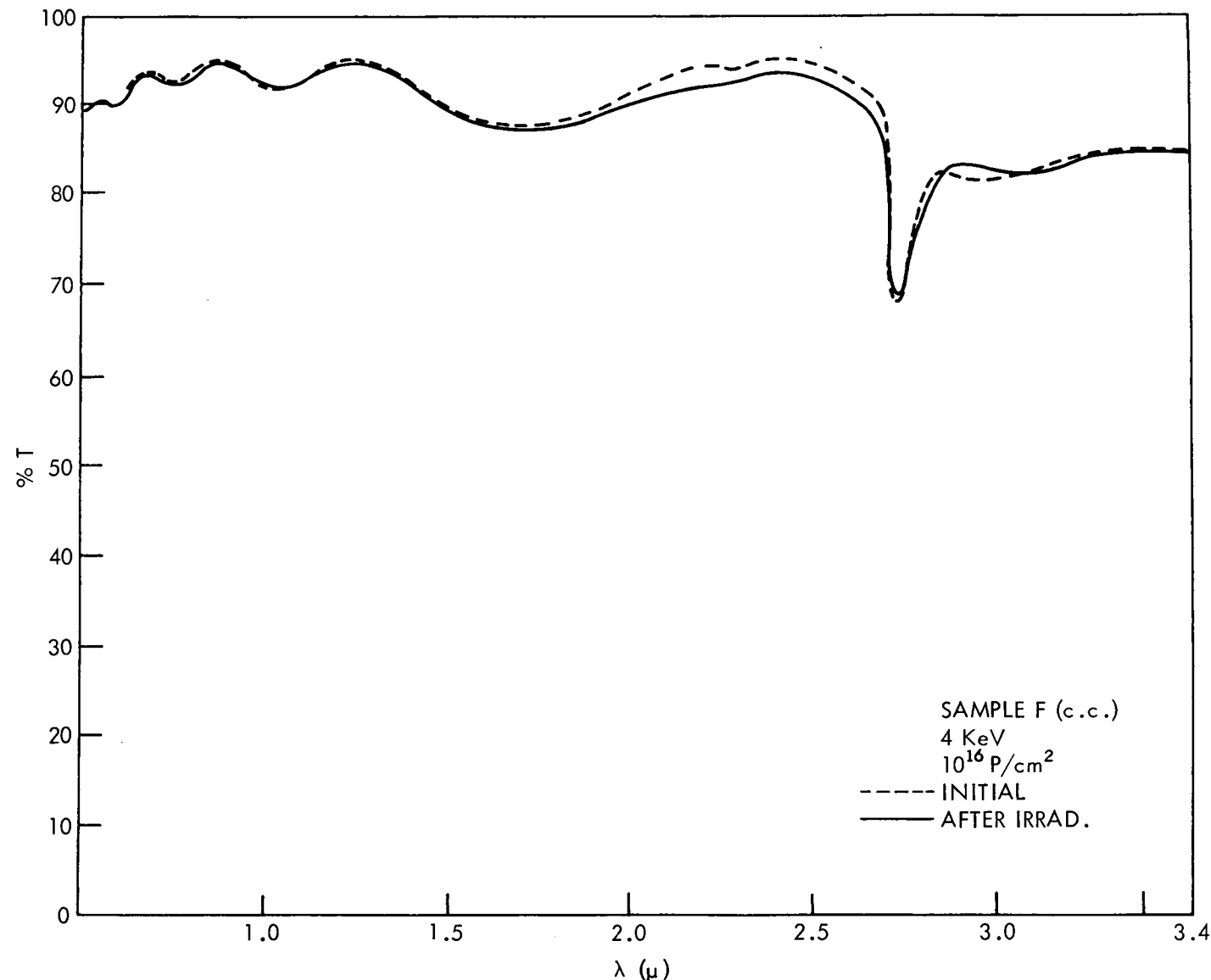


Figure 30.

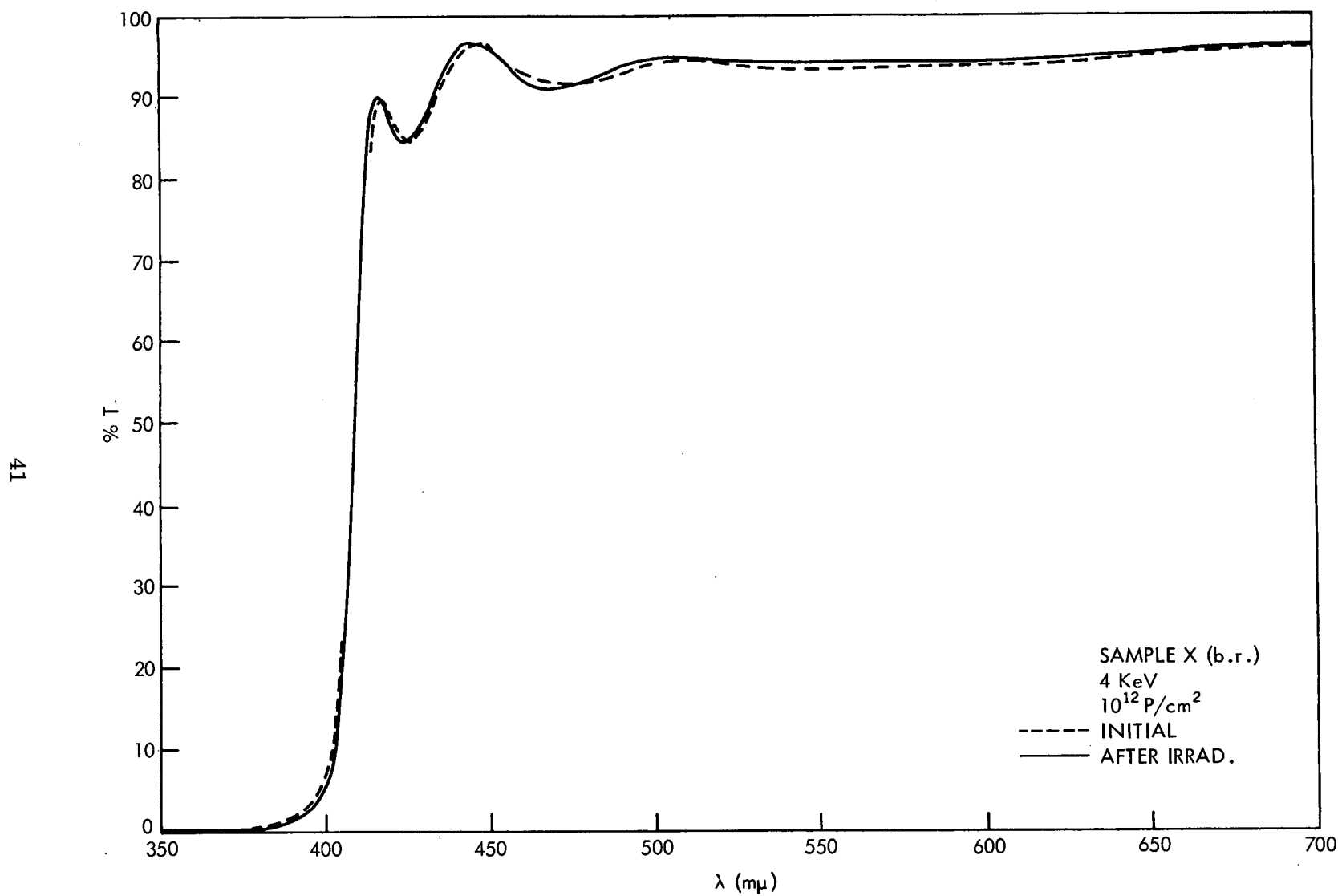


Figure 31.

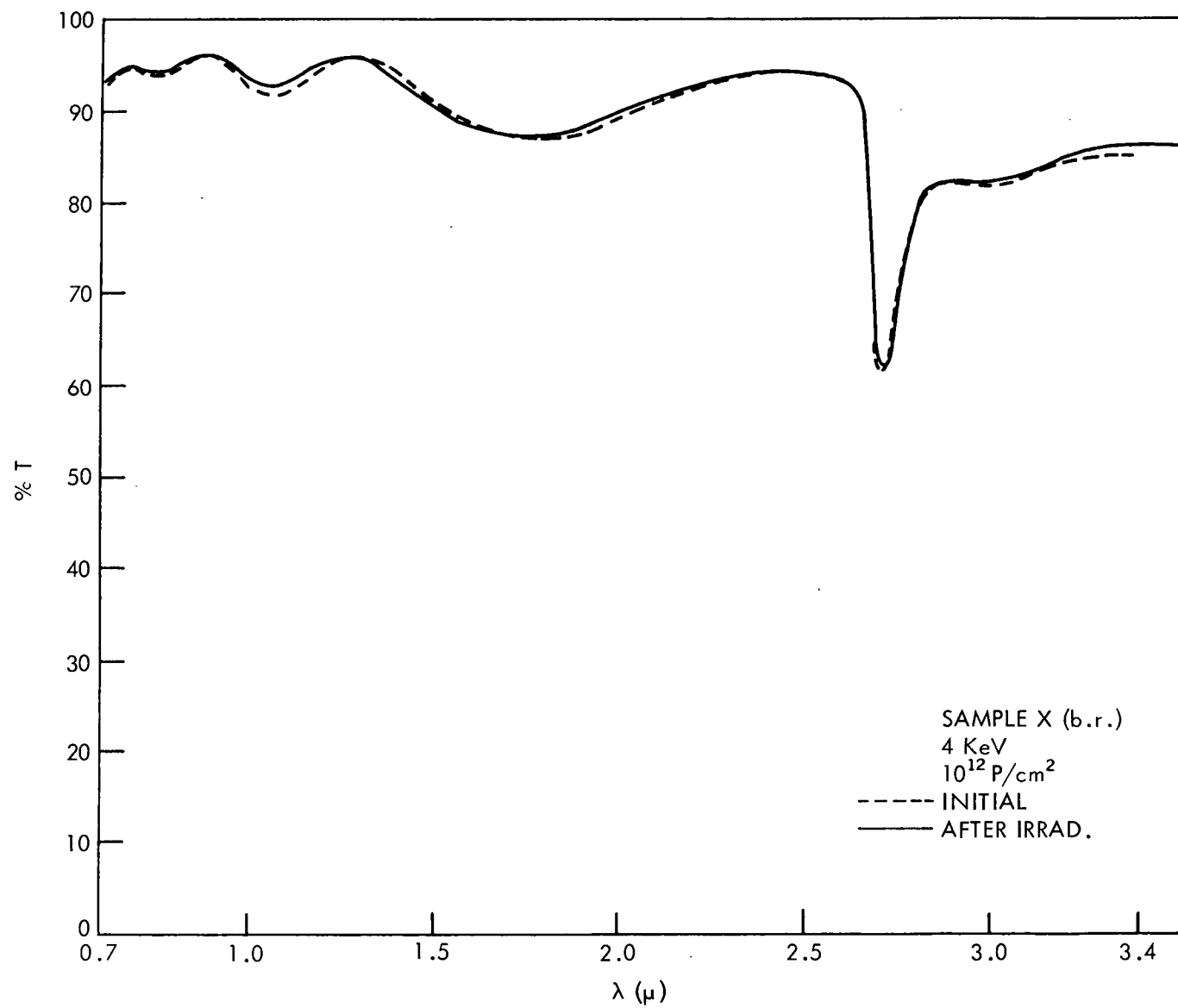


Figure 32.

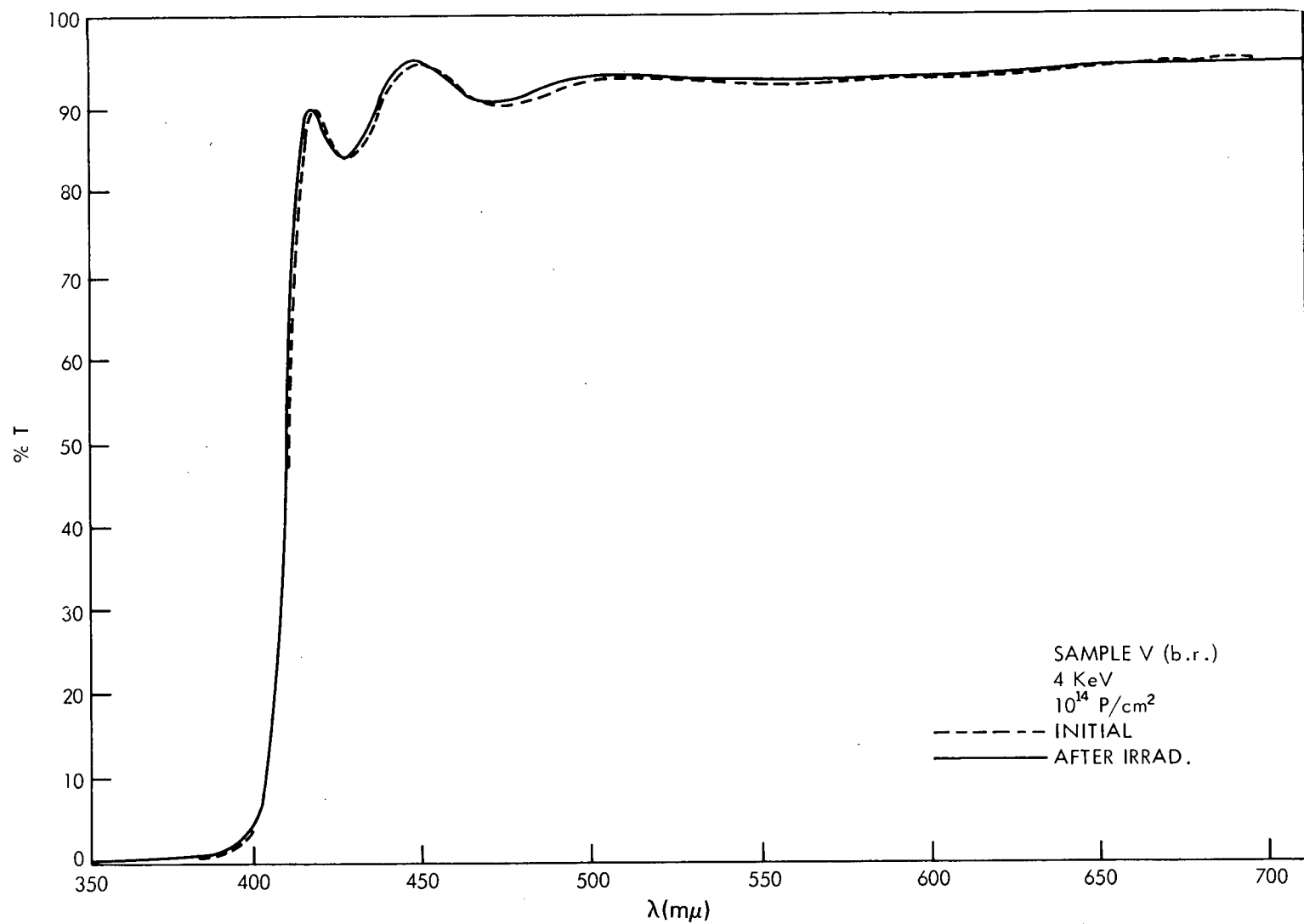


Figure 33.

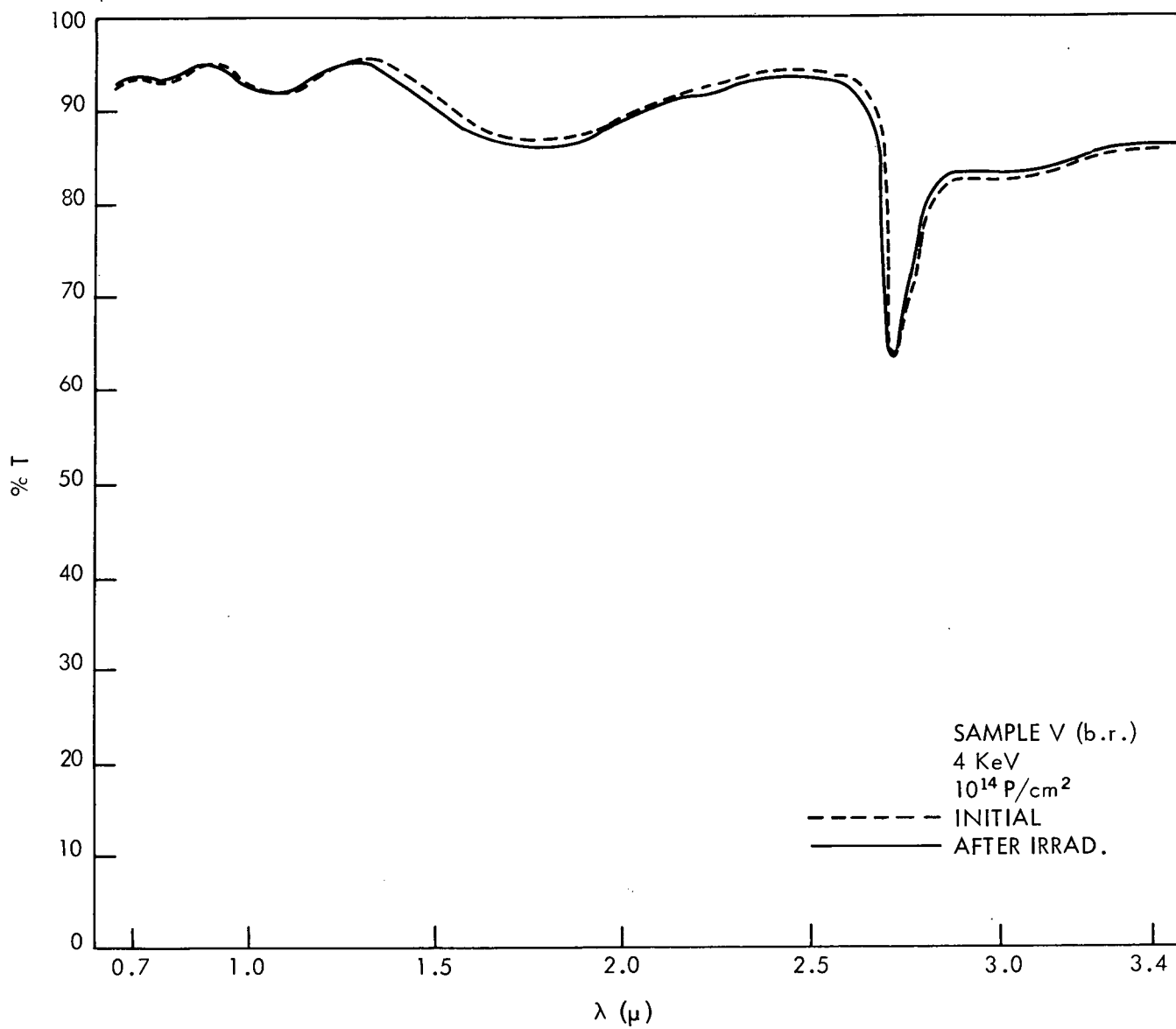


Figure 34.

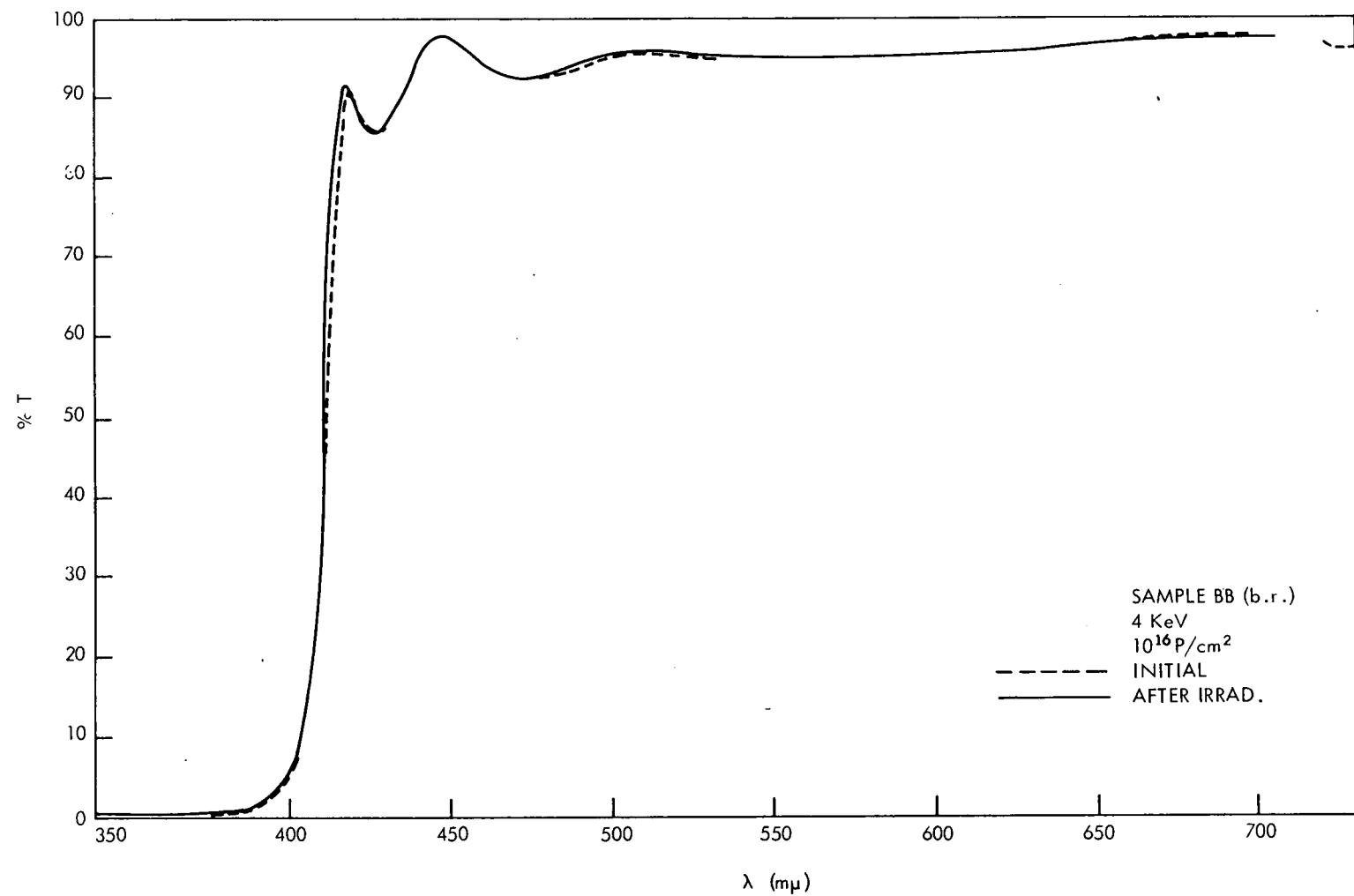


Figure 35.

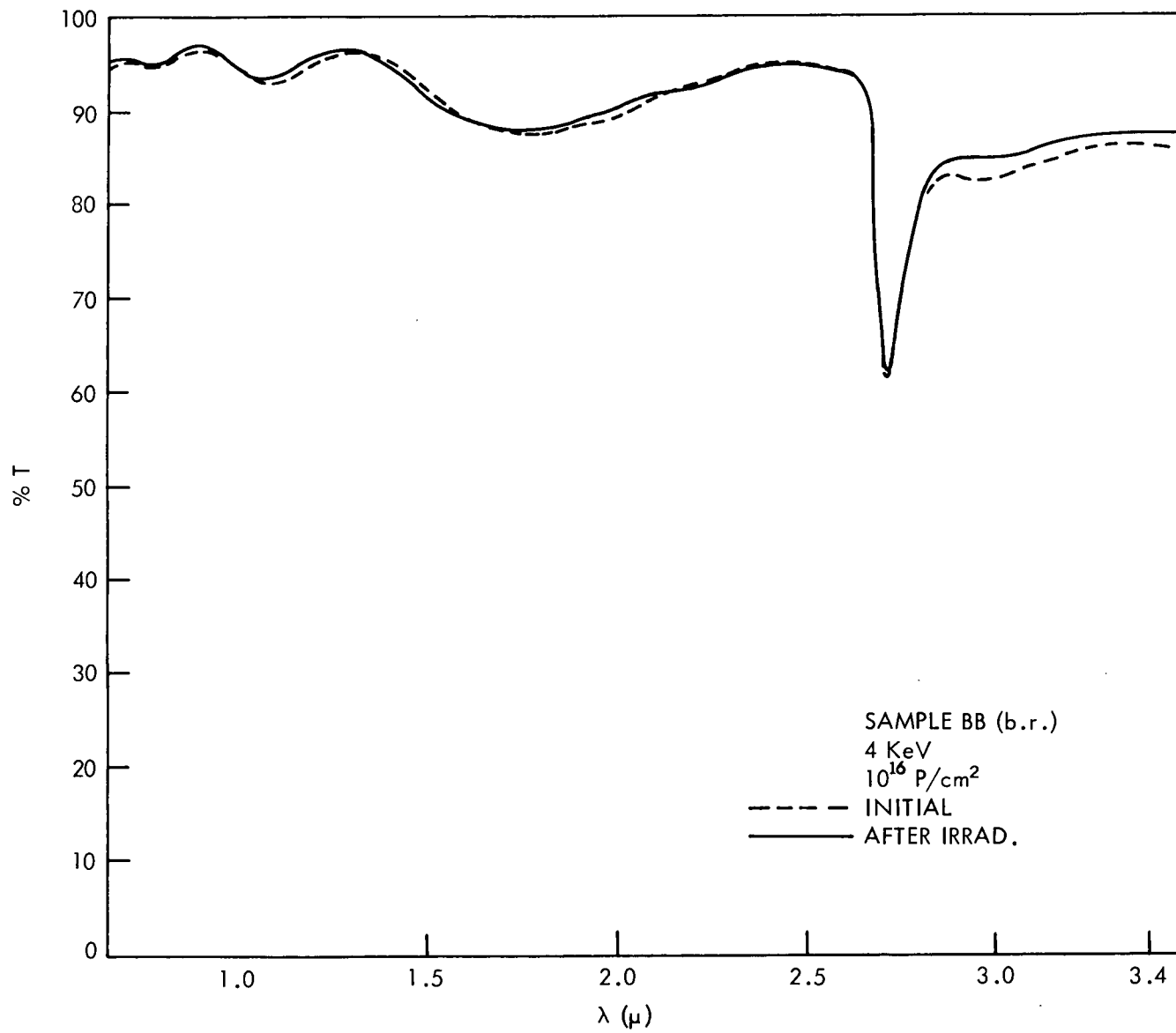


Figure 36.

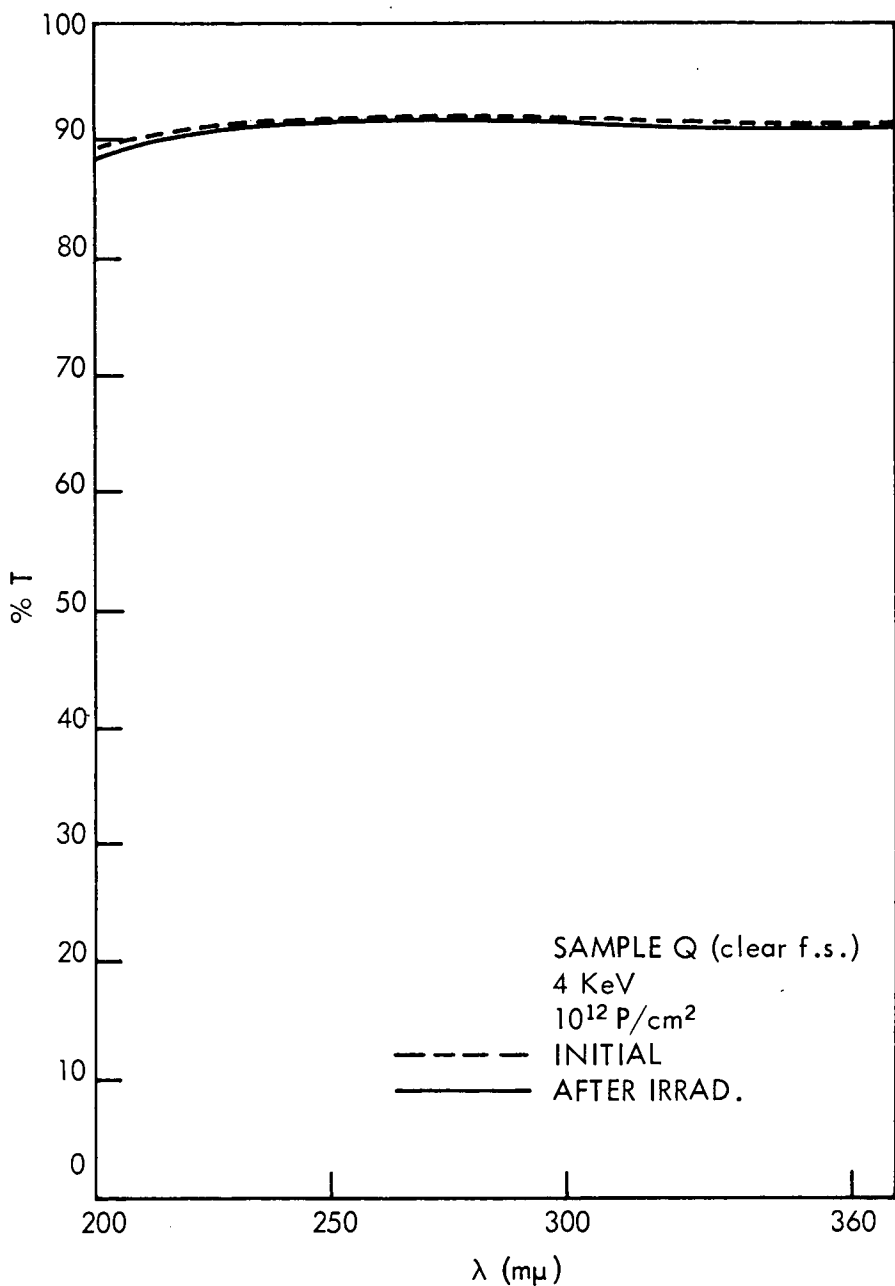


Figure 37.

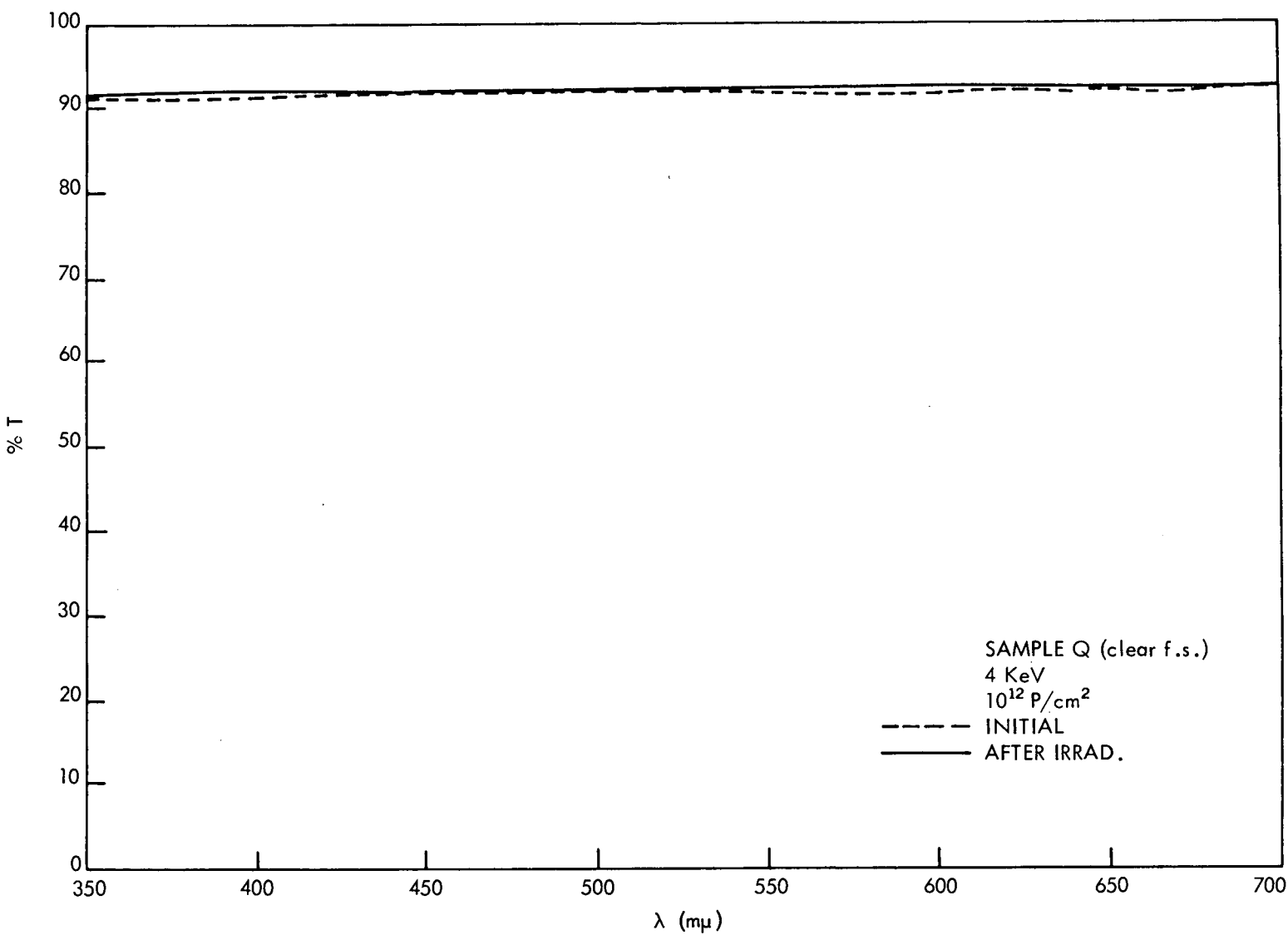


Figure 38.

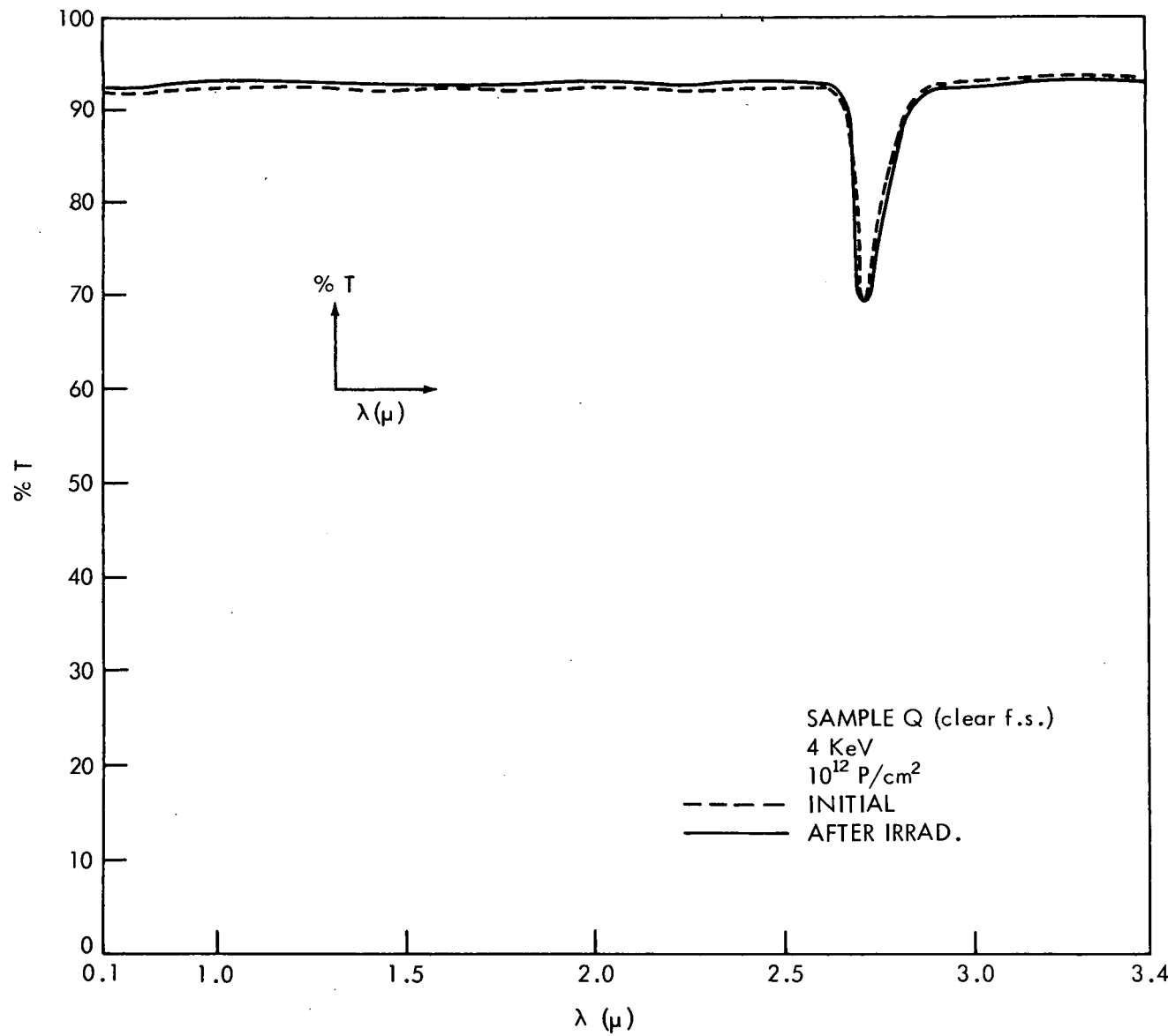


Figure 39.

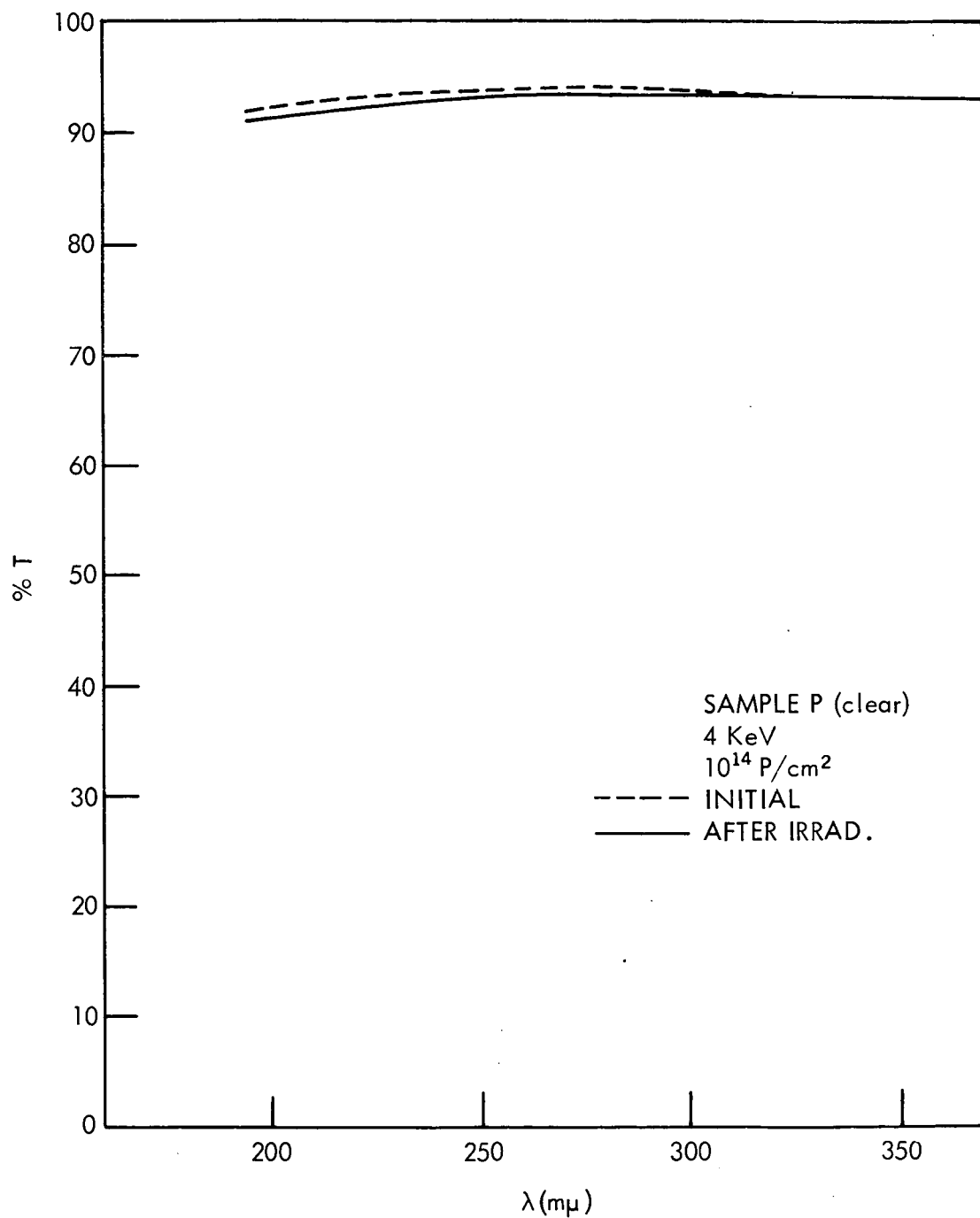


Figure 40.

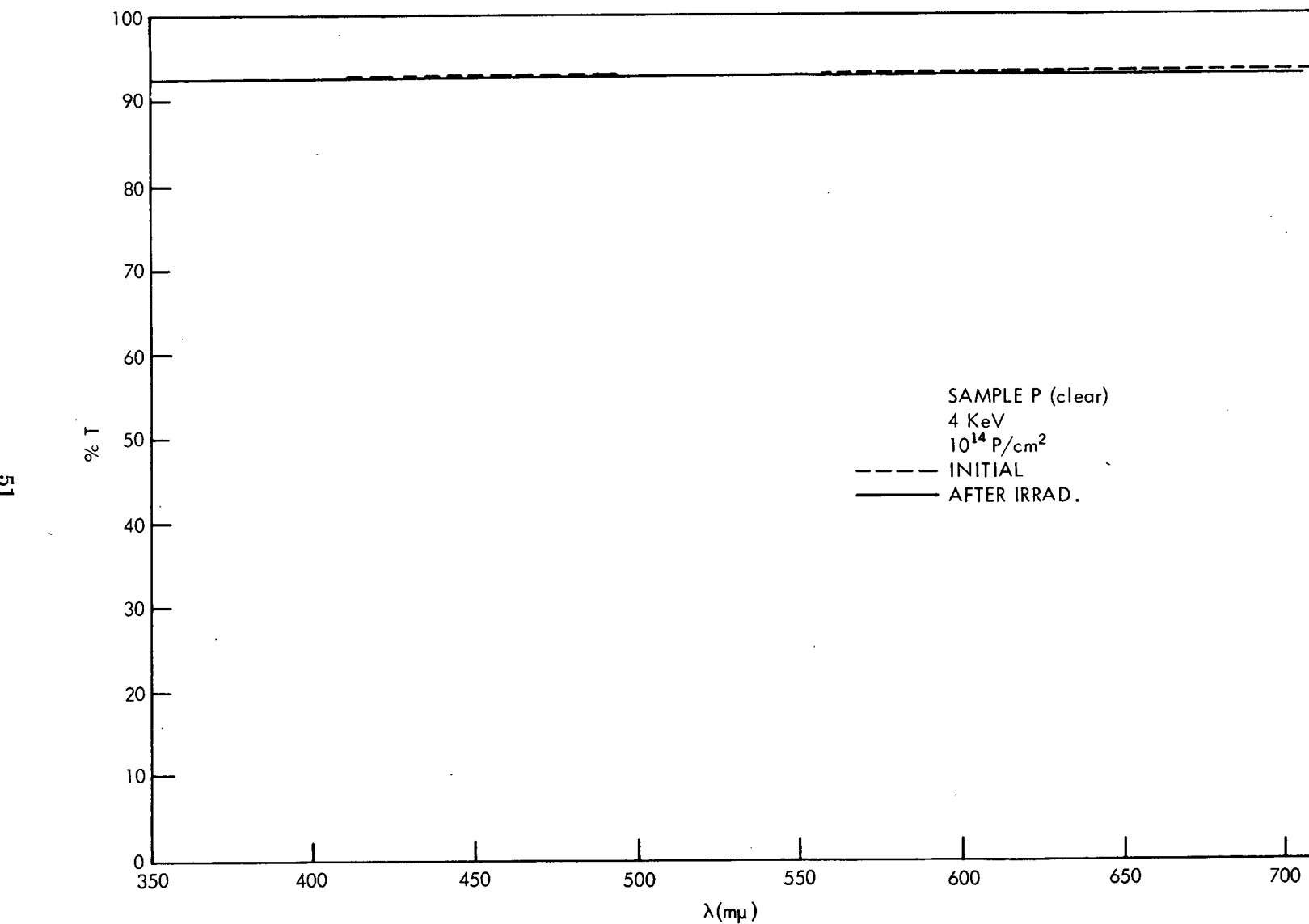


Figure 41.

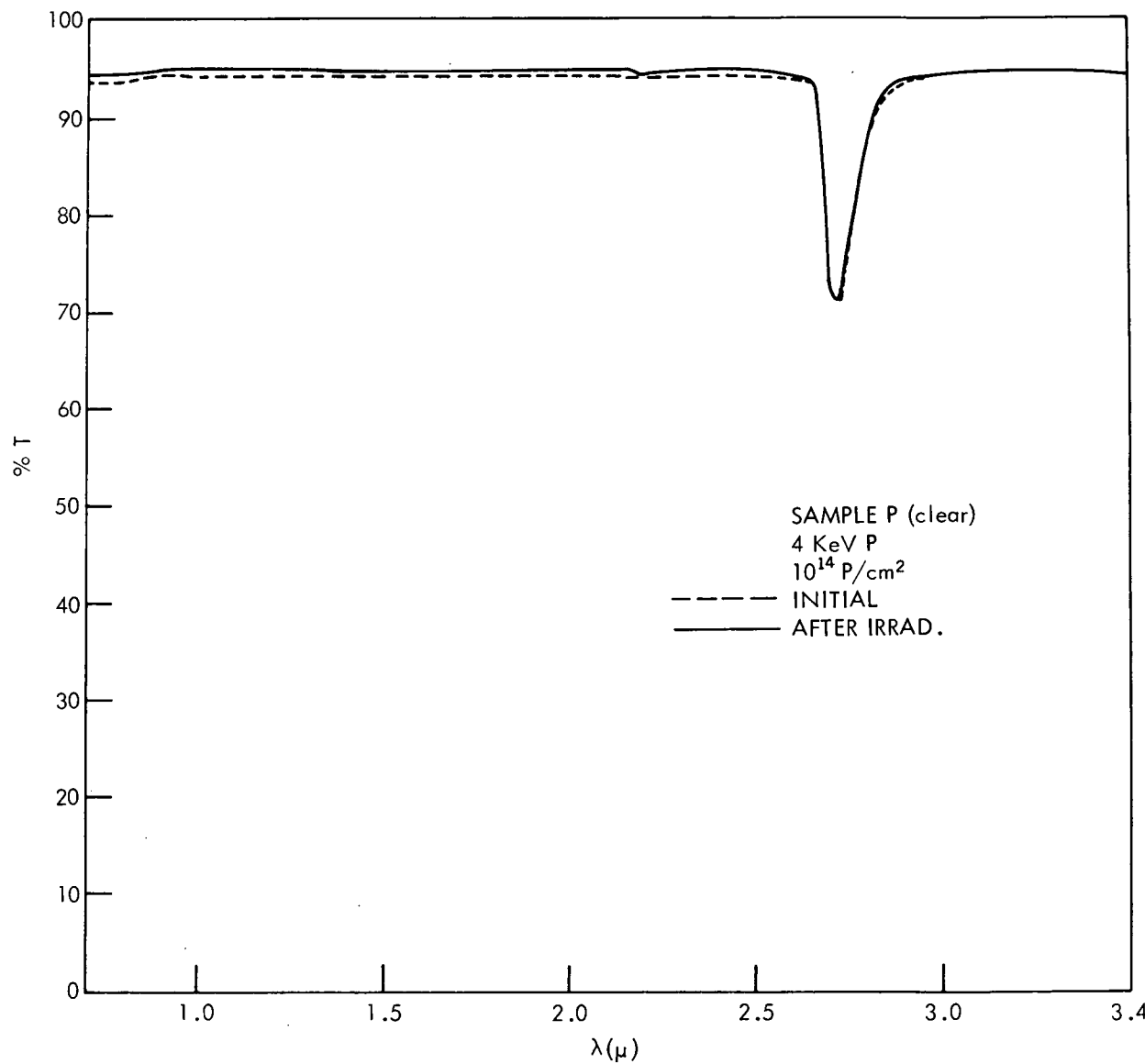


Figure 42.

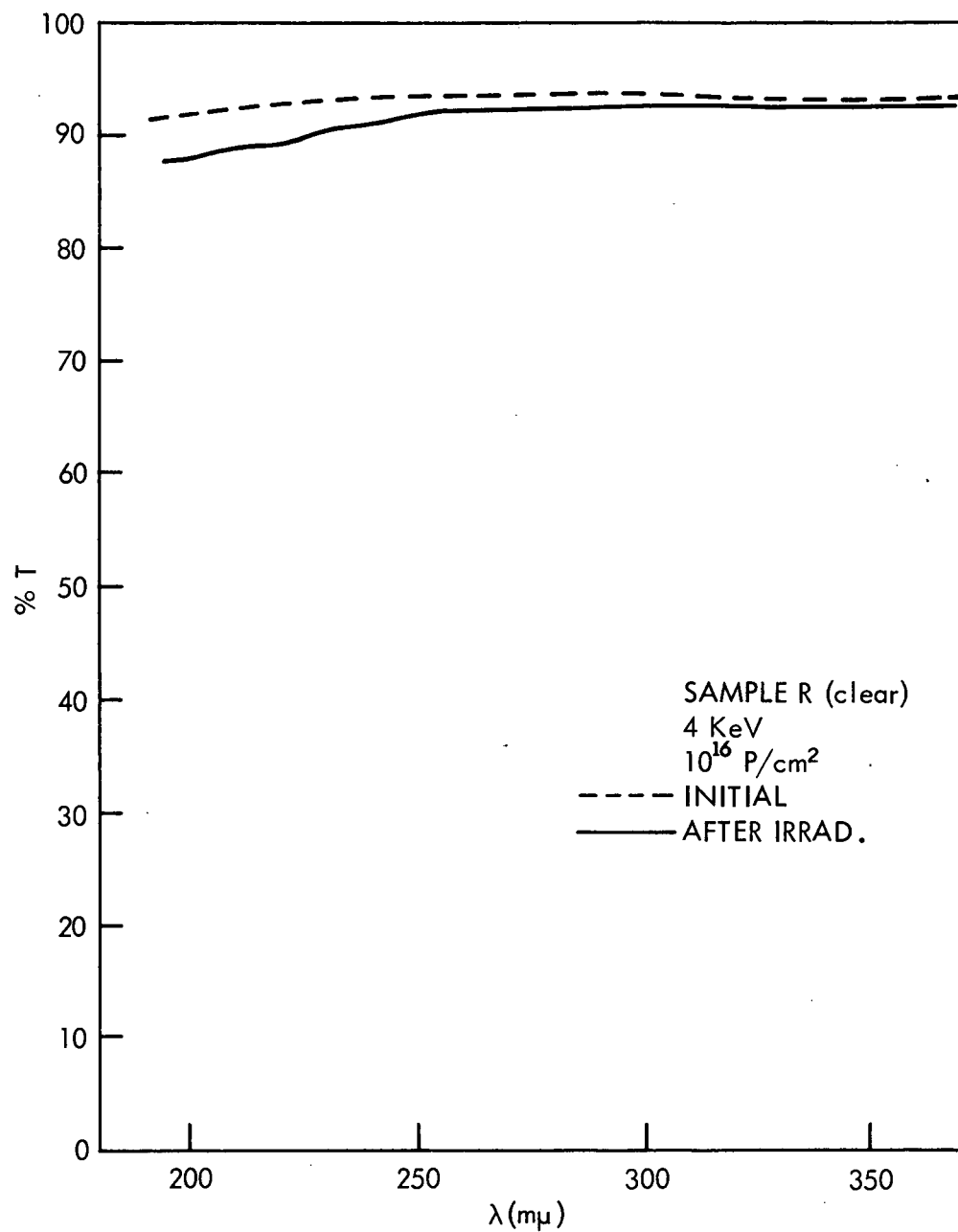


Figure 43.

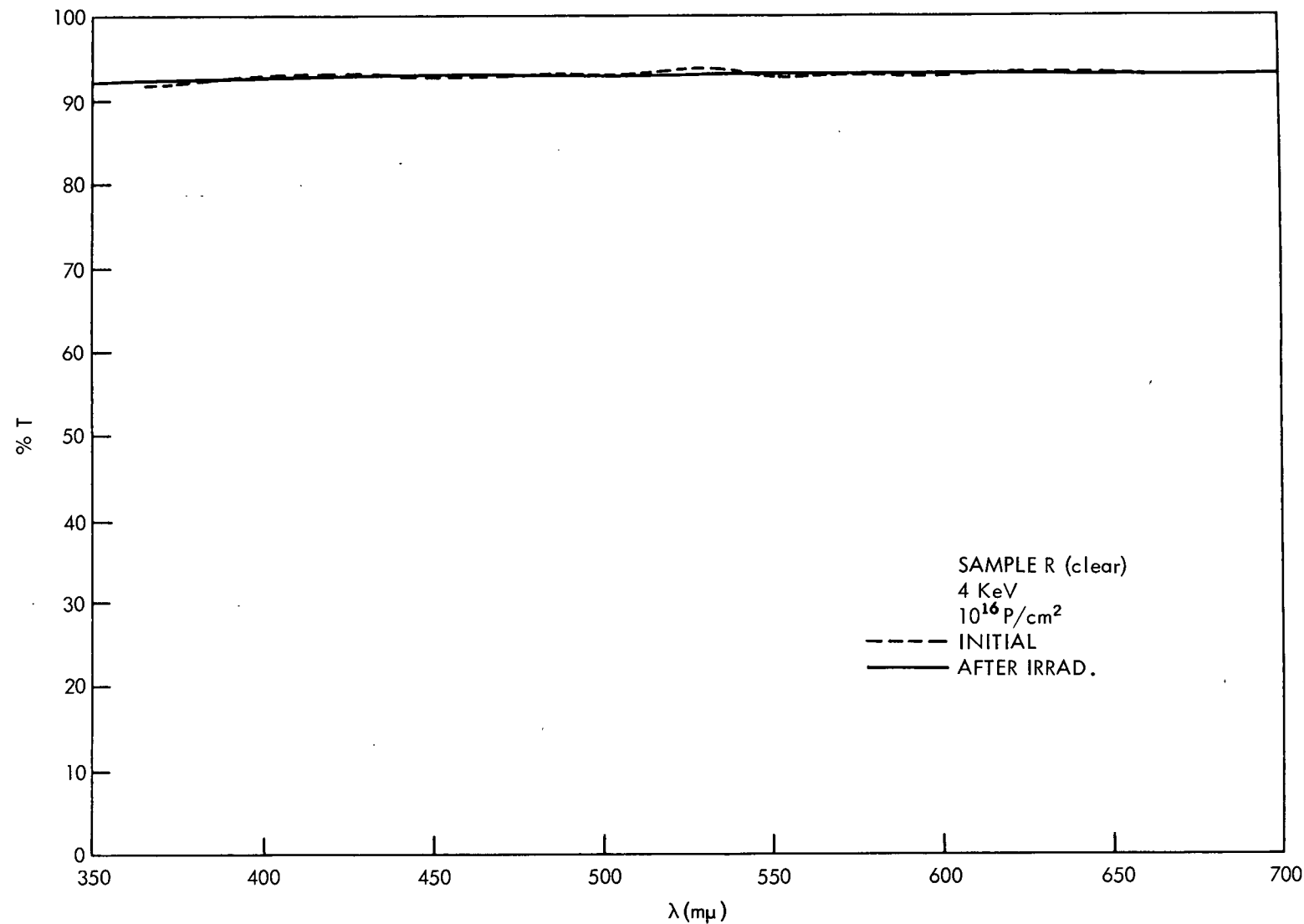


Figure 44.

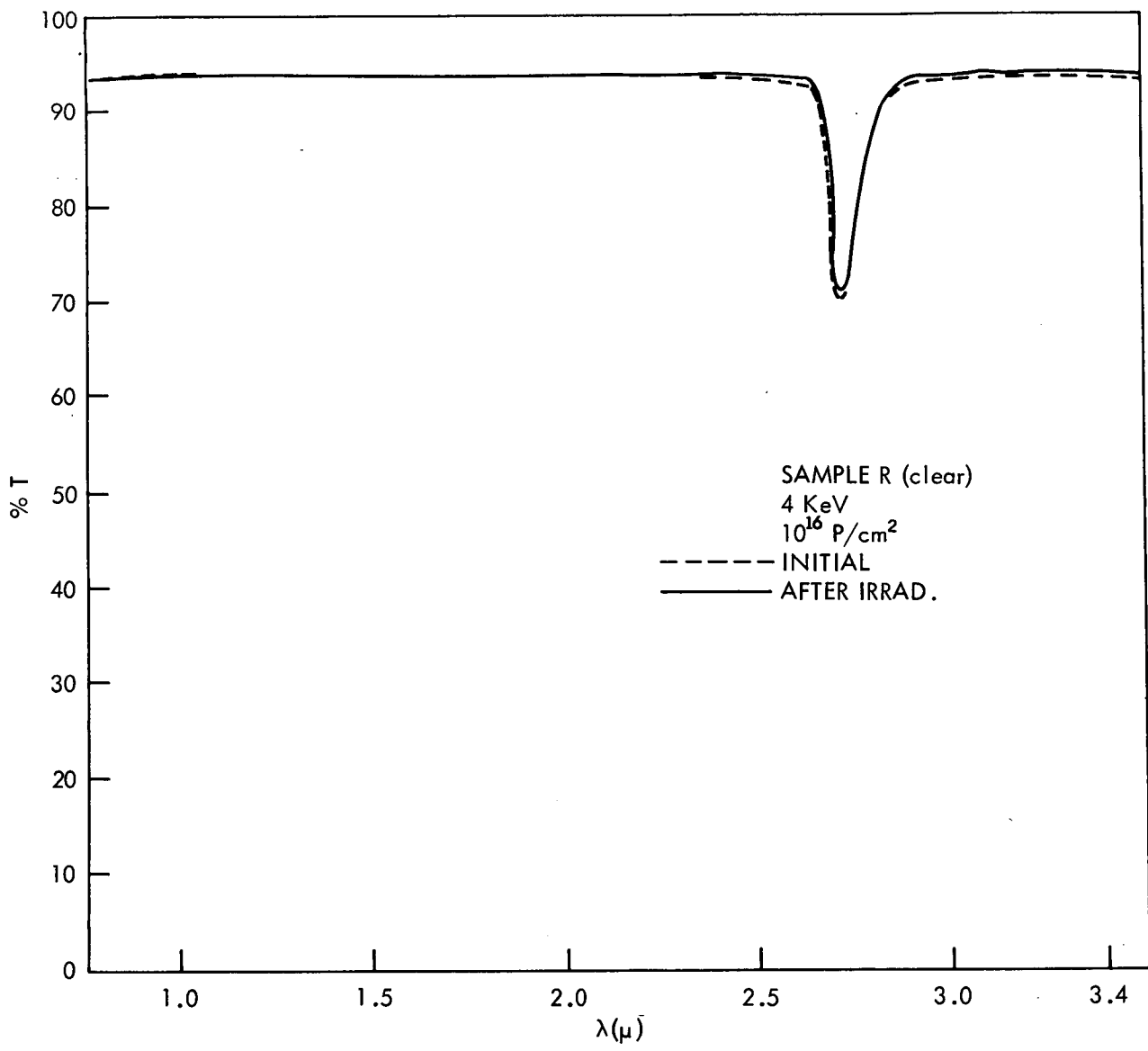


Figure 45.

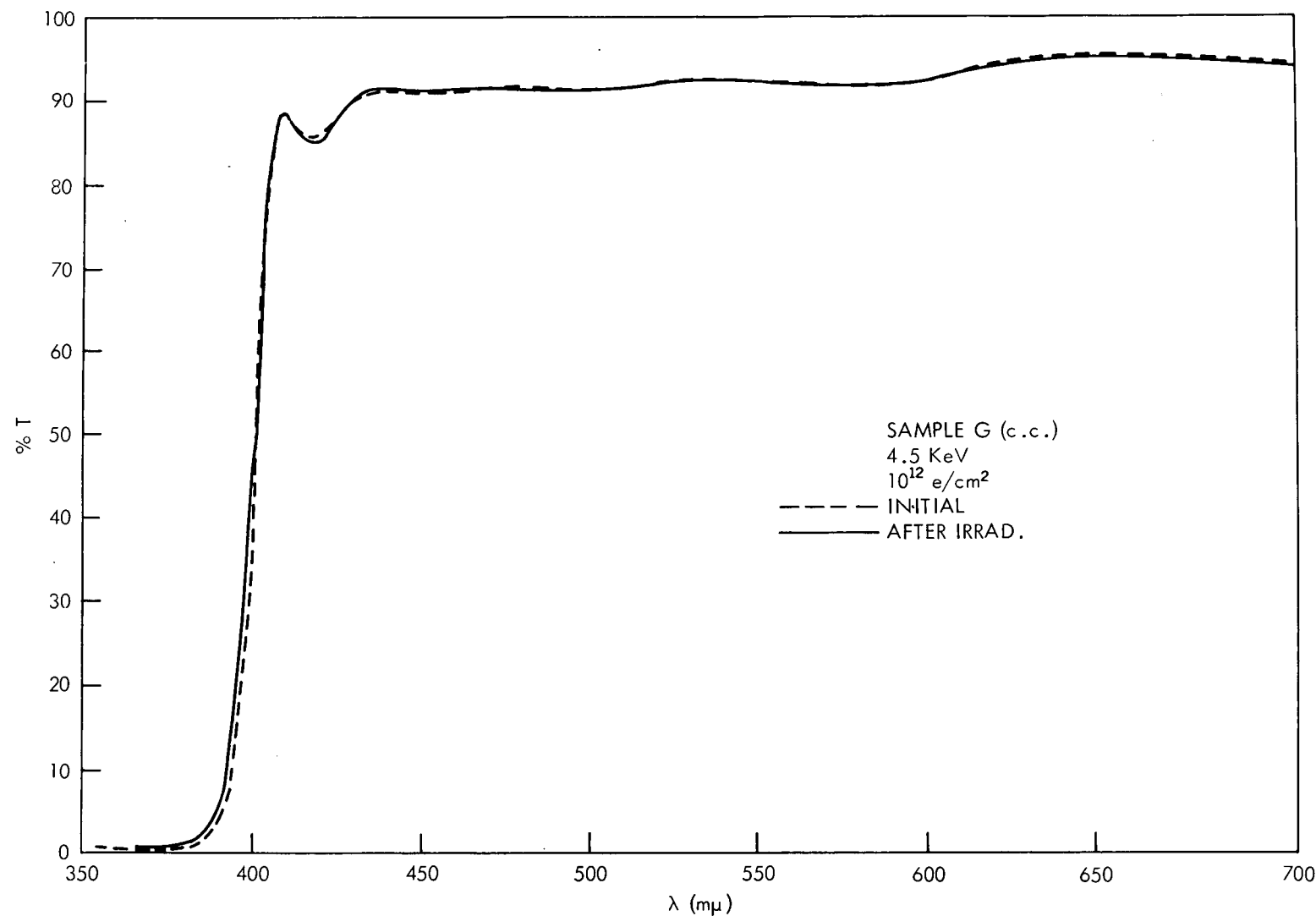


Figure 46.

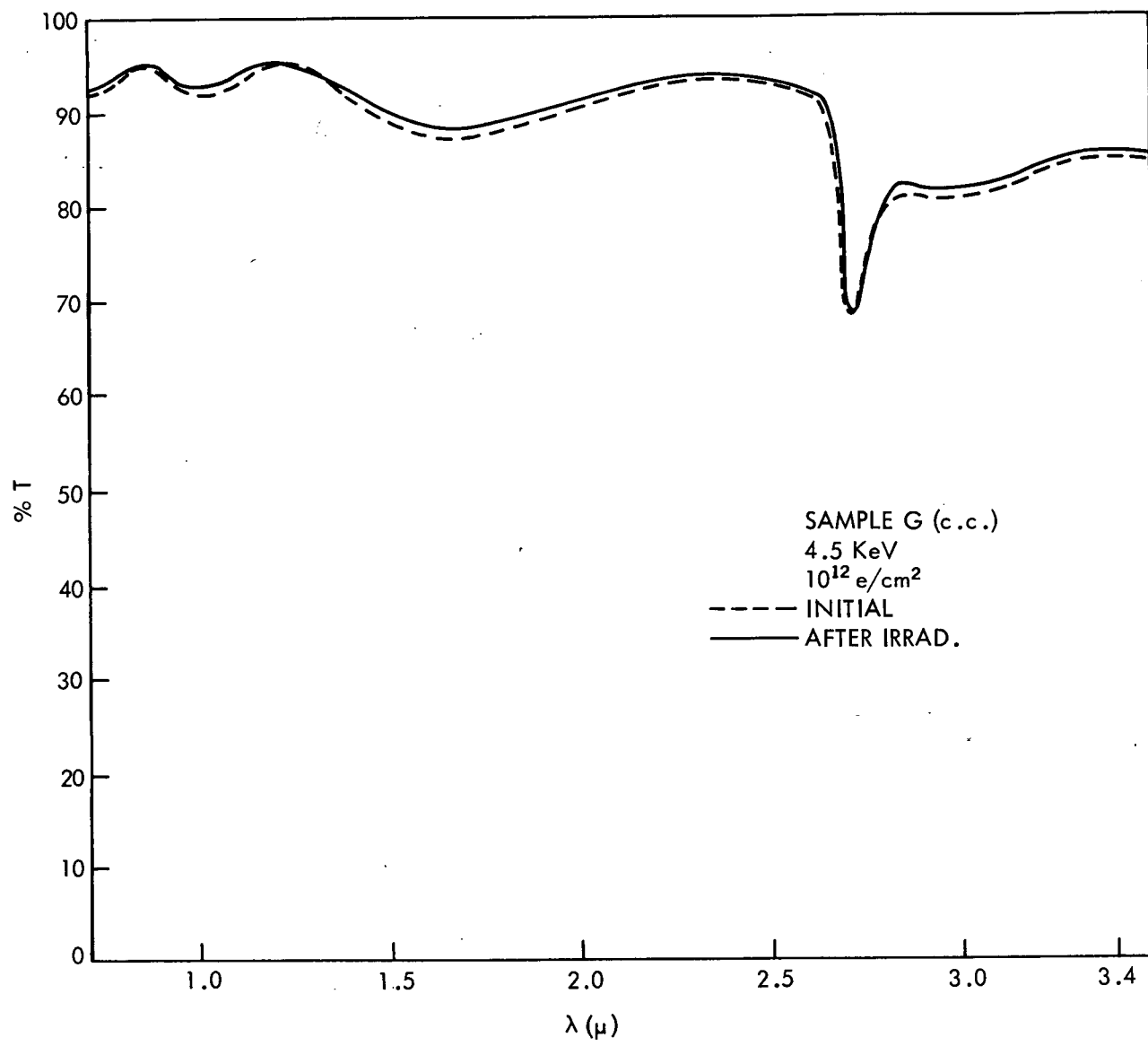


Figure 47.

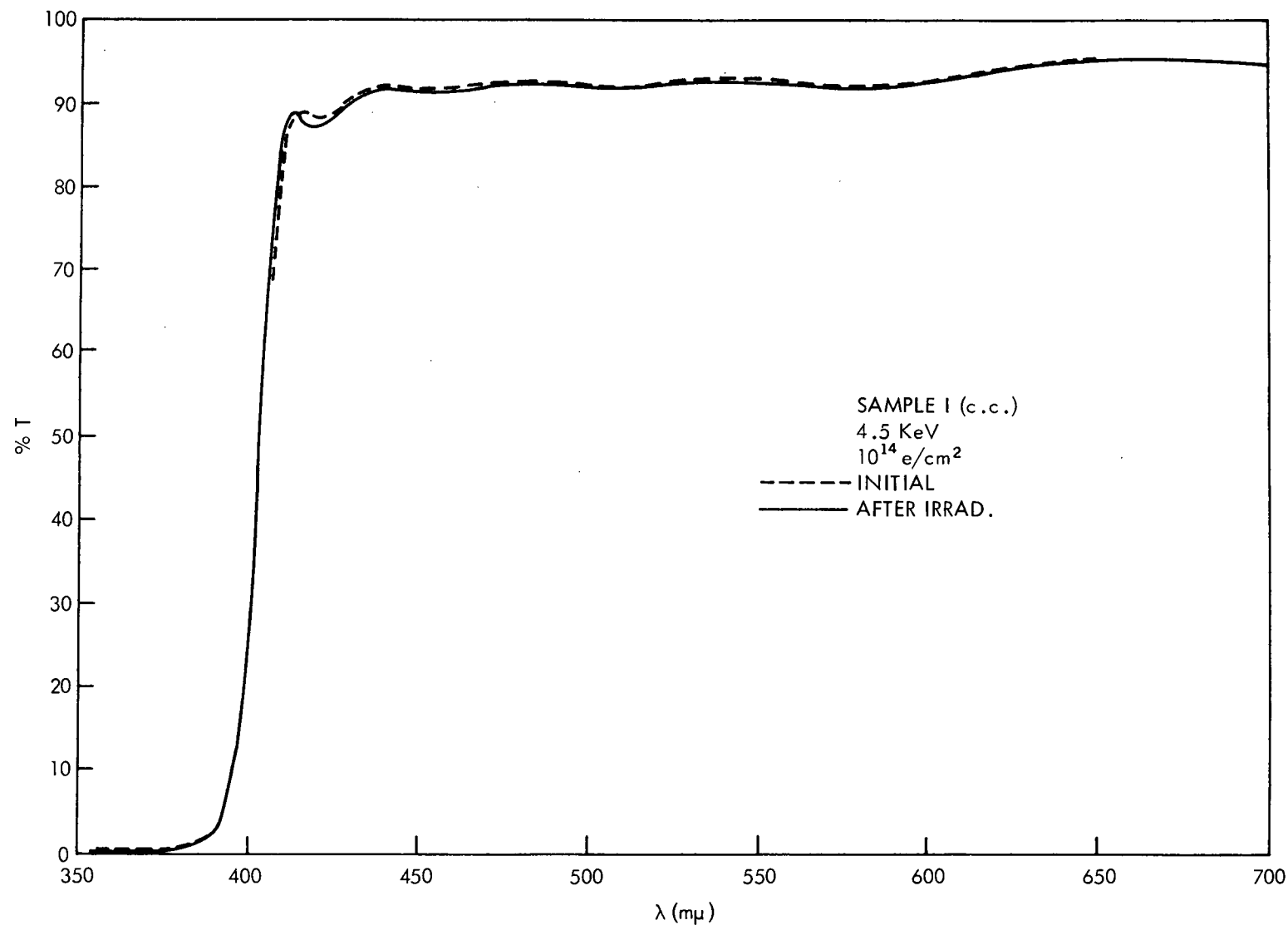


Figure 48.

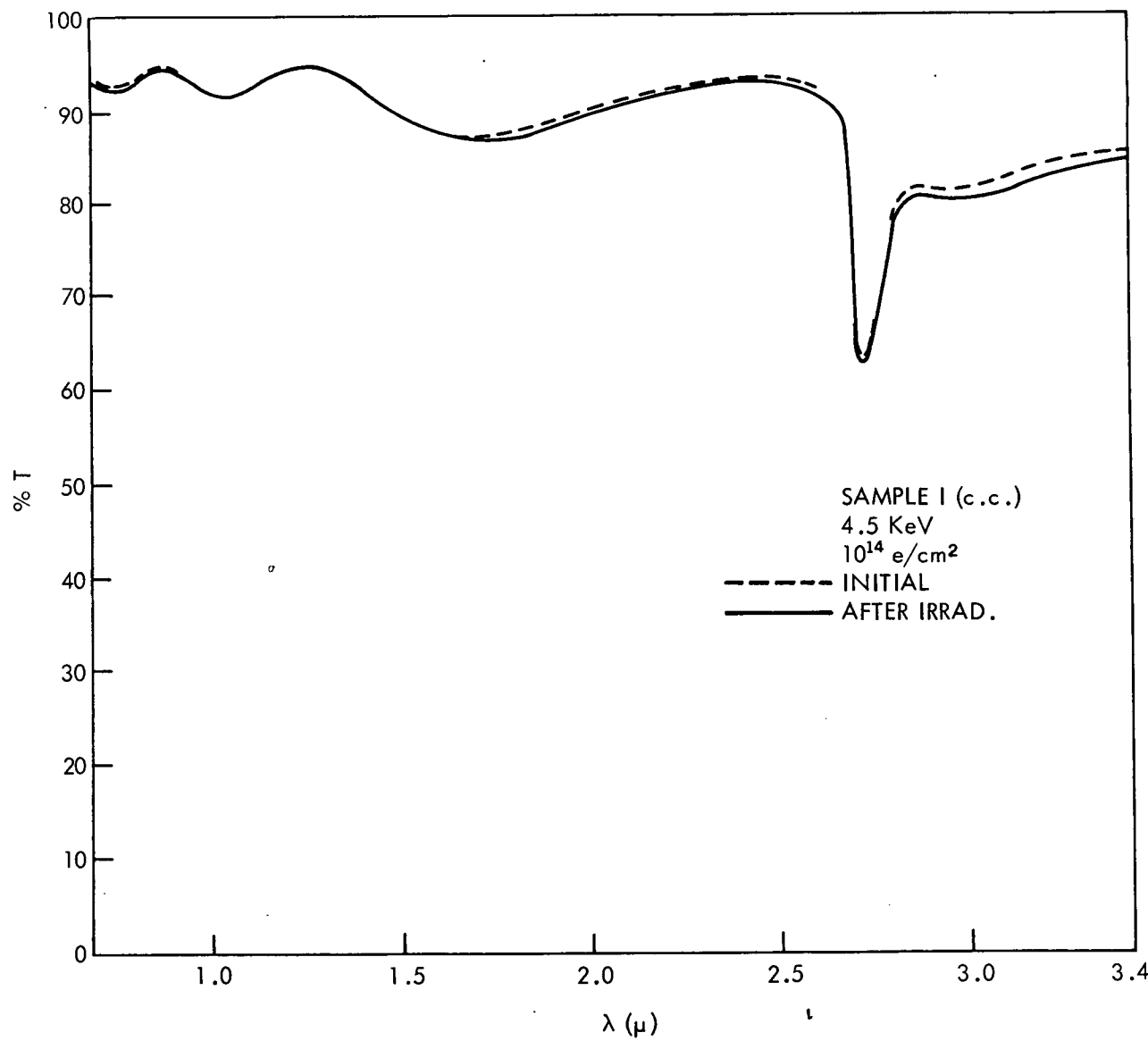


Figure 49.

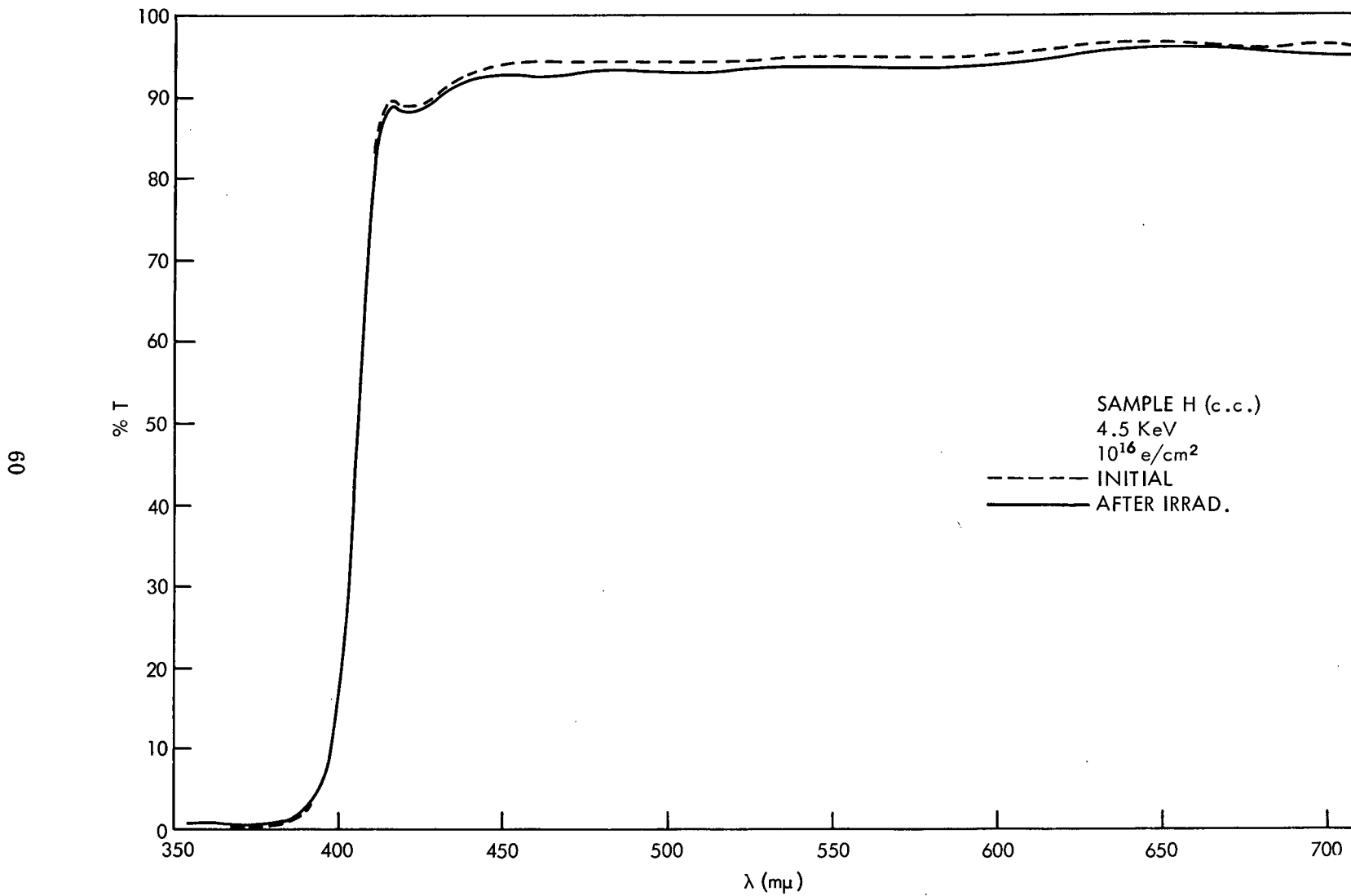


Figure 50.

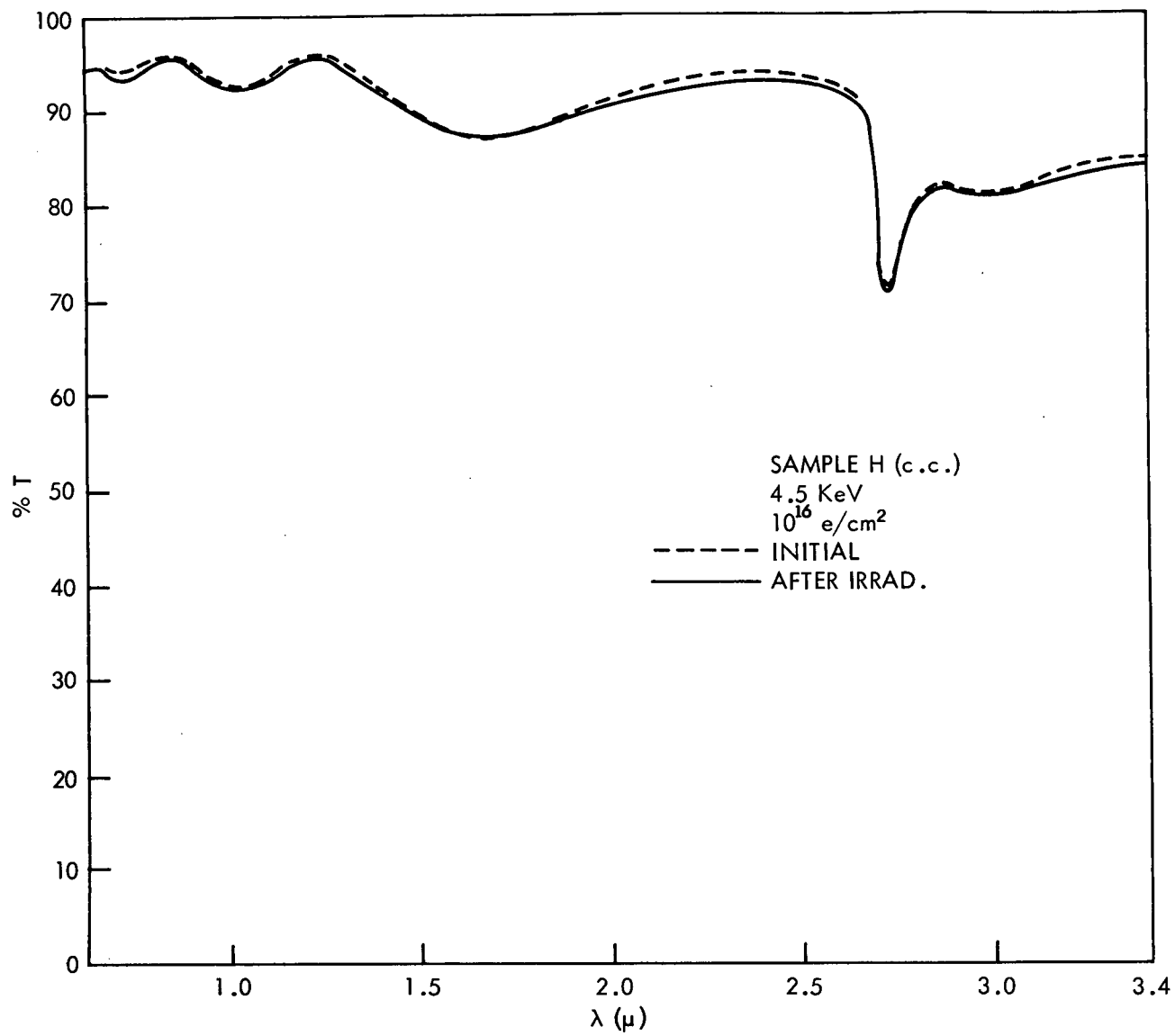


Figure 51.

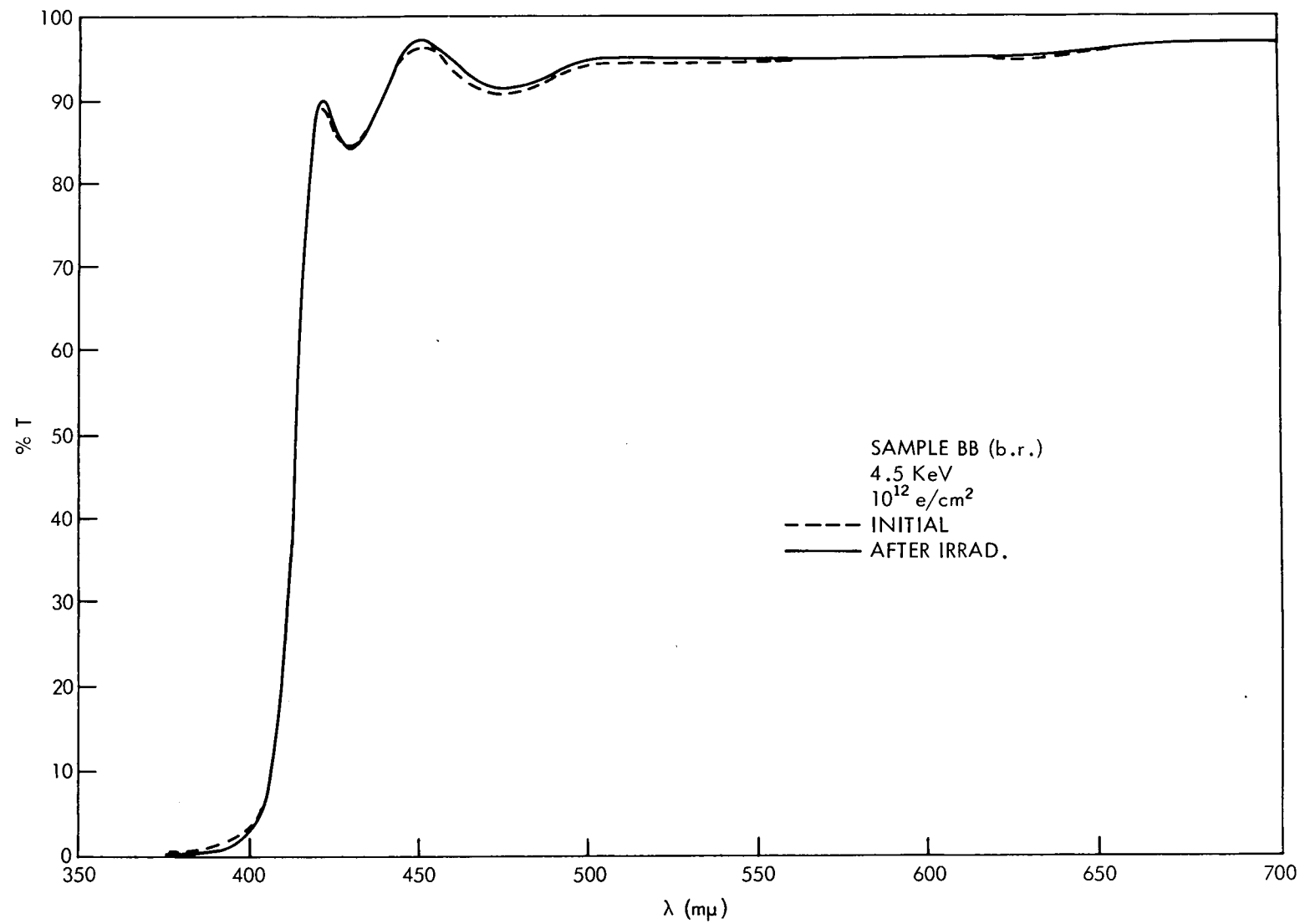


Figure 52.

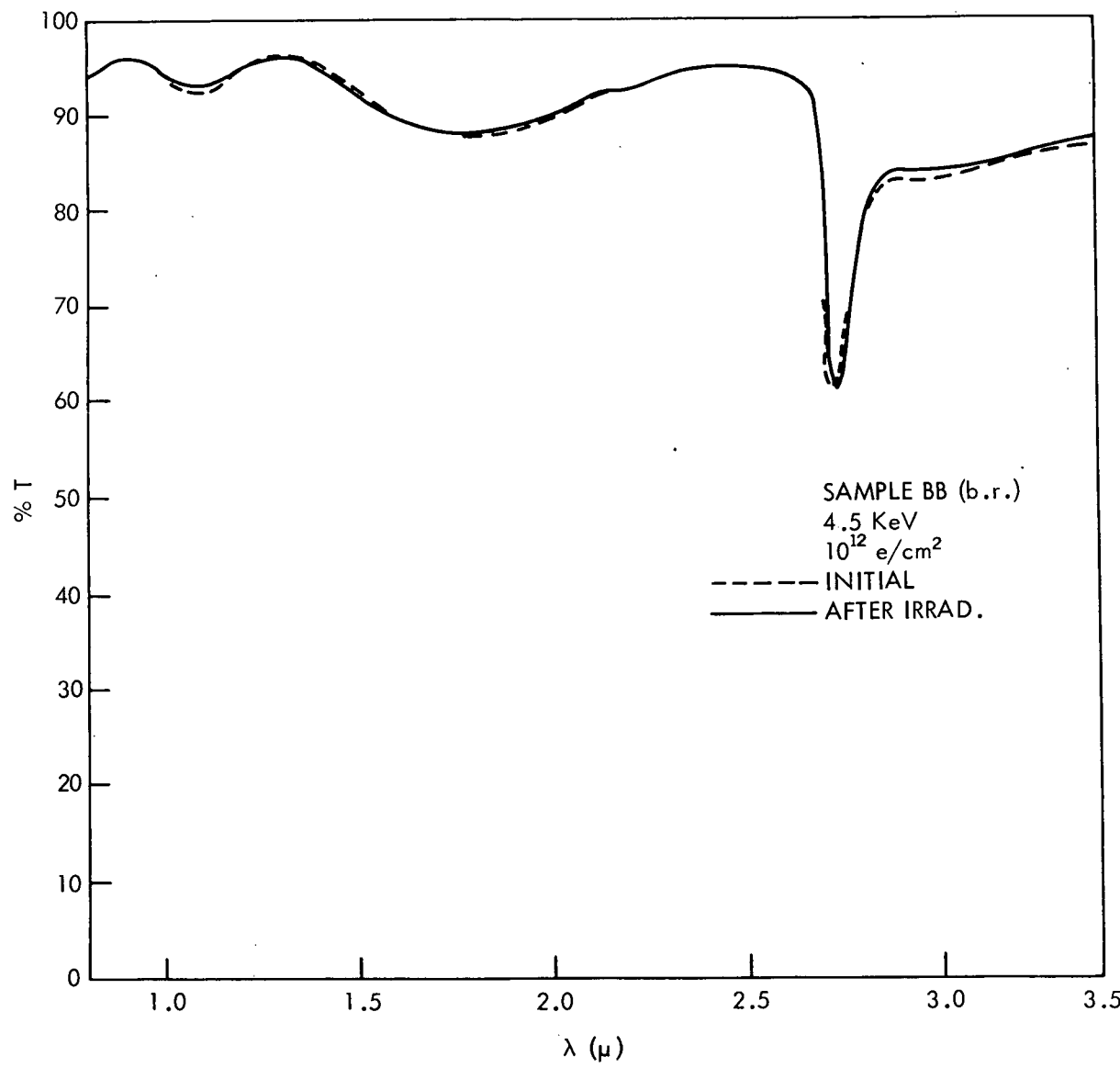


Figure 53.

49

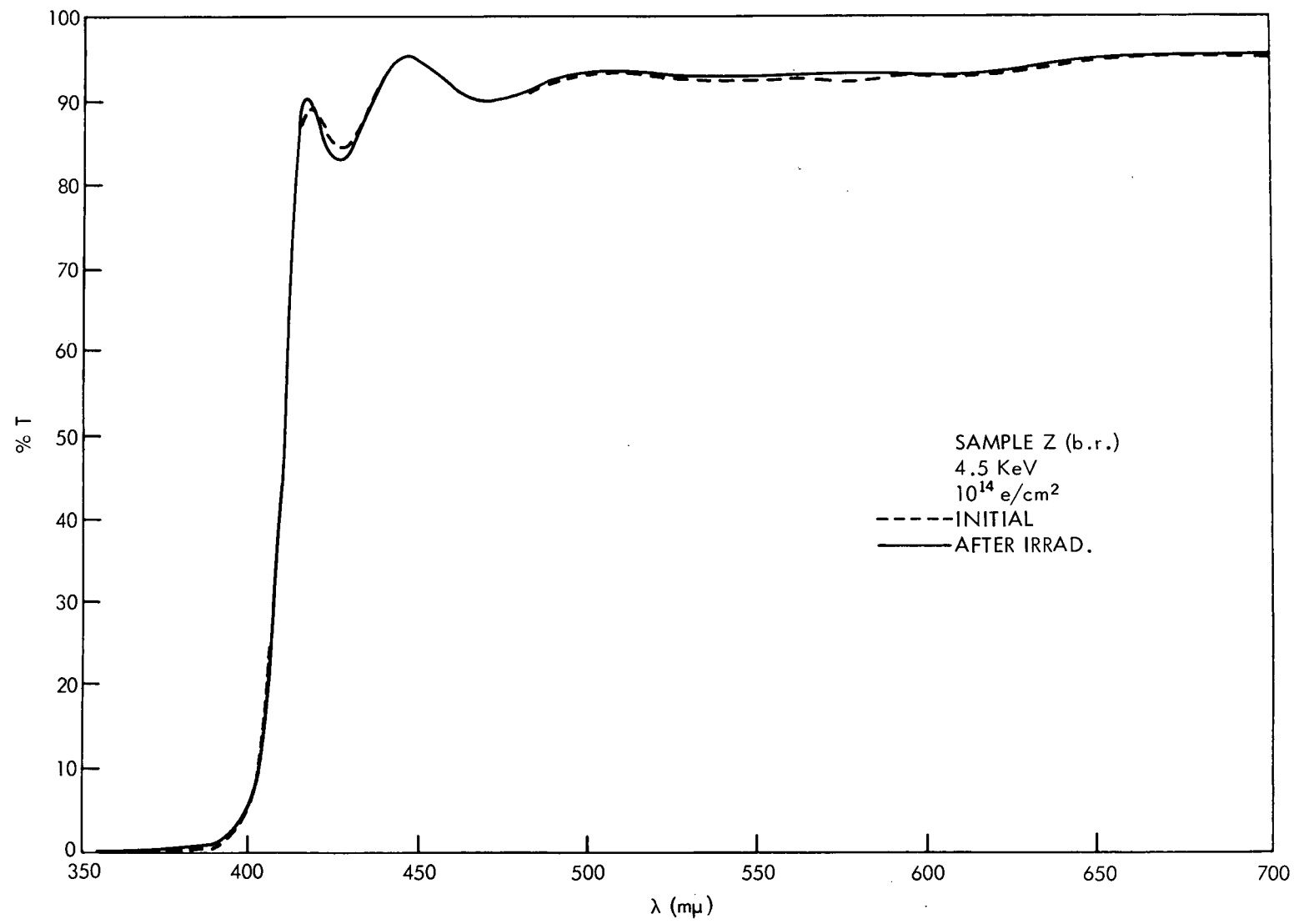


Figure 54.

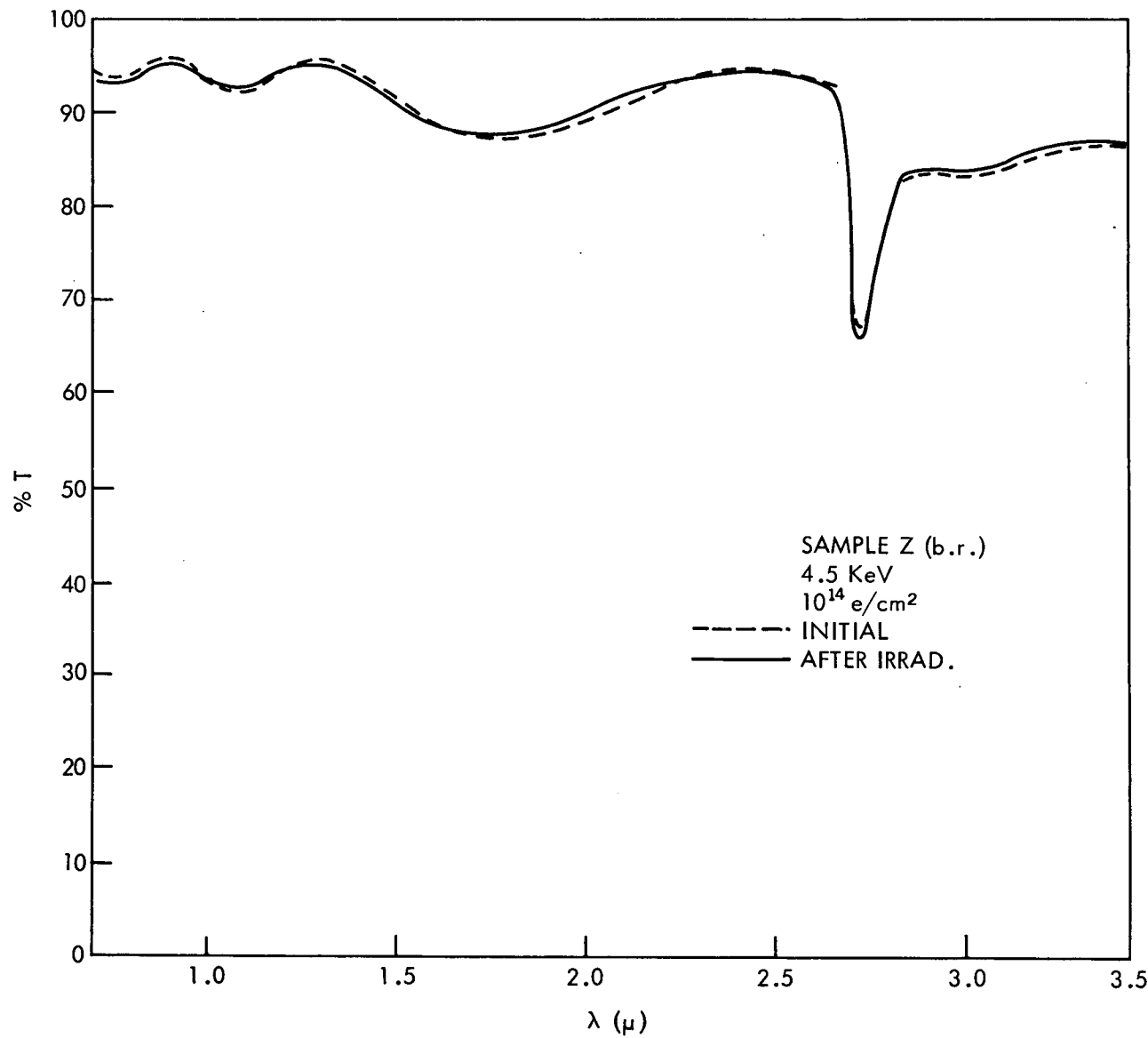


Figure 55.

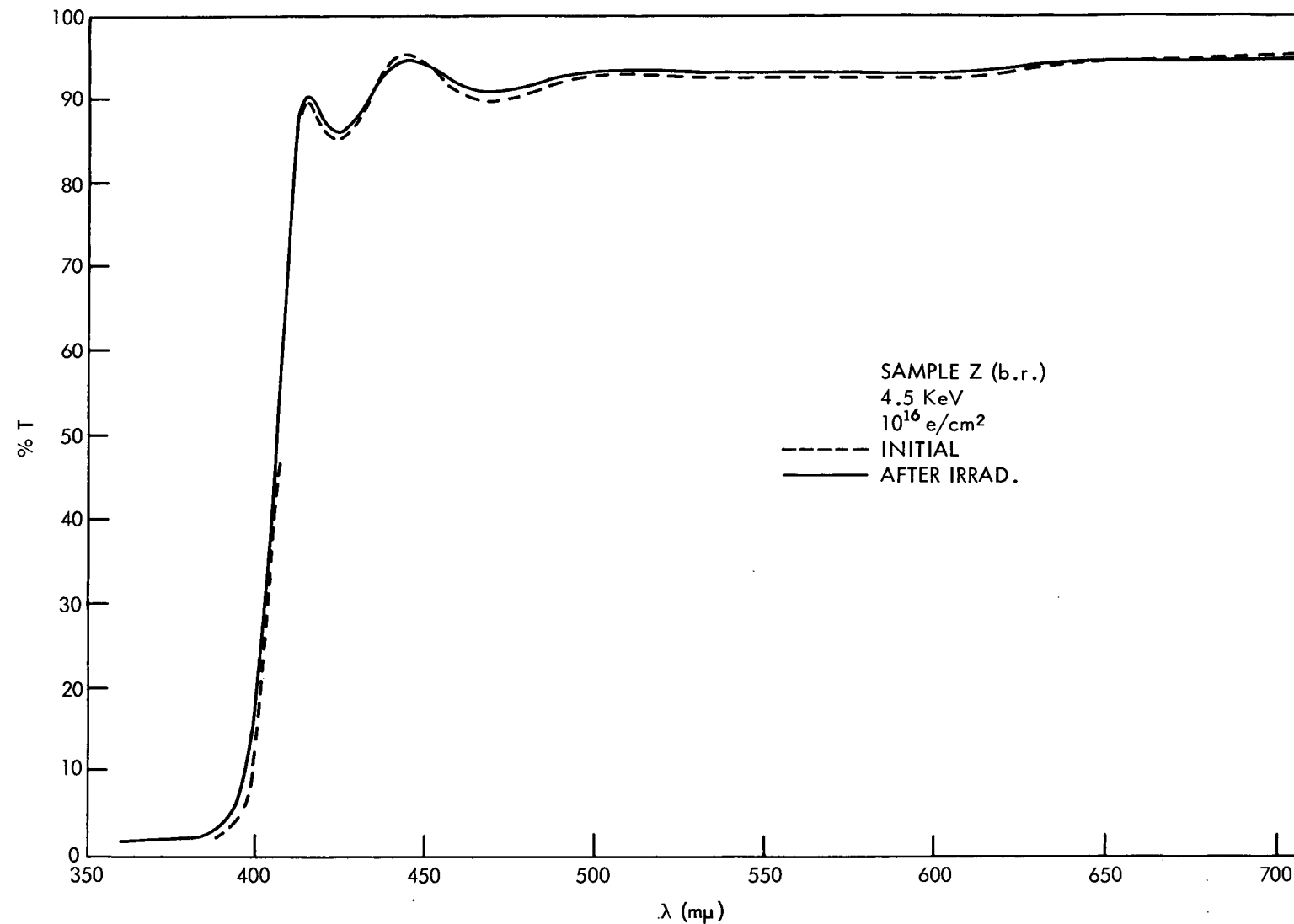


Figure 56.

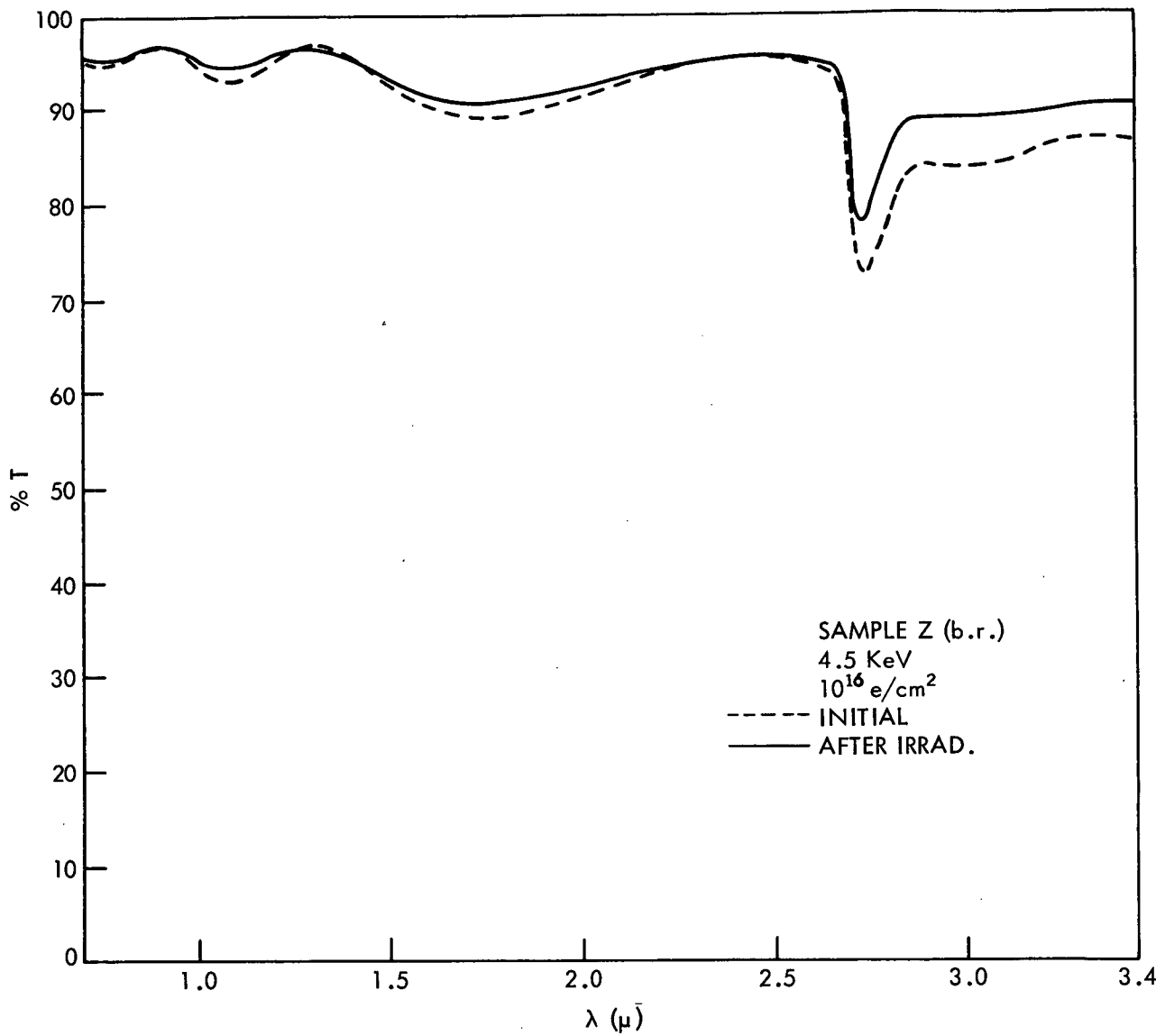


Figure 57.

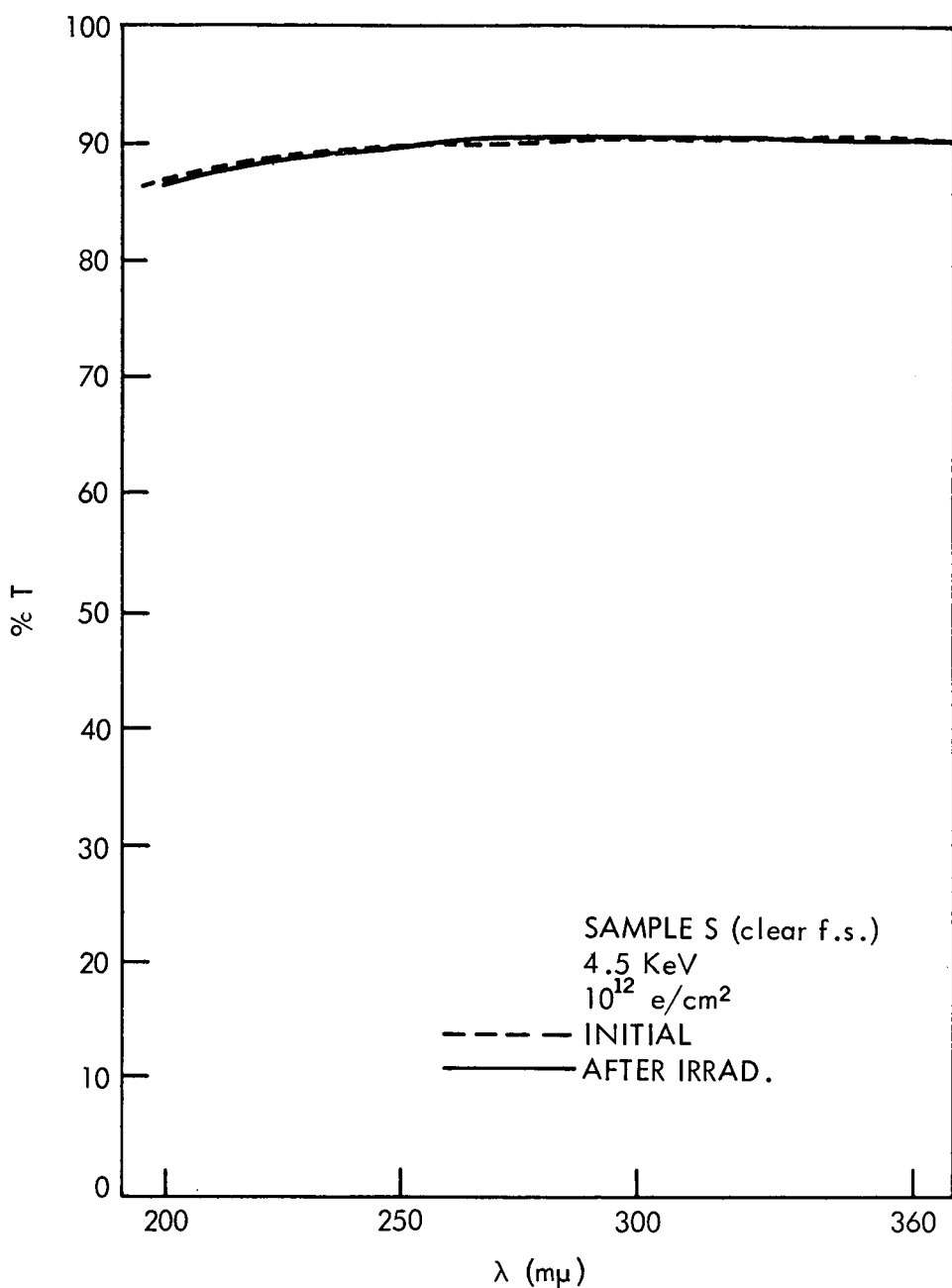


Figure 58.

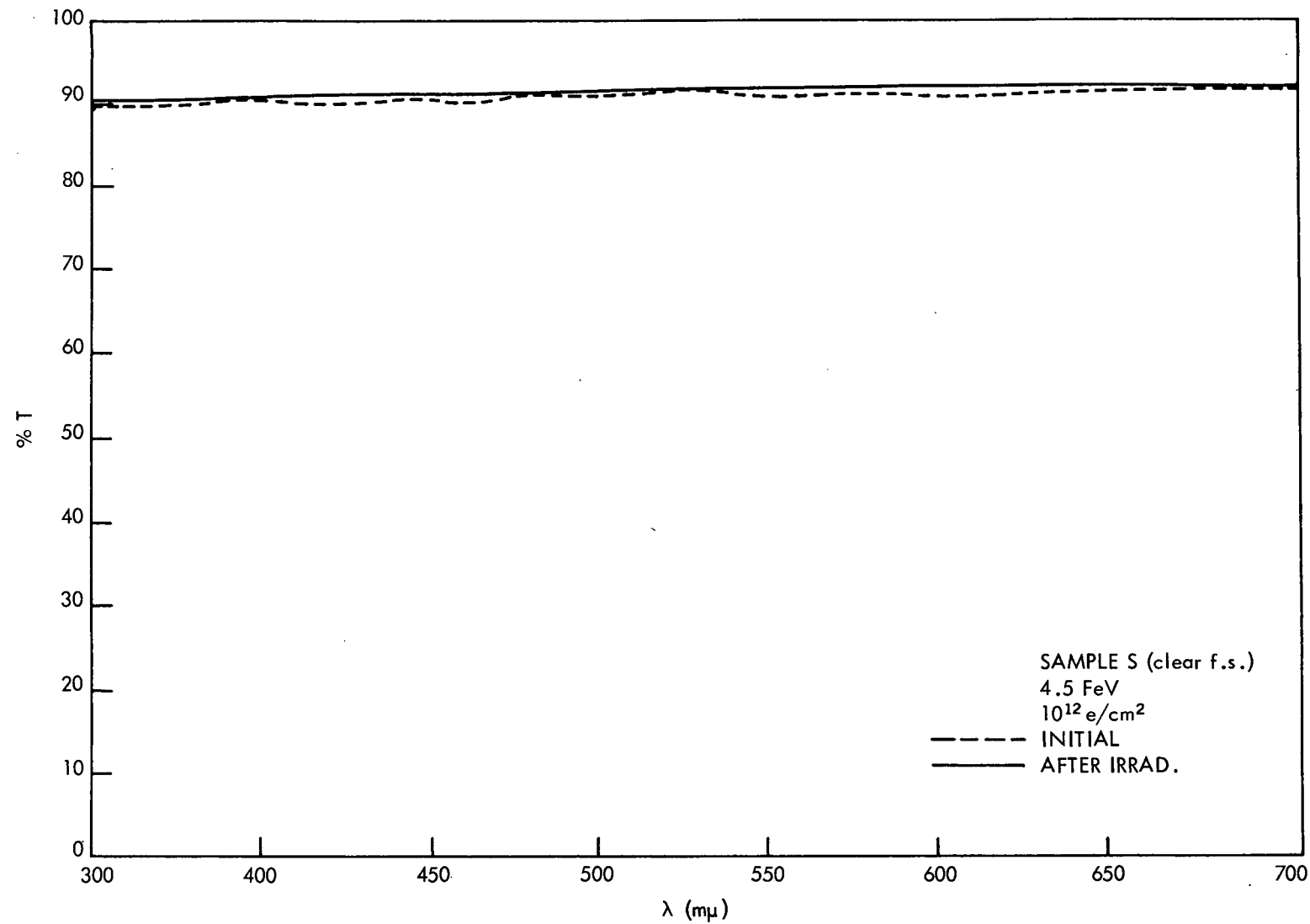


Figure 59.

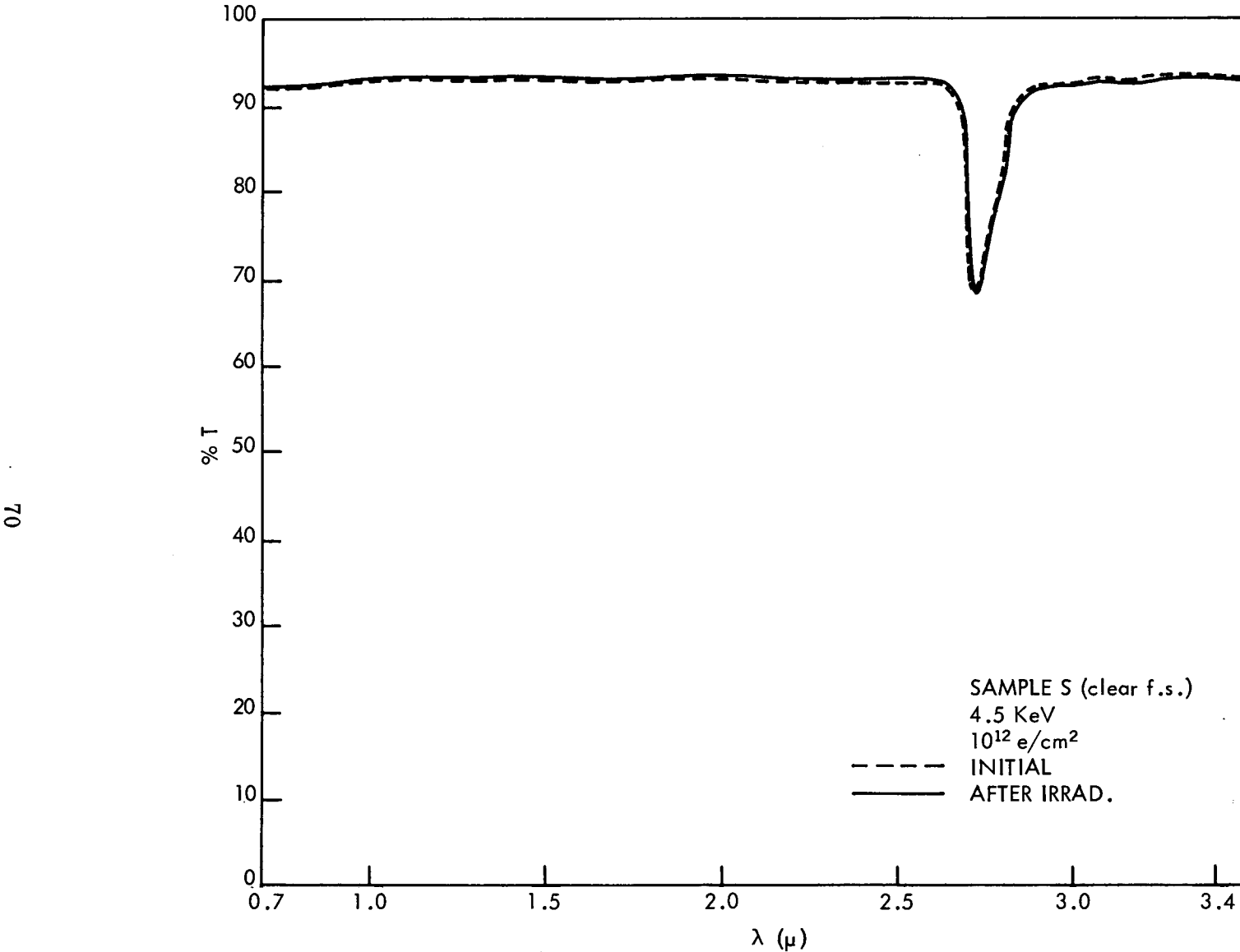


Figure 60.

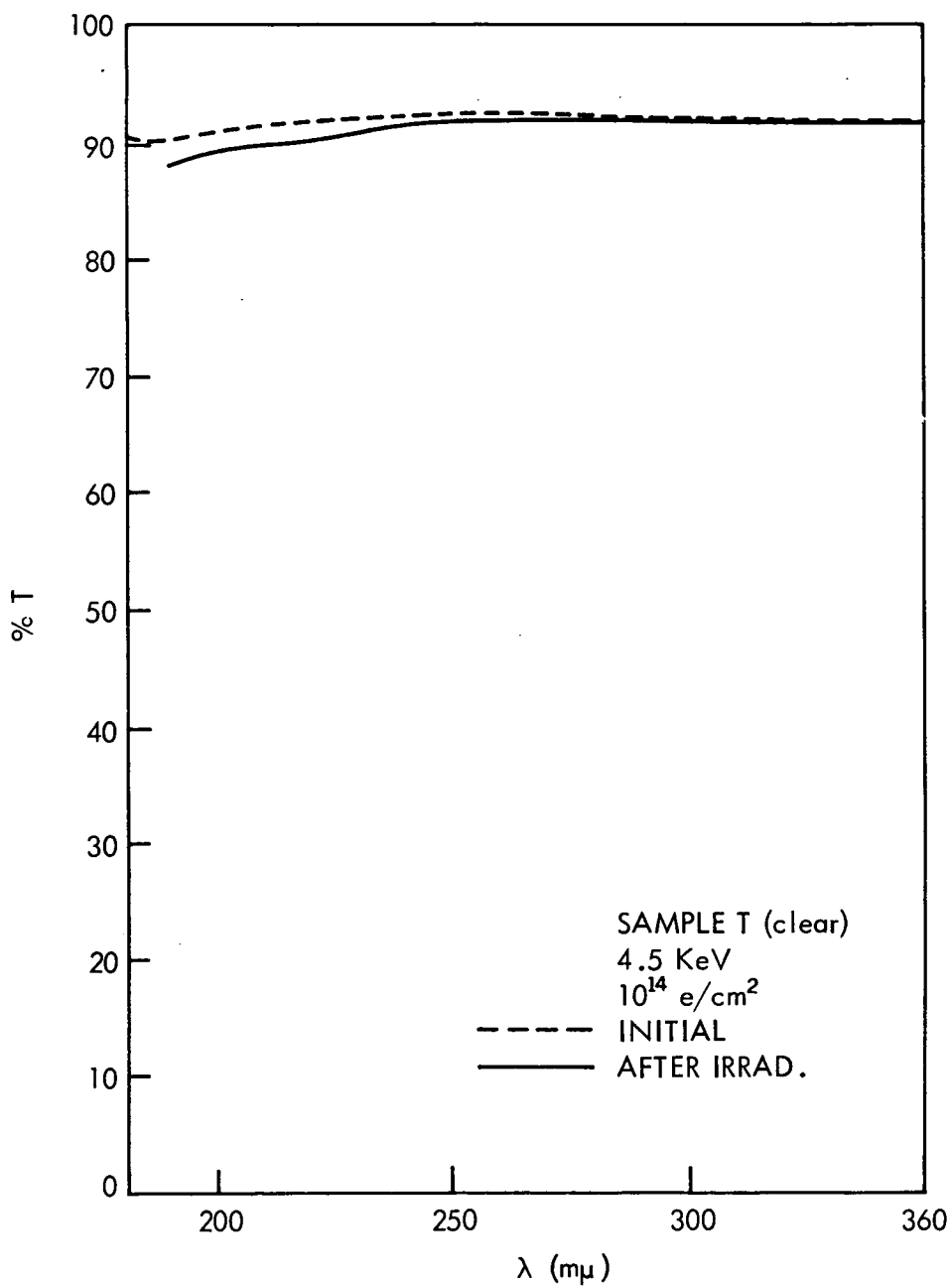


Figure 61.

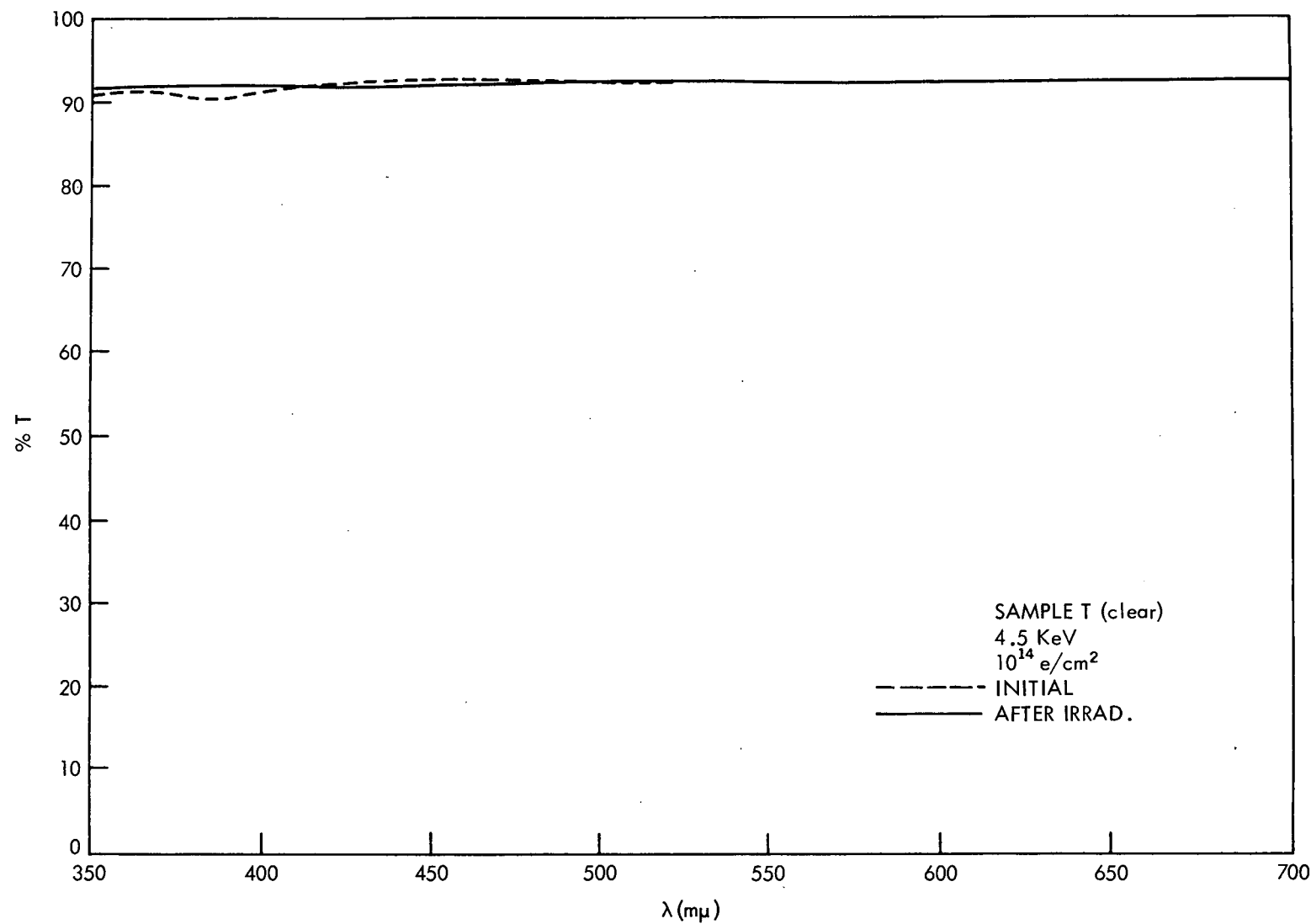


Figure 62.

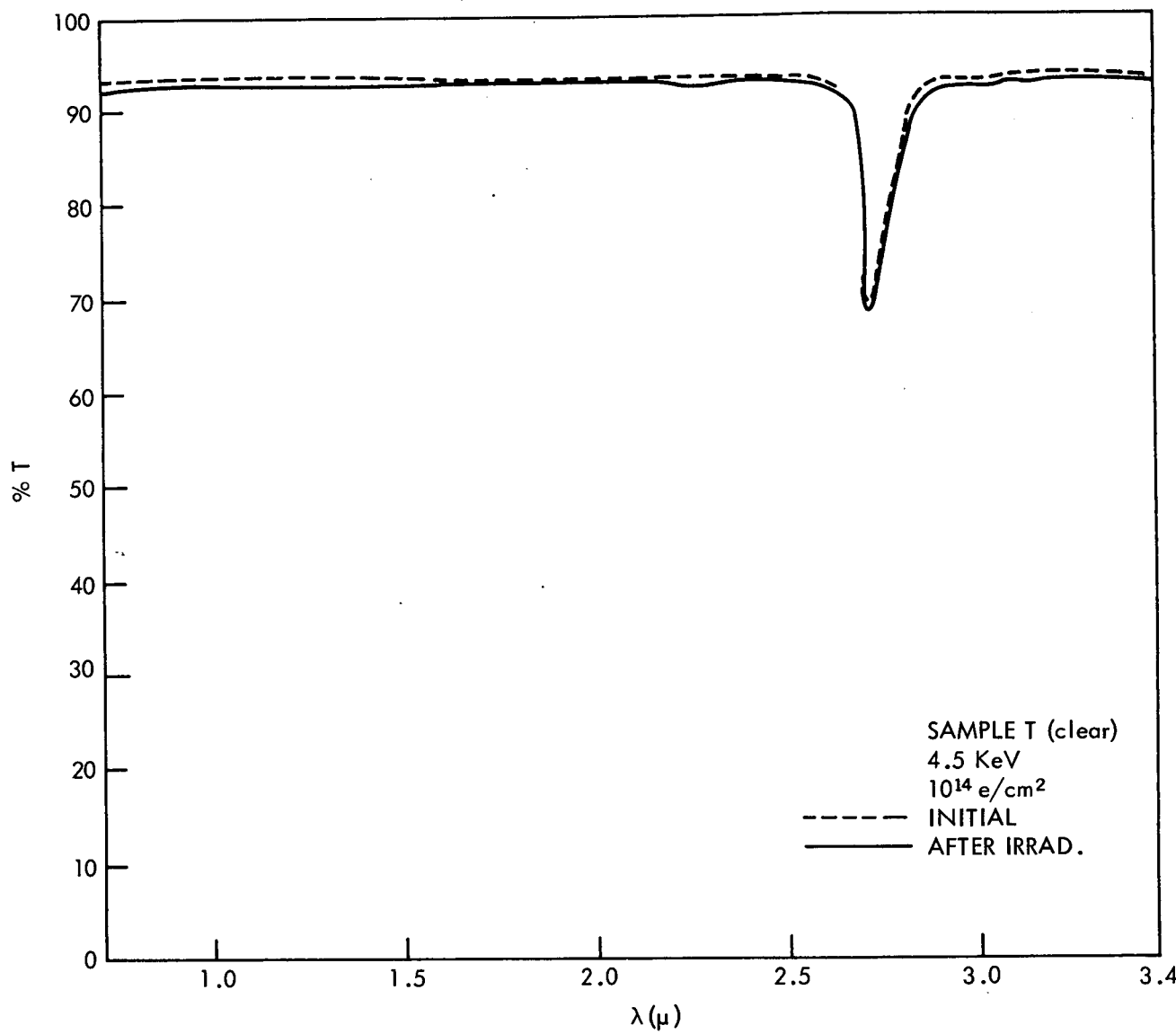


Figure 63.

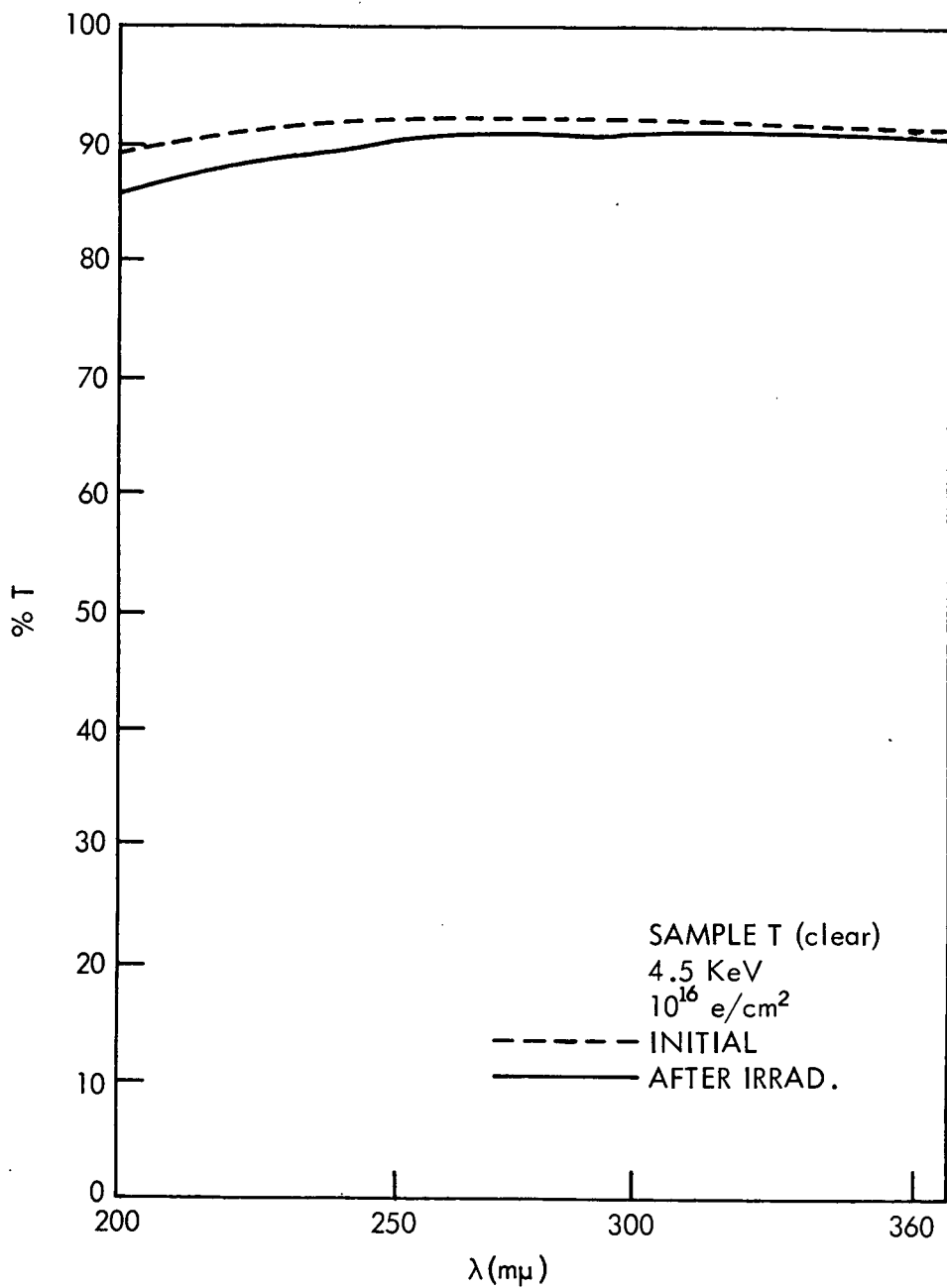


Figure 64.

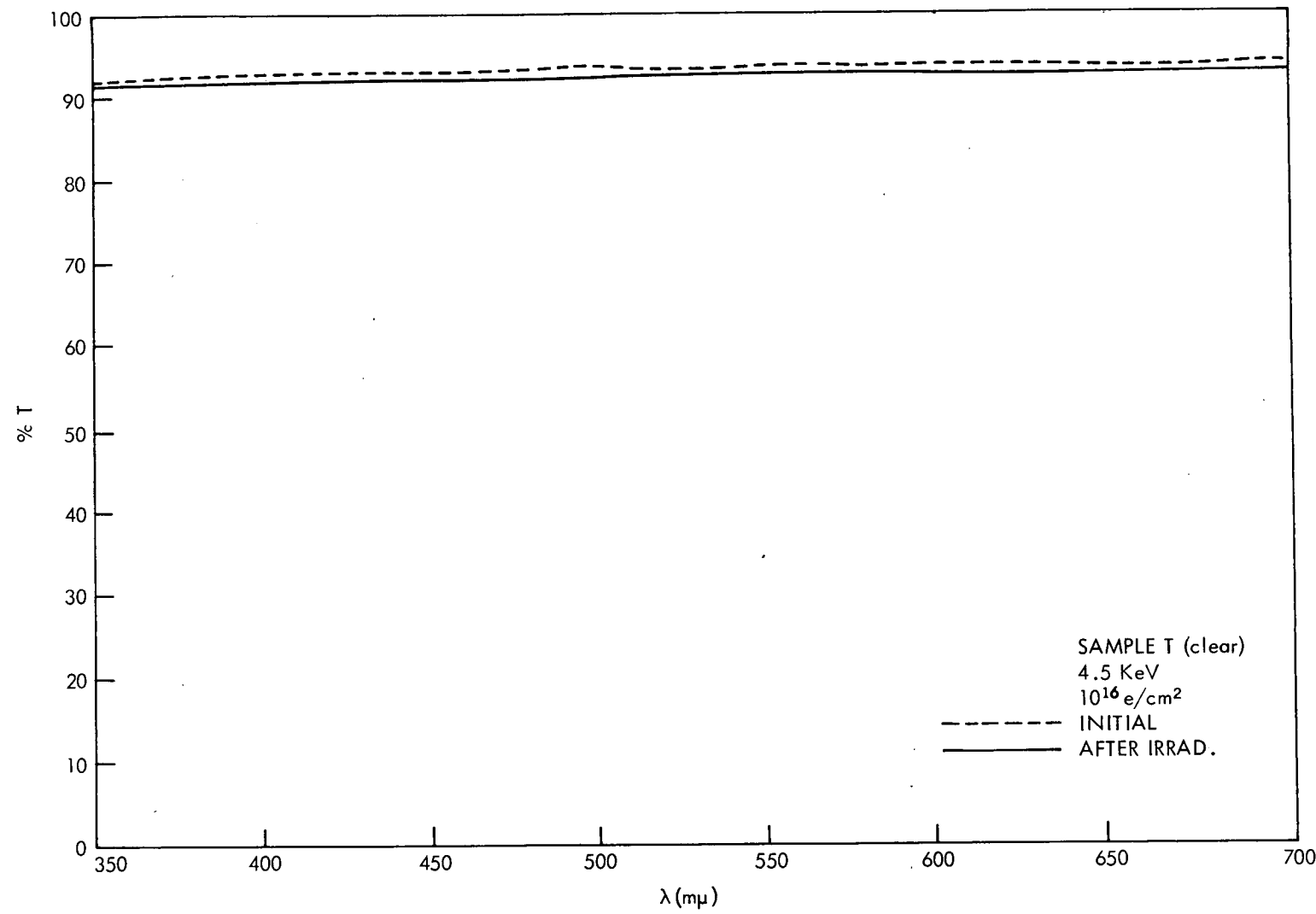


Figure 65.

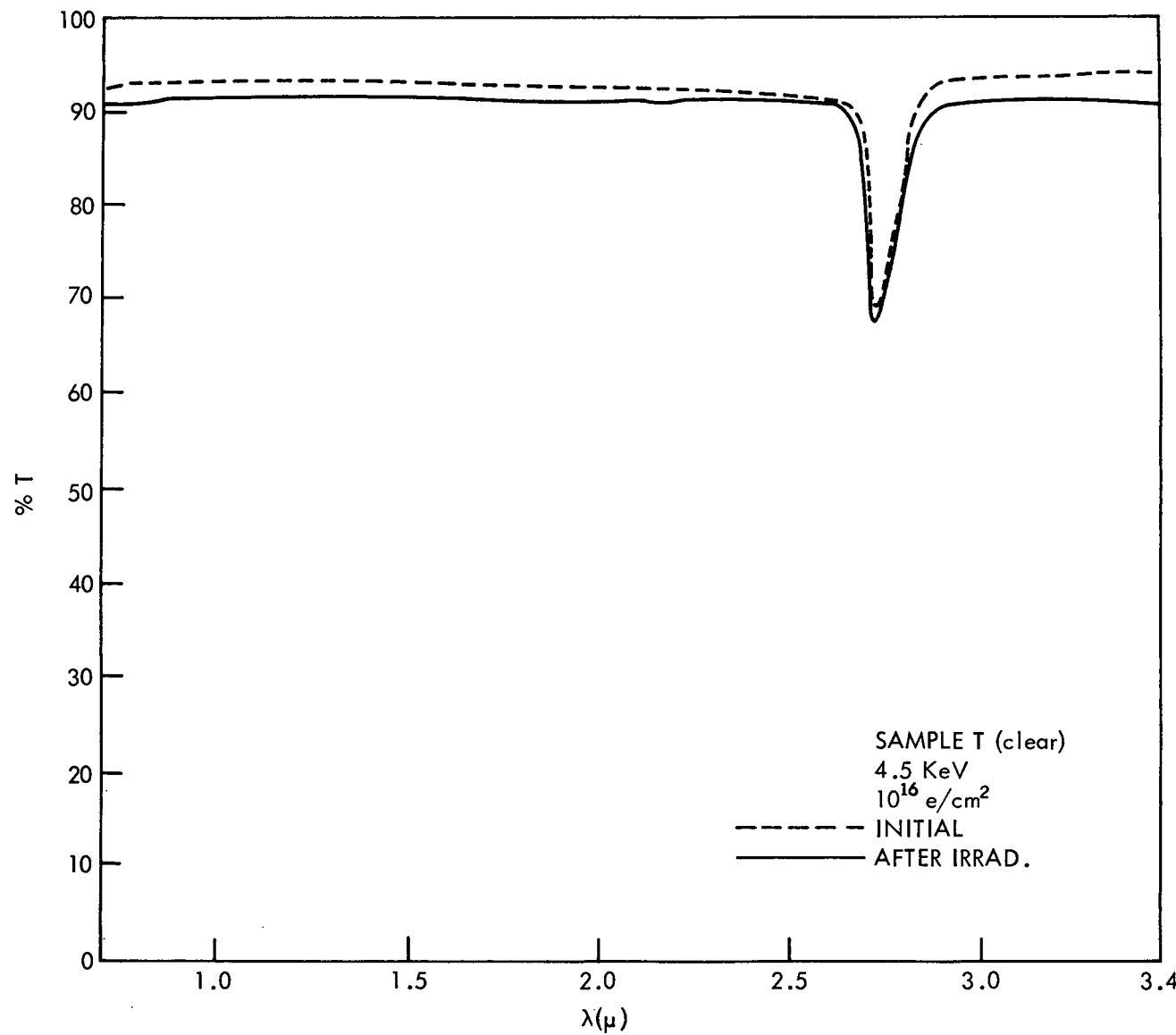


Figure 66.

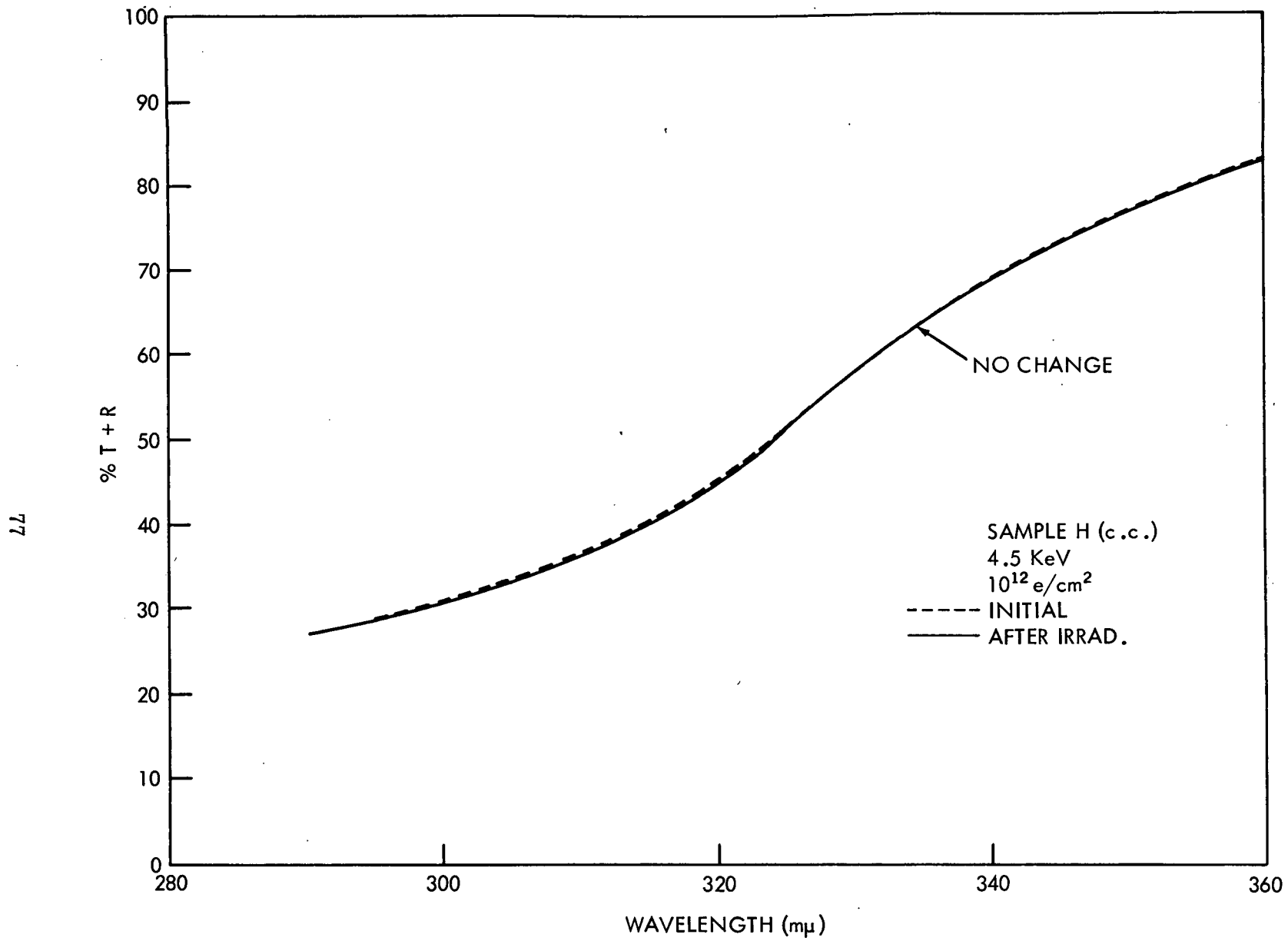


Figure 67.

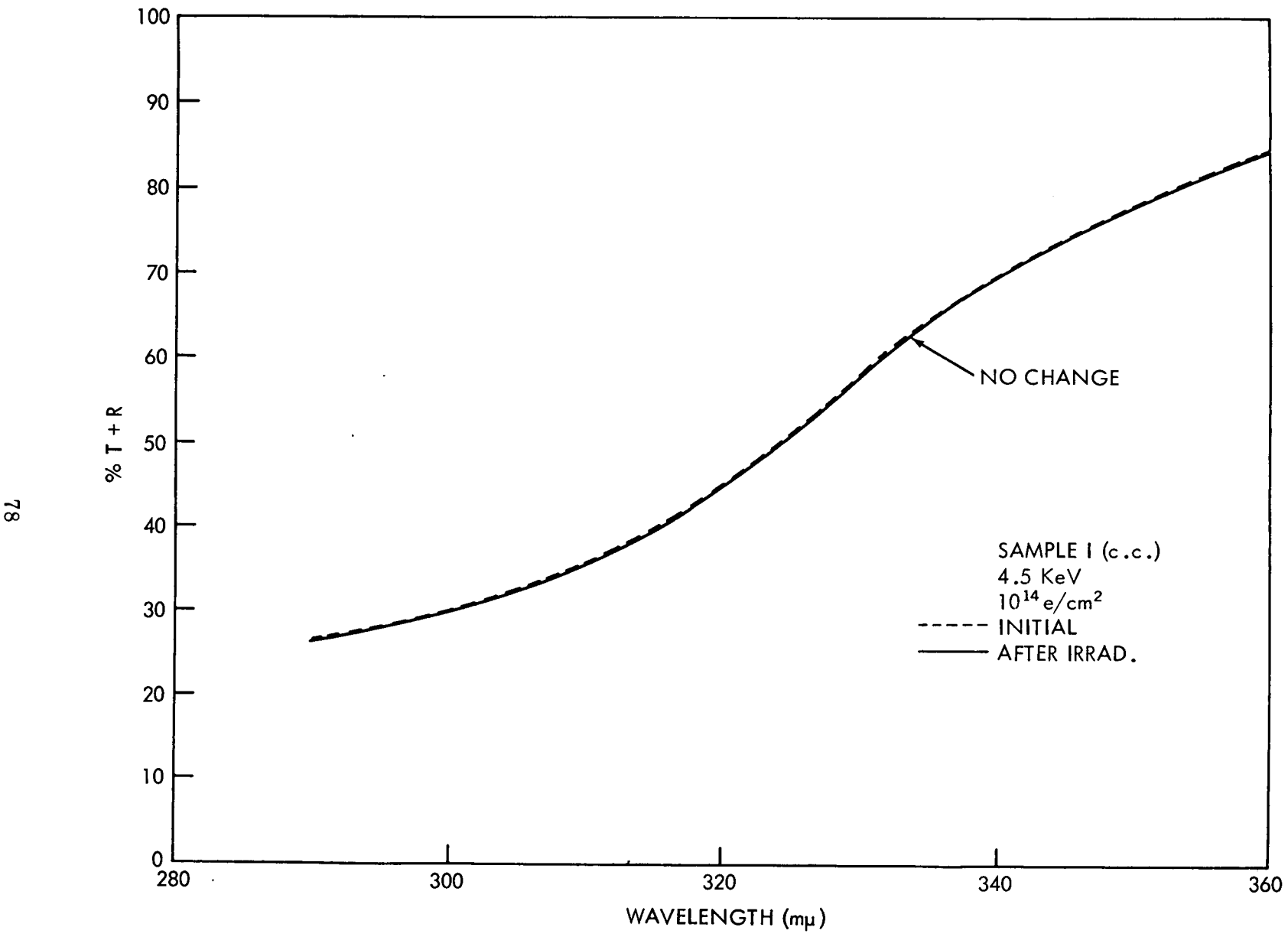


Figure 68.

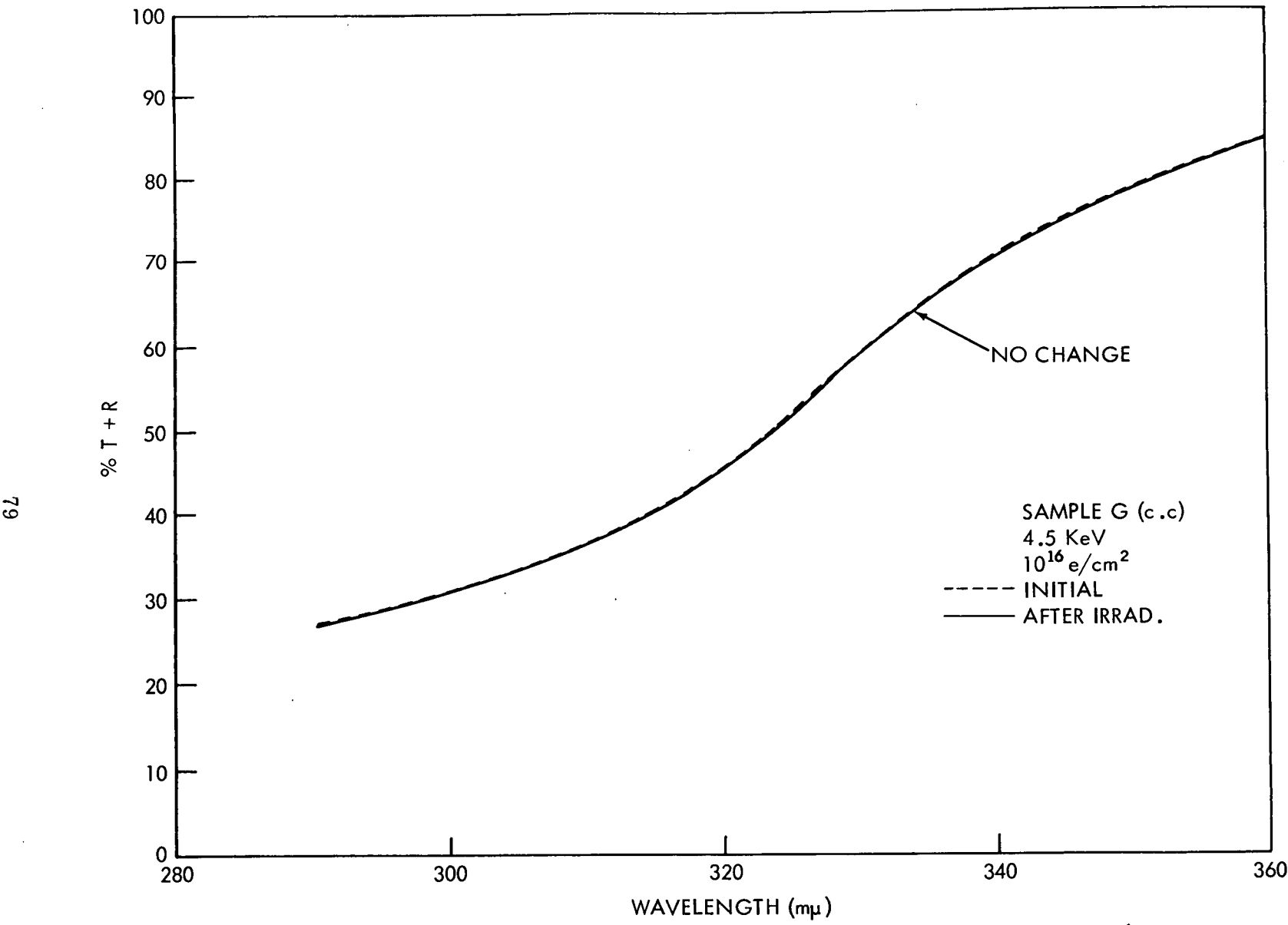


Figure 69.

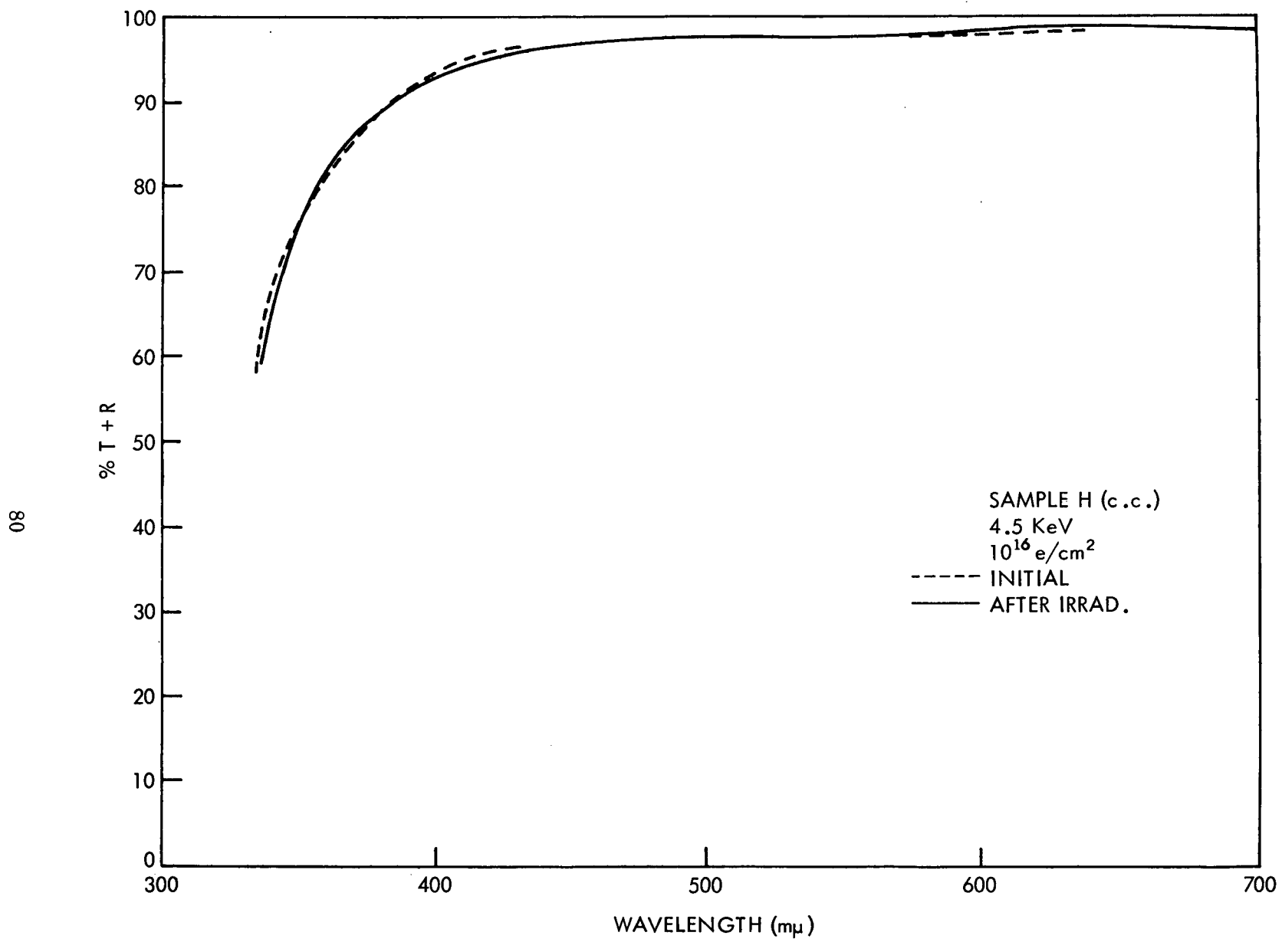


Figure 70.

81

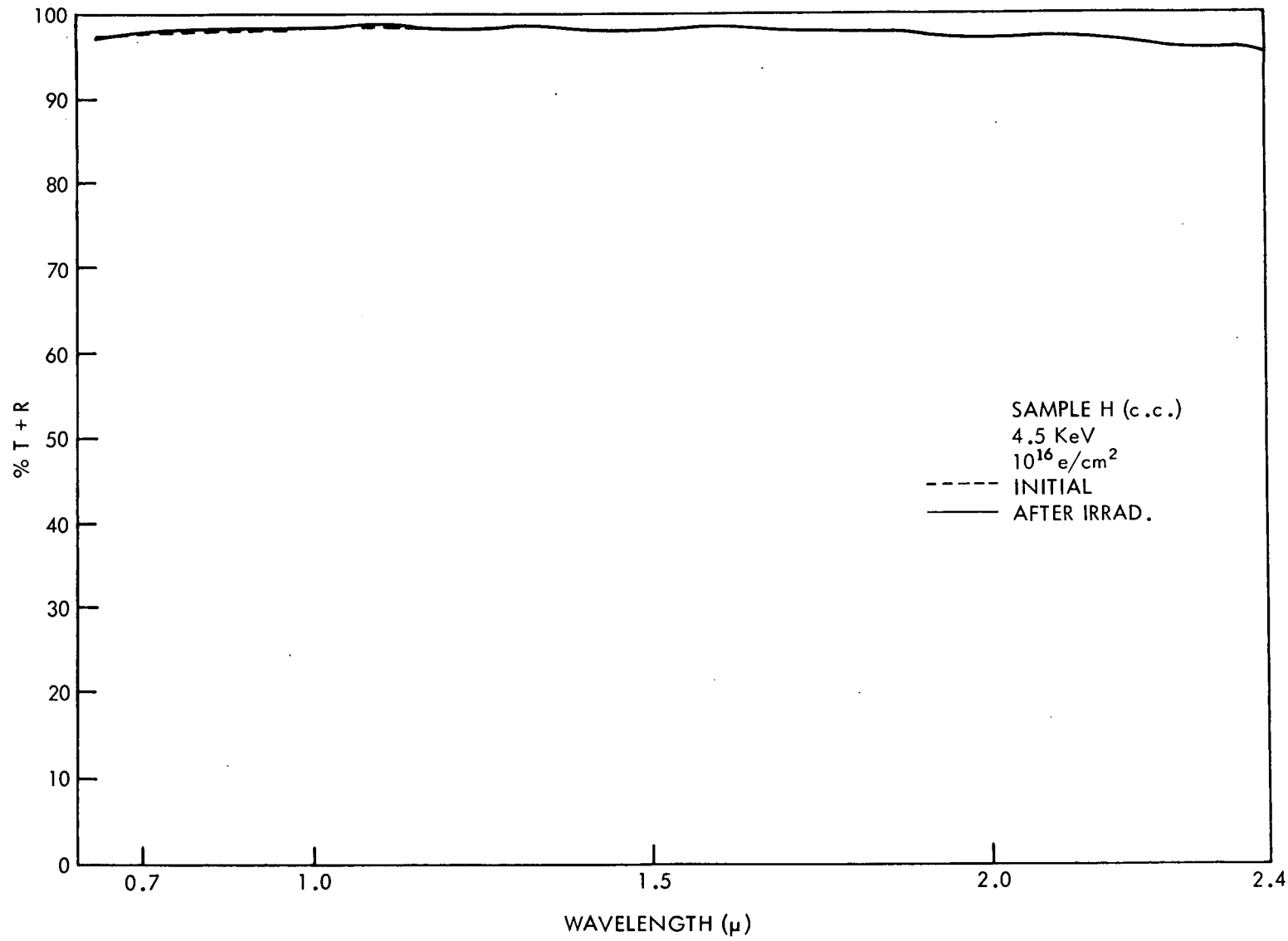


Figure 71.

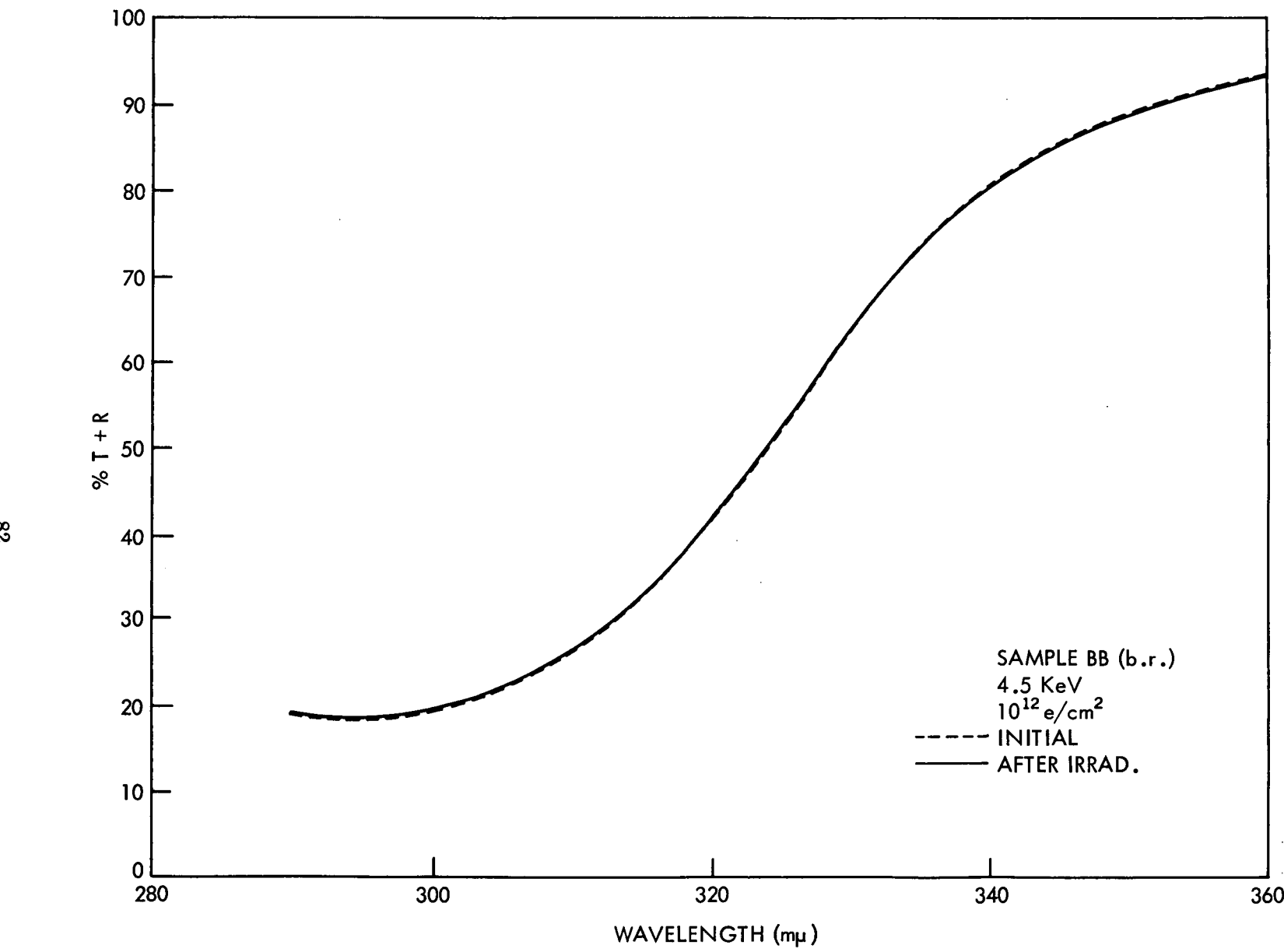


Figure 72.

88

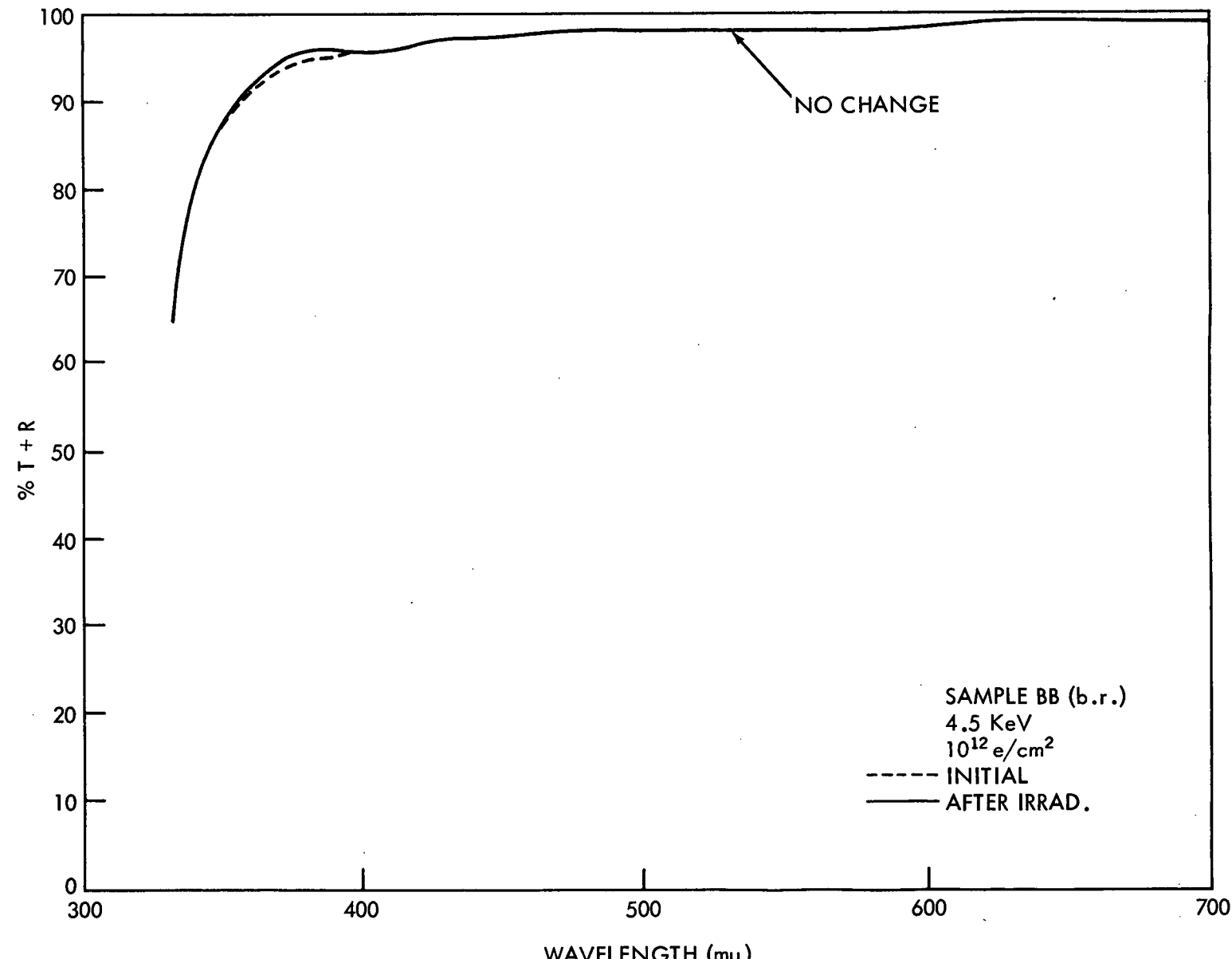


Figure 73.

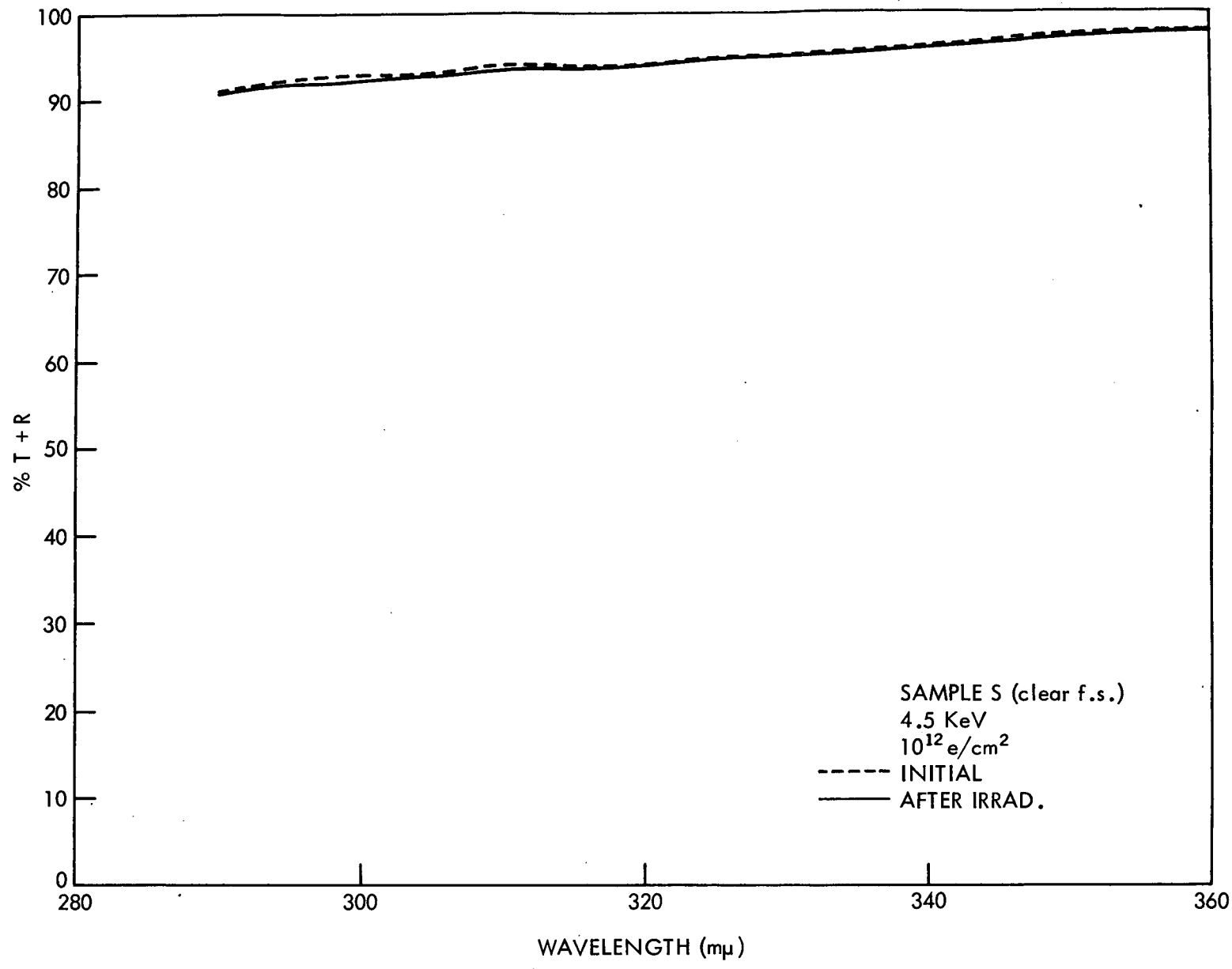


Figure 74.

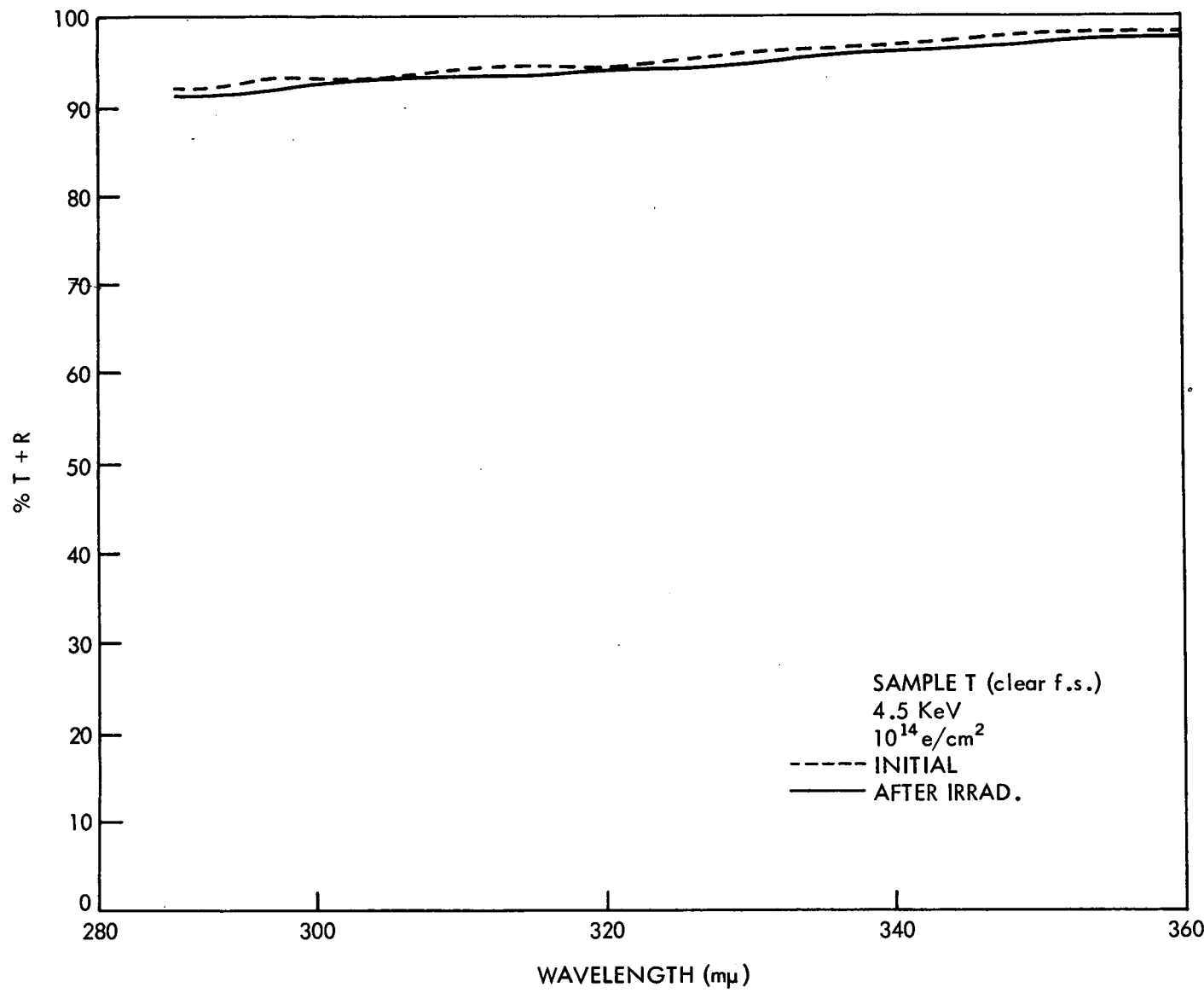


Figure 75.

98

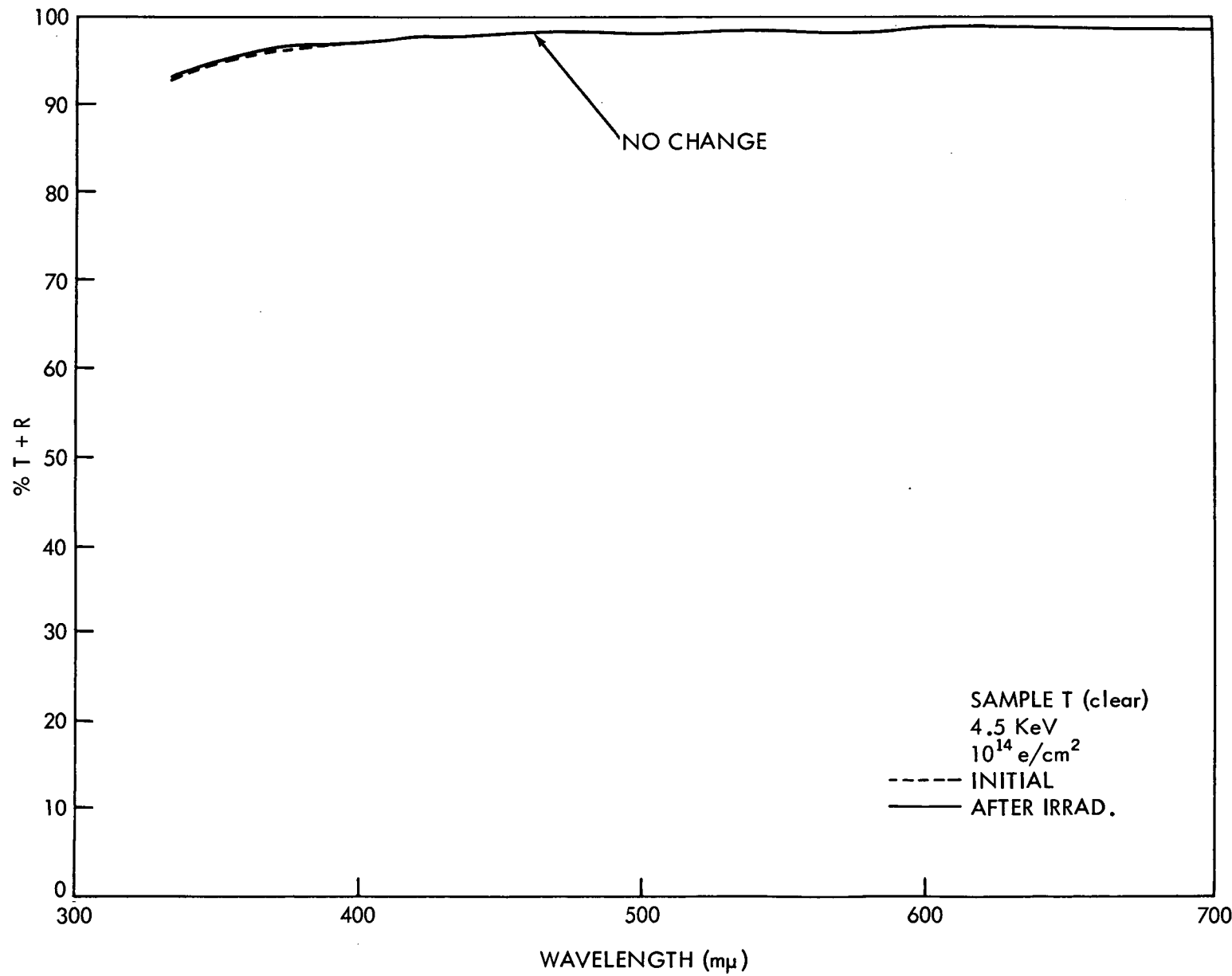


Figure 76.

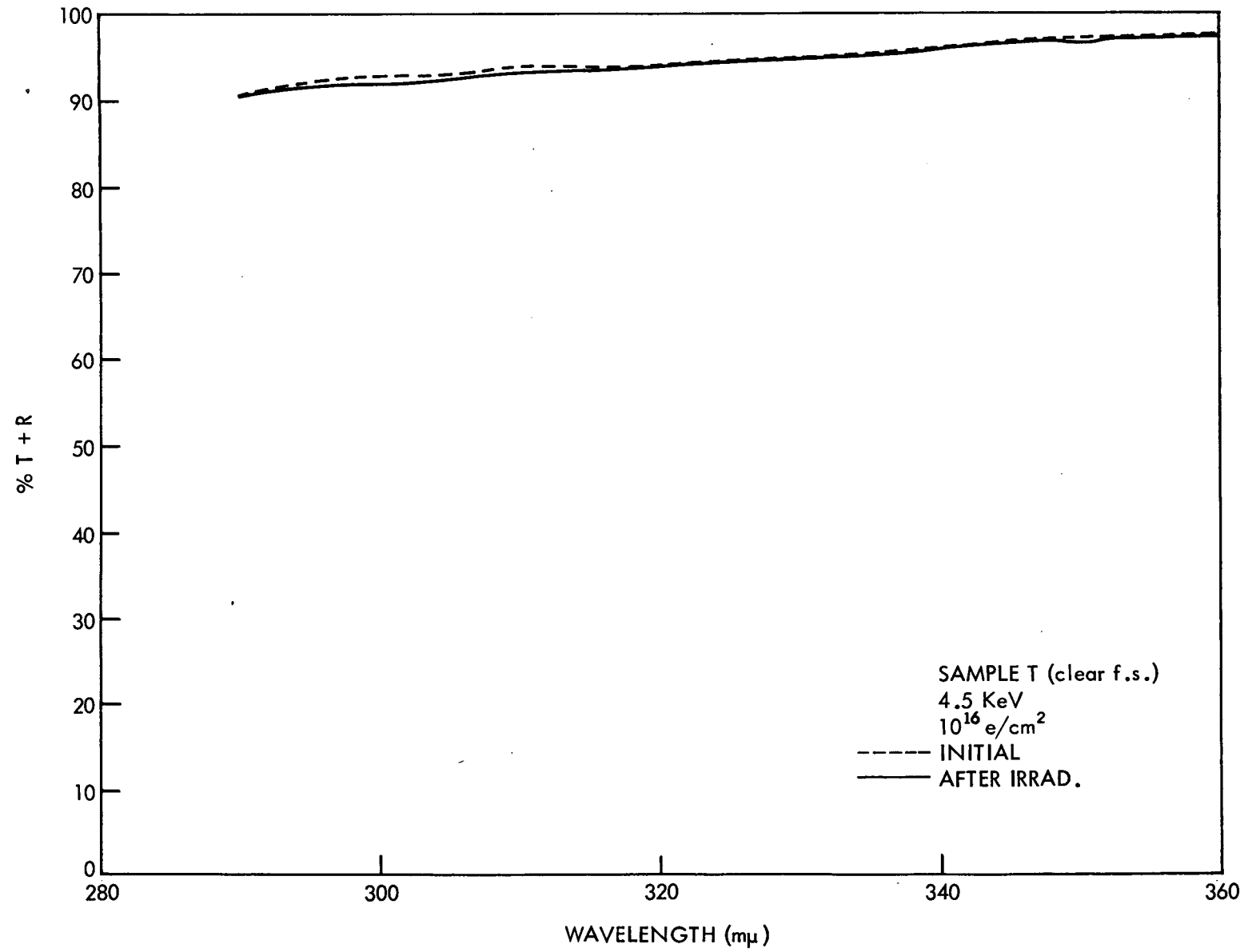


Figure 77.

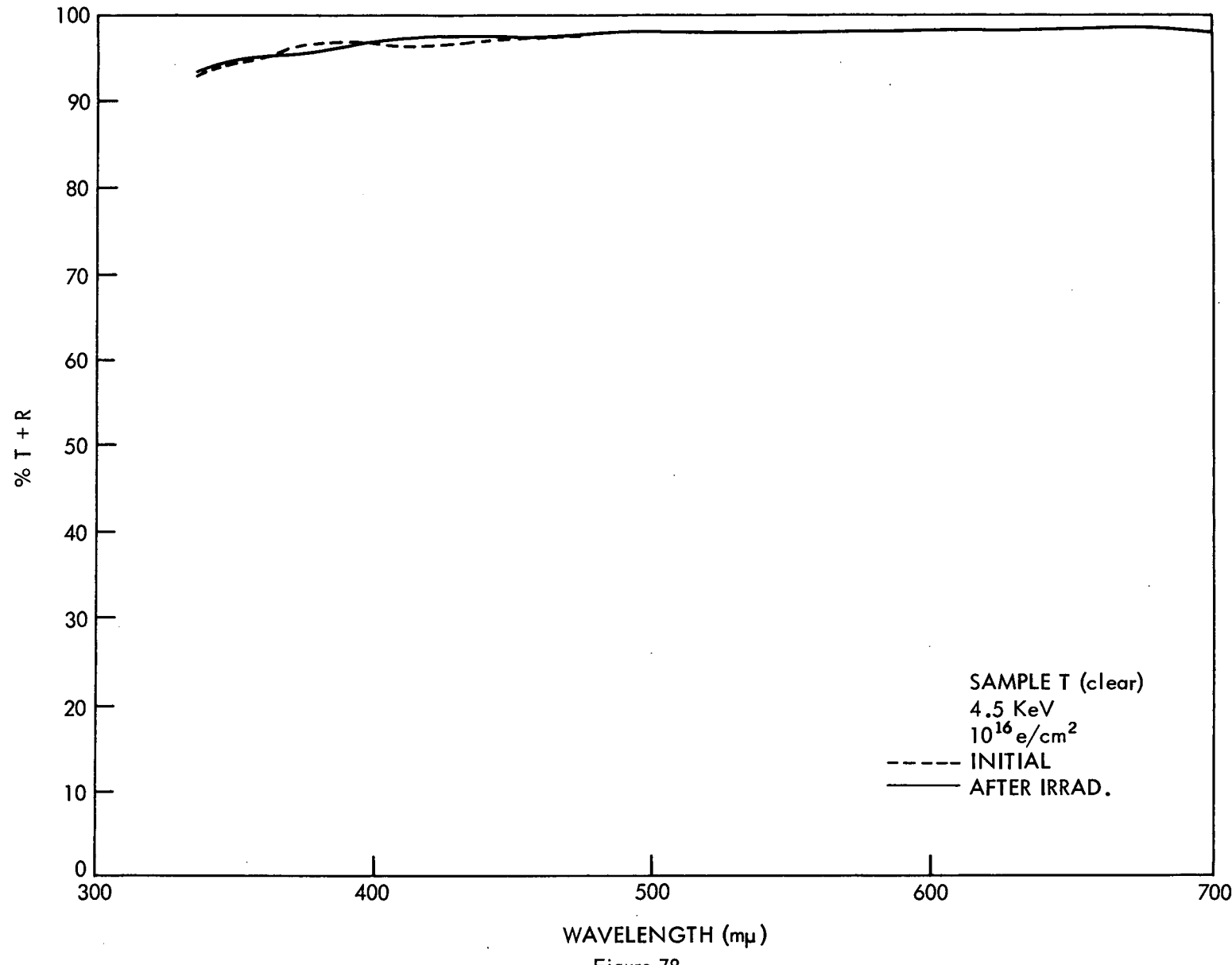


Figure 78.

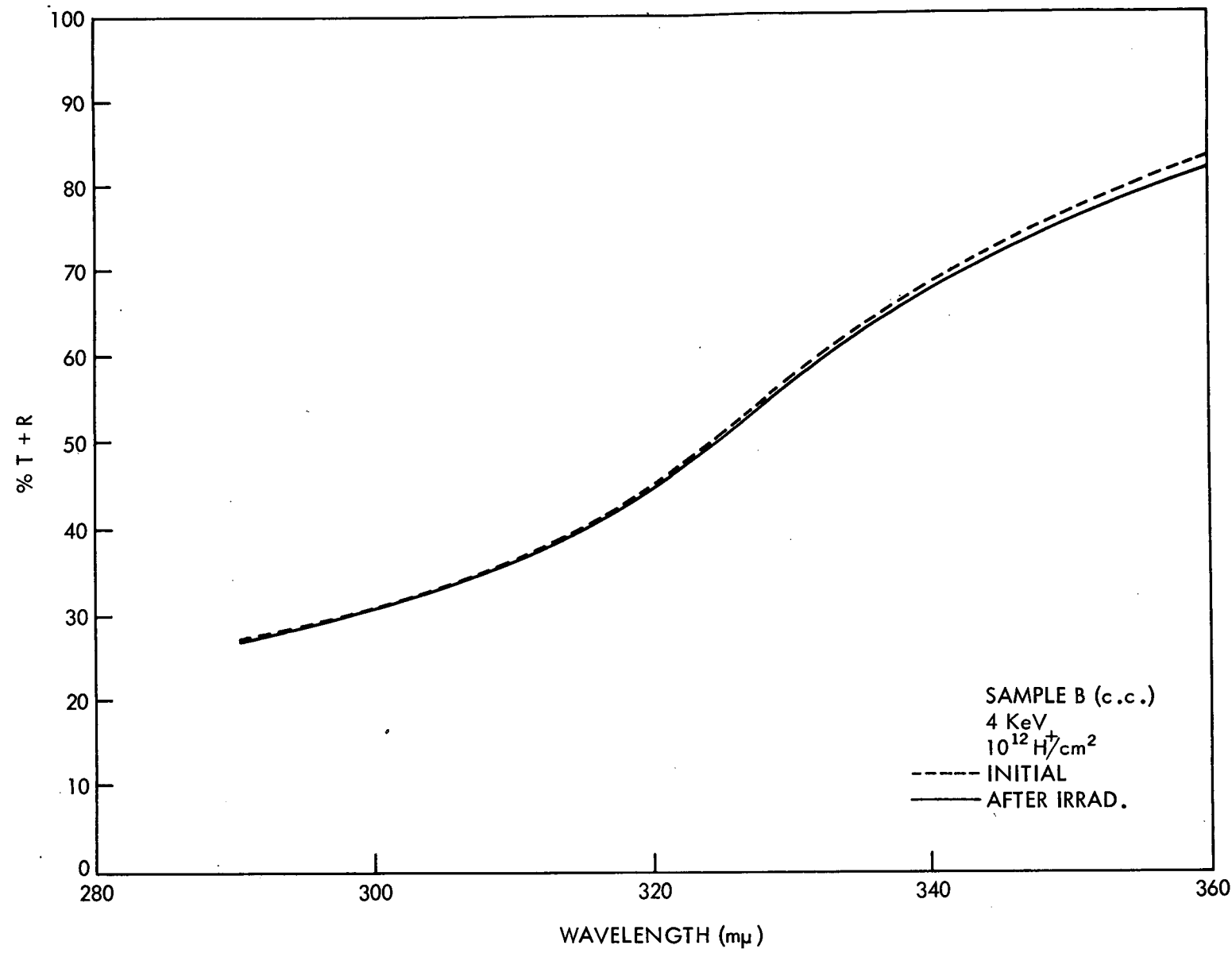


Figure 79.

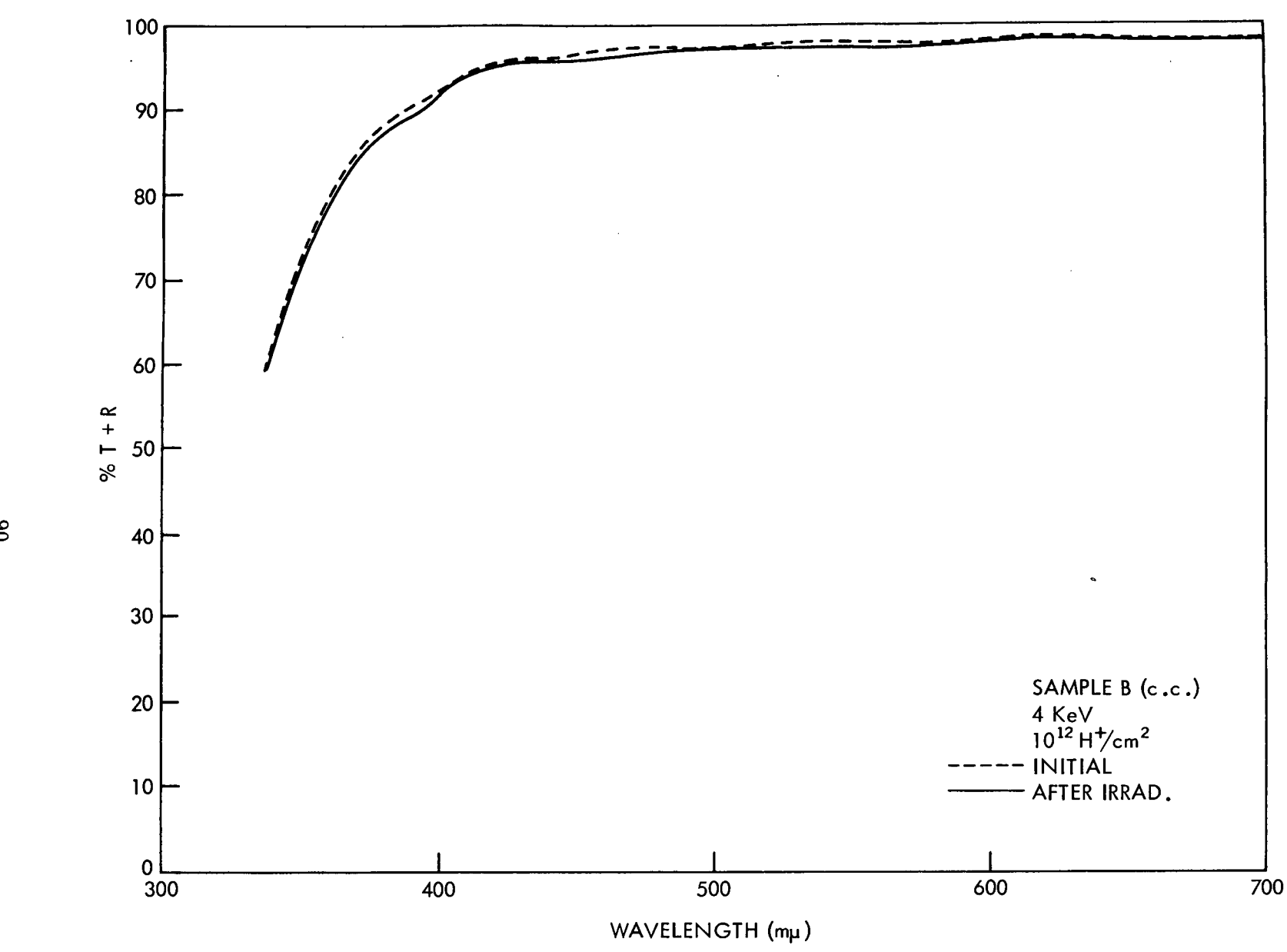


Figure 30.

16

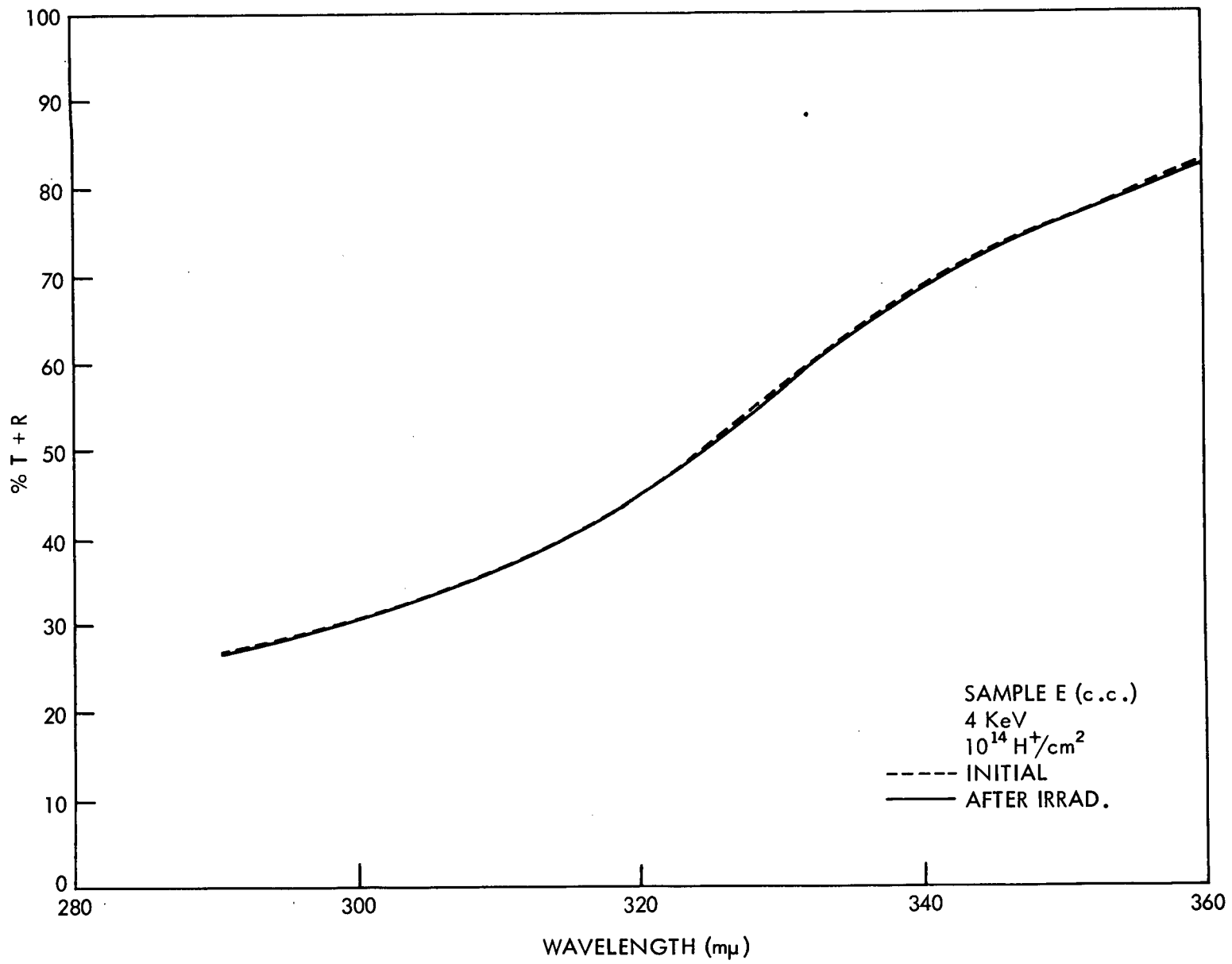


Figure 81.

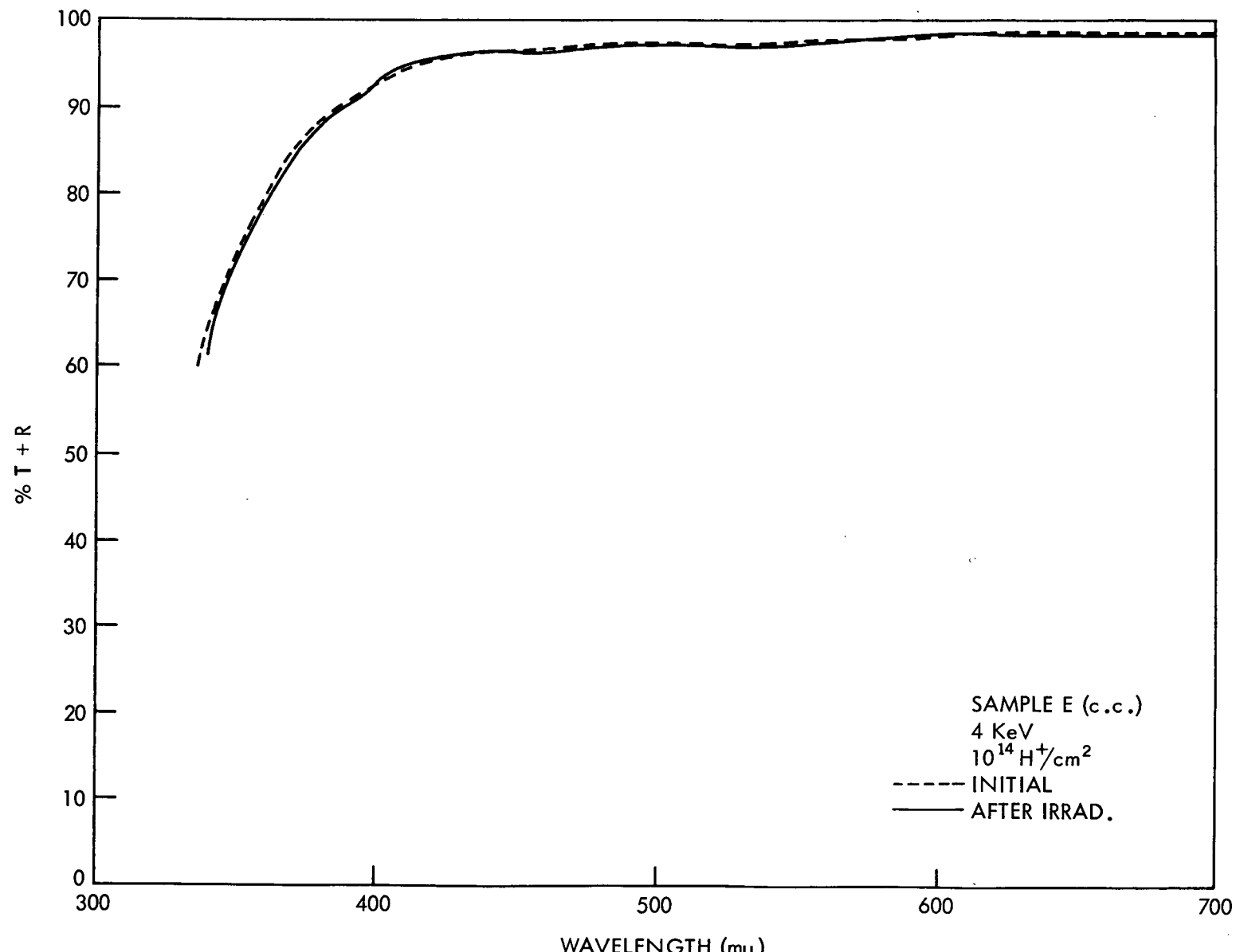


Figure 82.

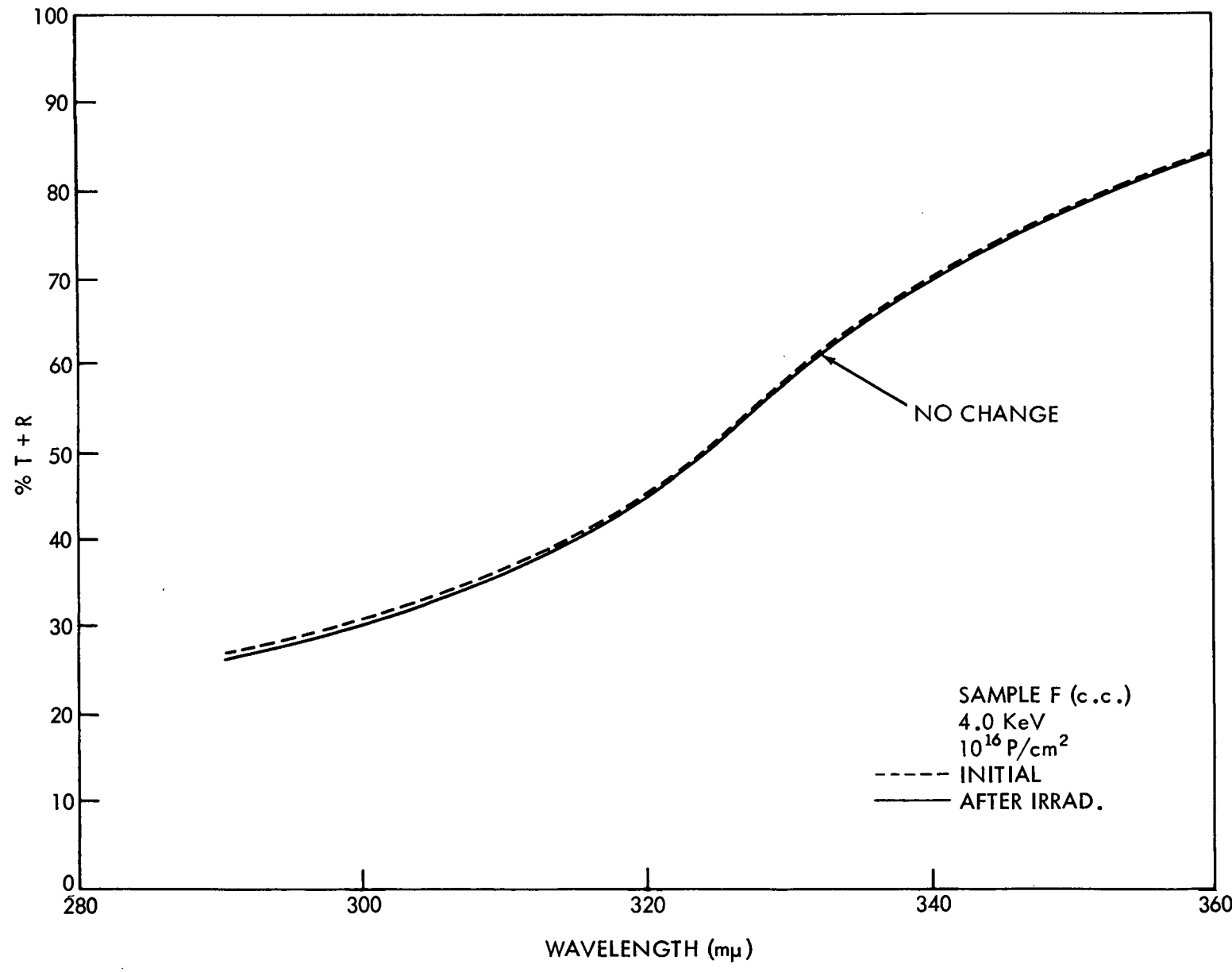


Figure 84.

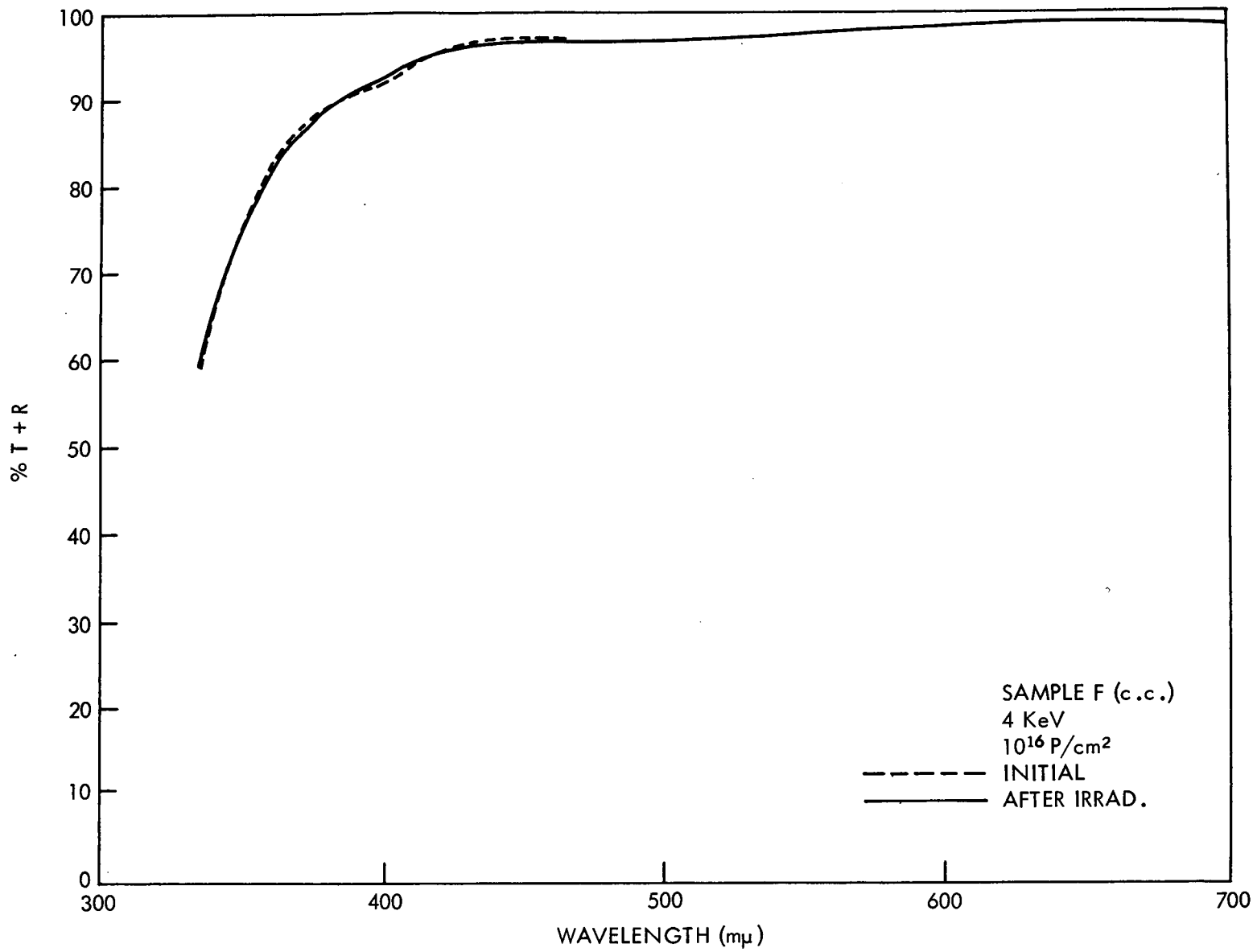


Figure 84.

C-2

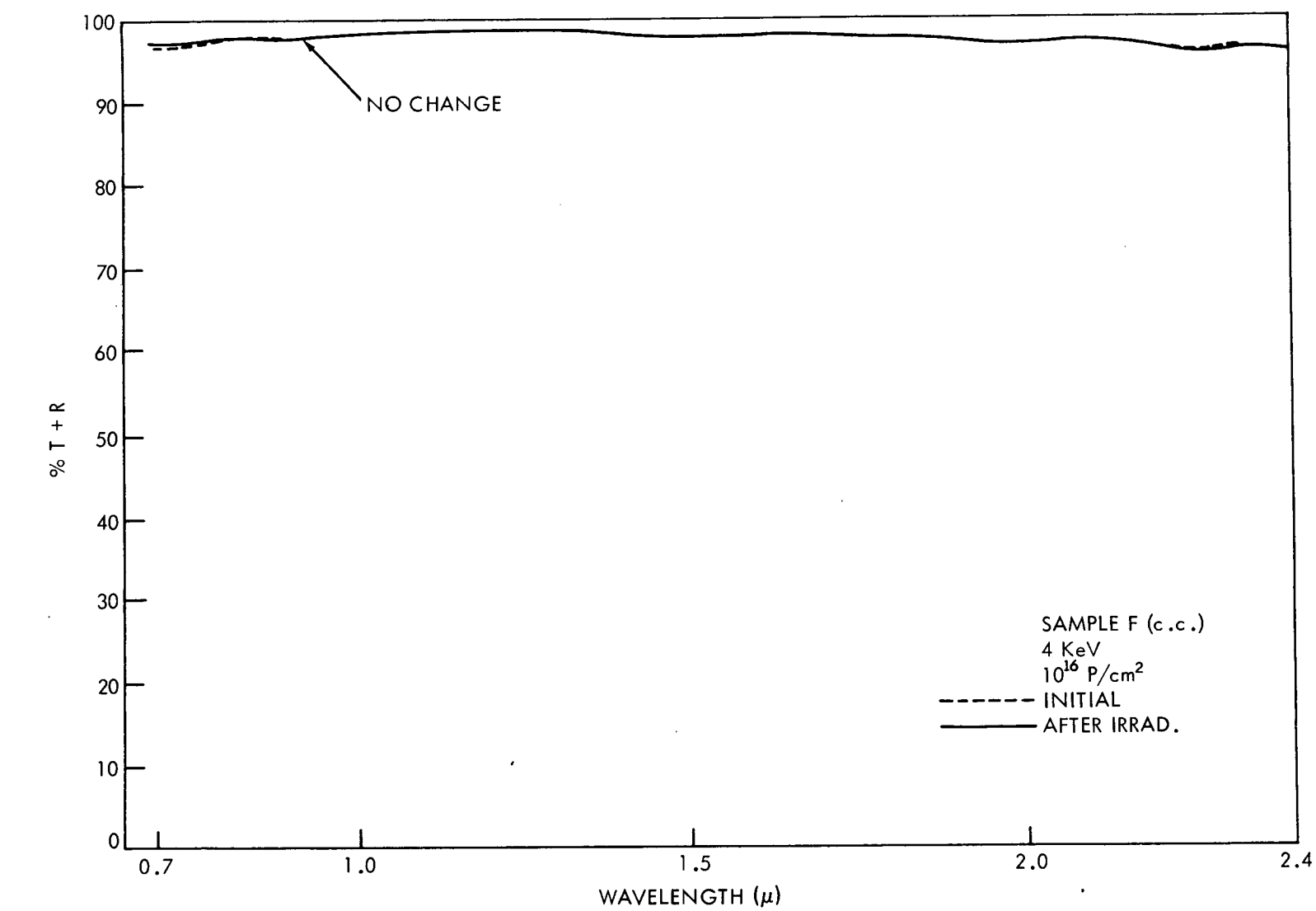


Figure 85.

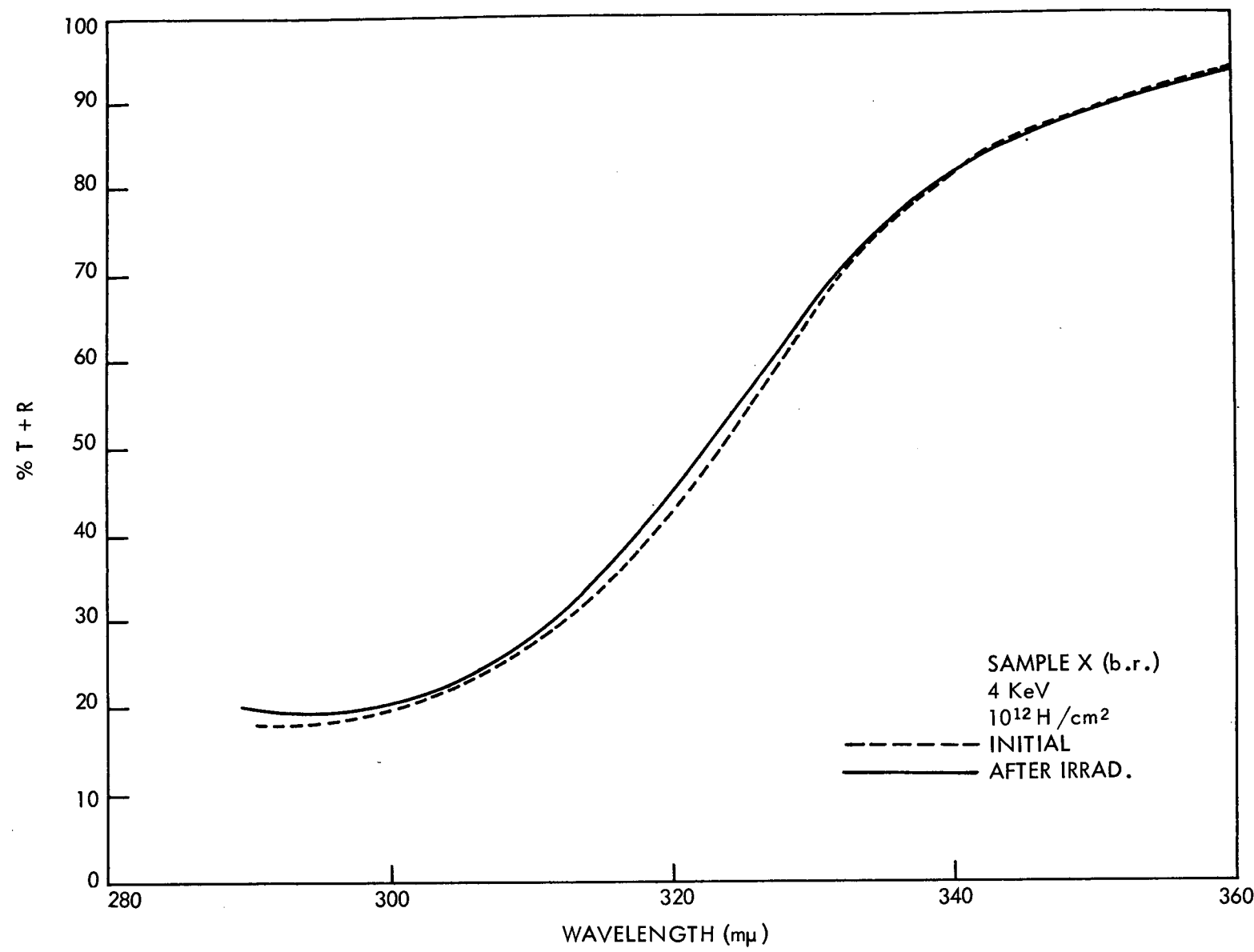


Figure 86.

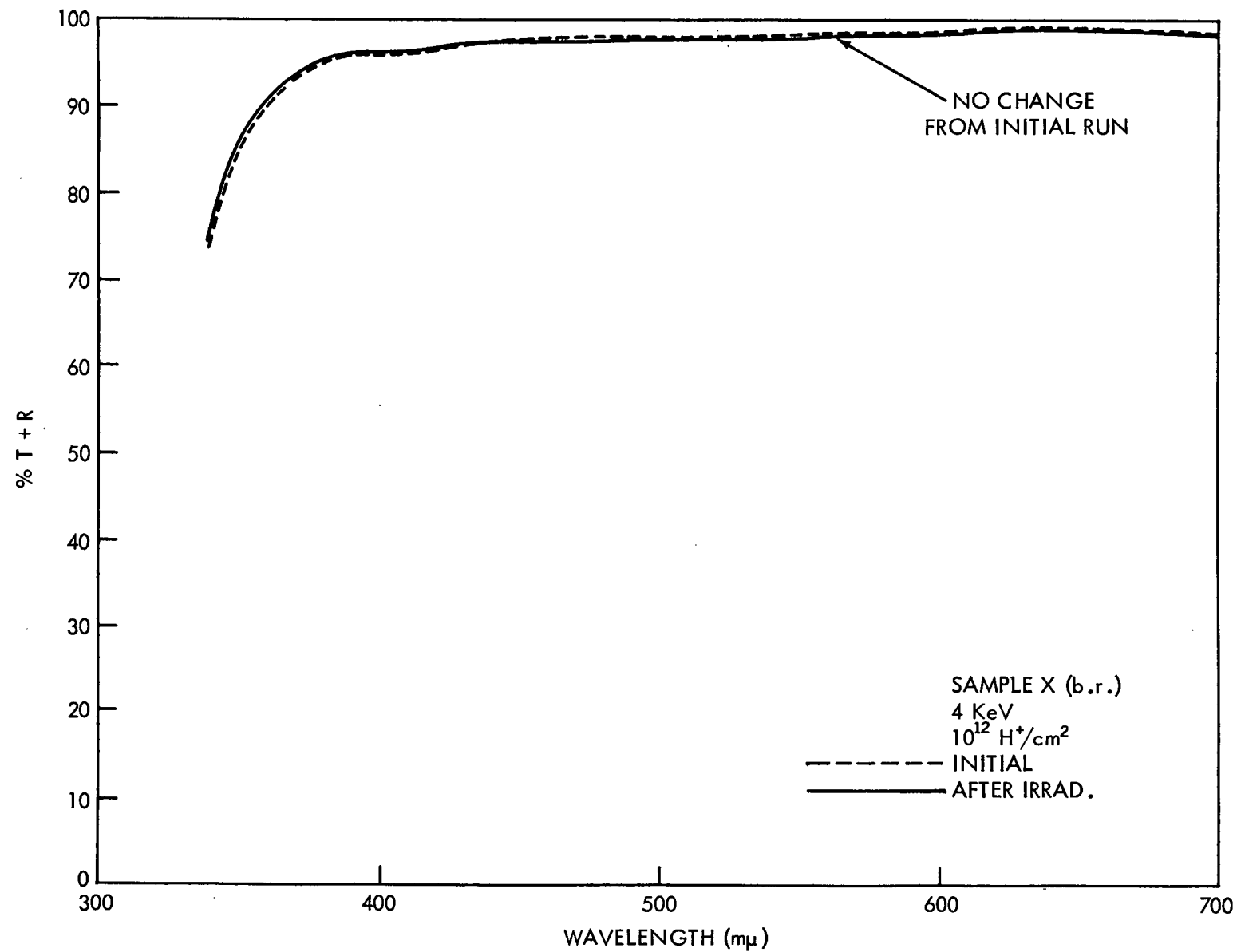


Figure 87.

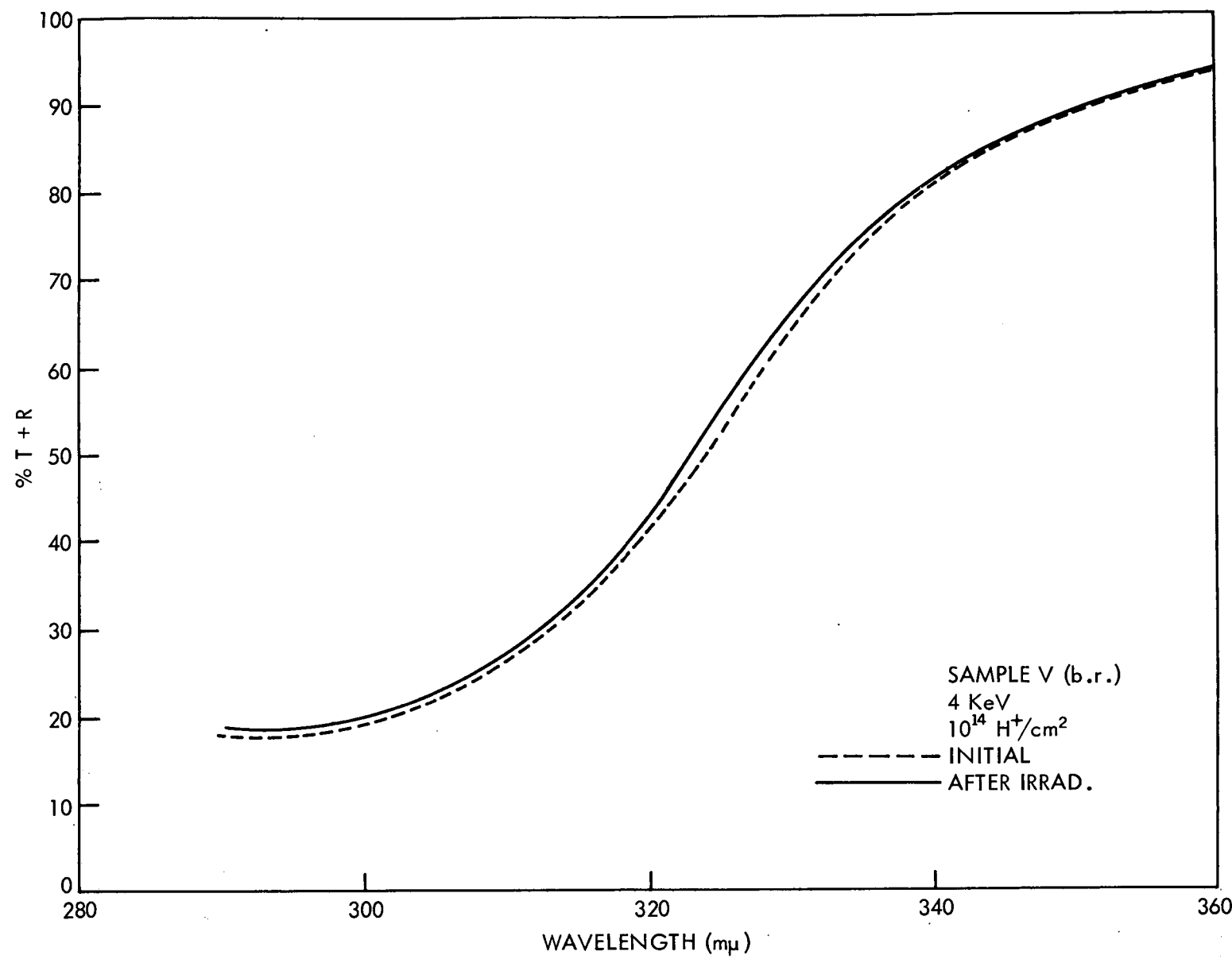


Figure 88.

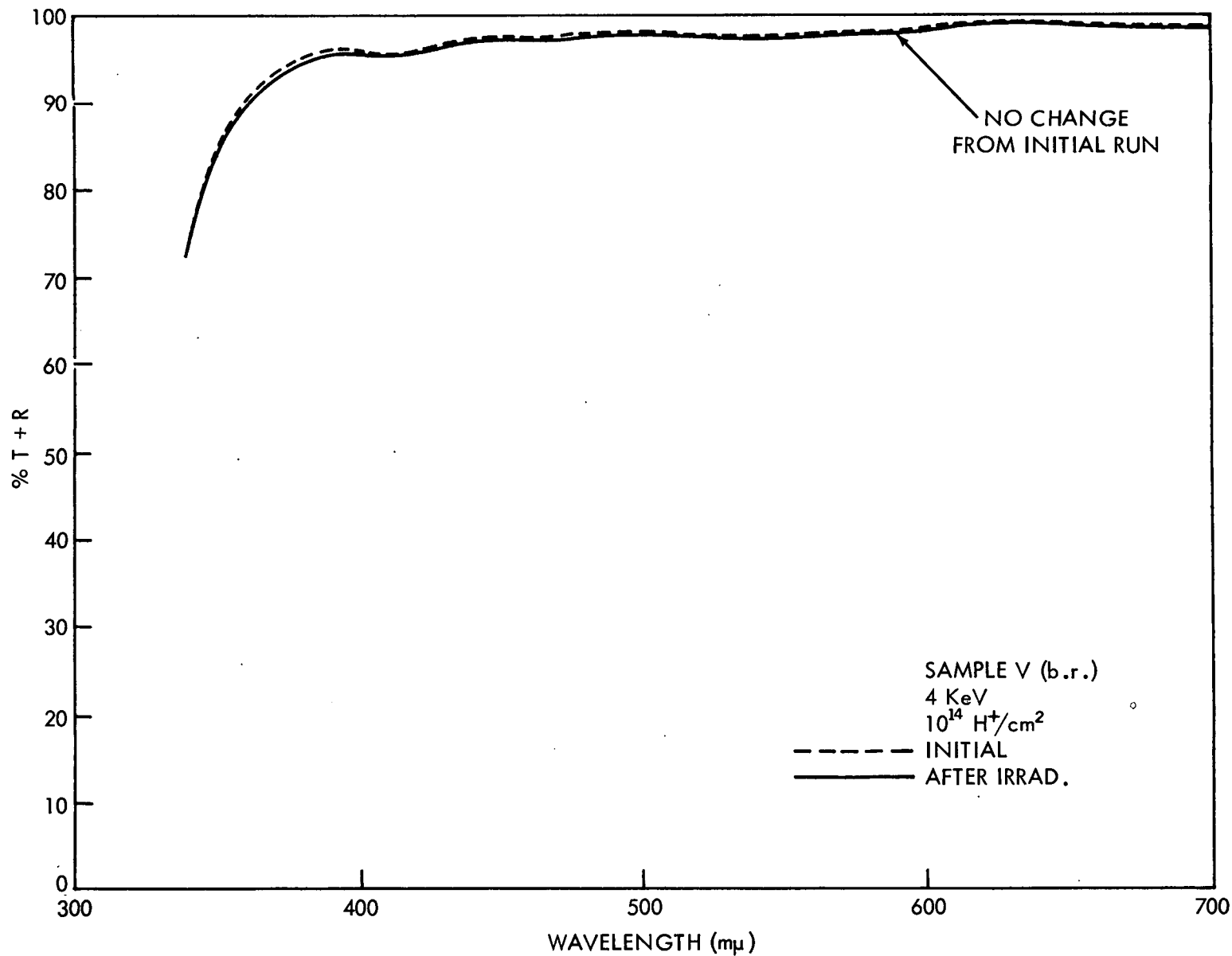


Figure 89.

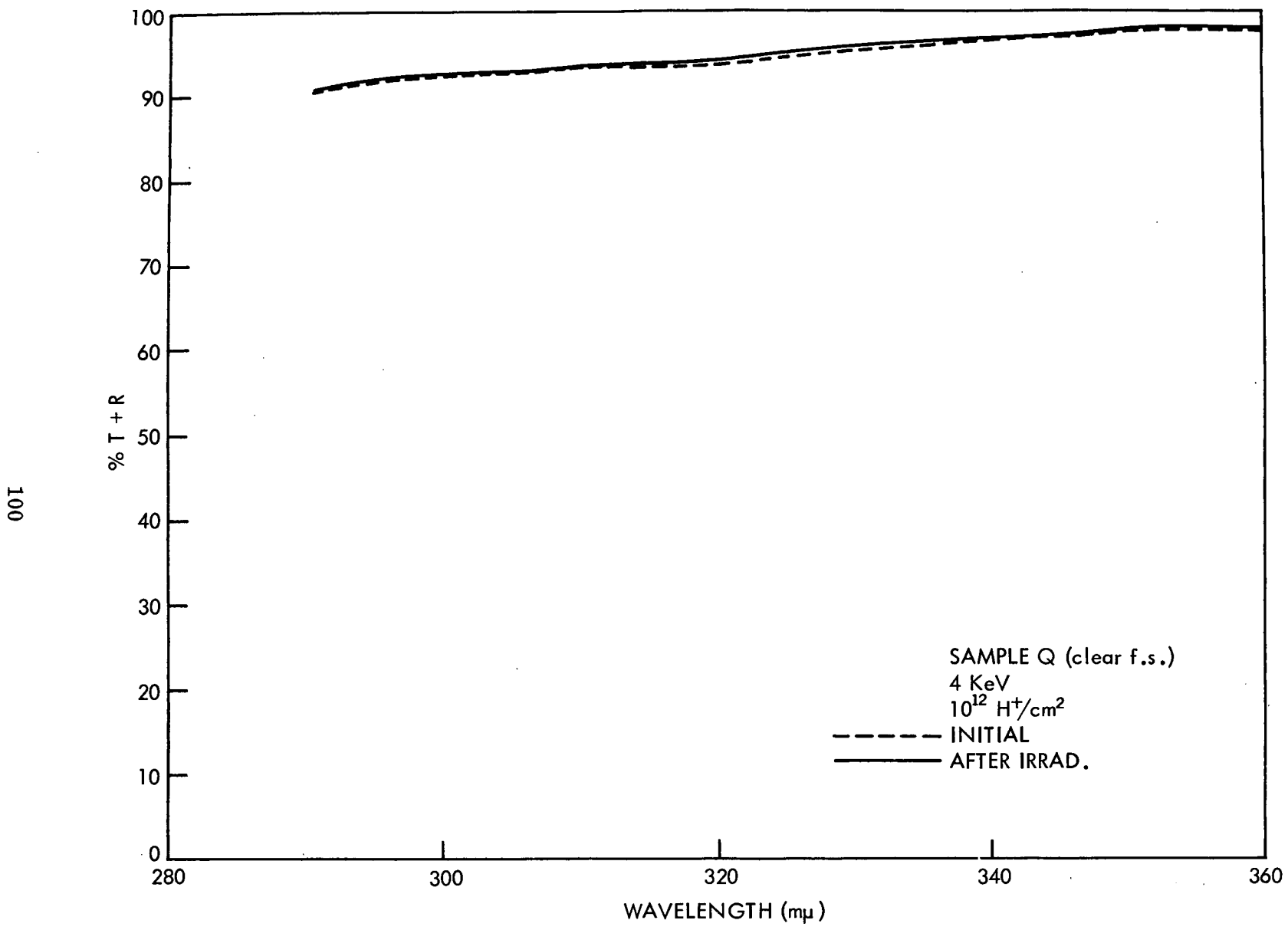


Figure 90.

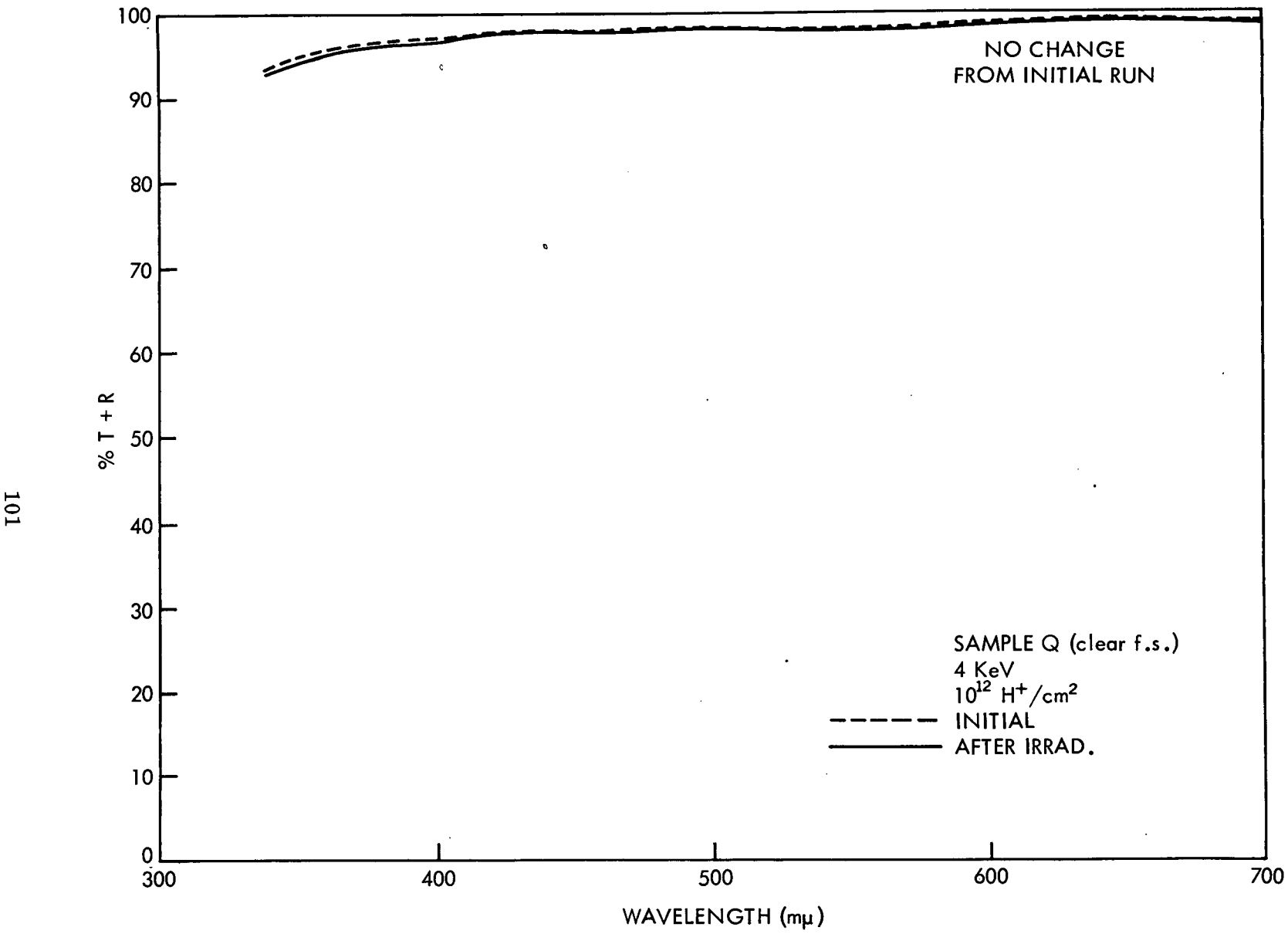


Figure 91.

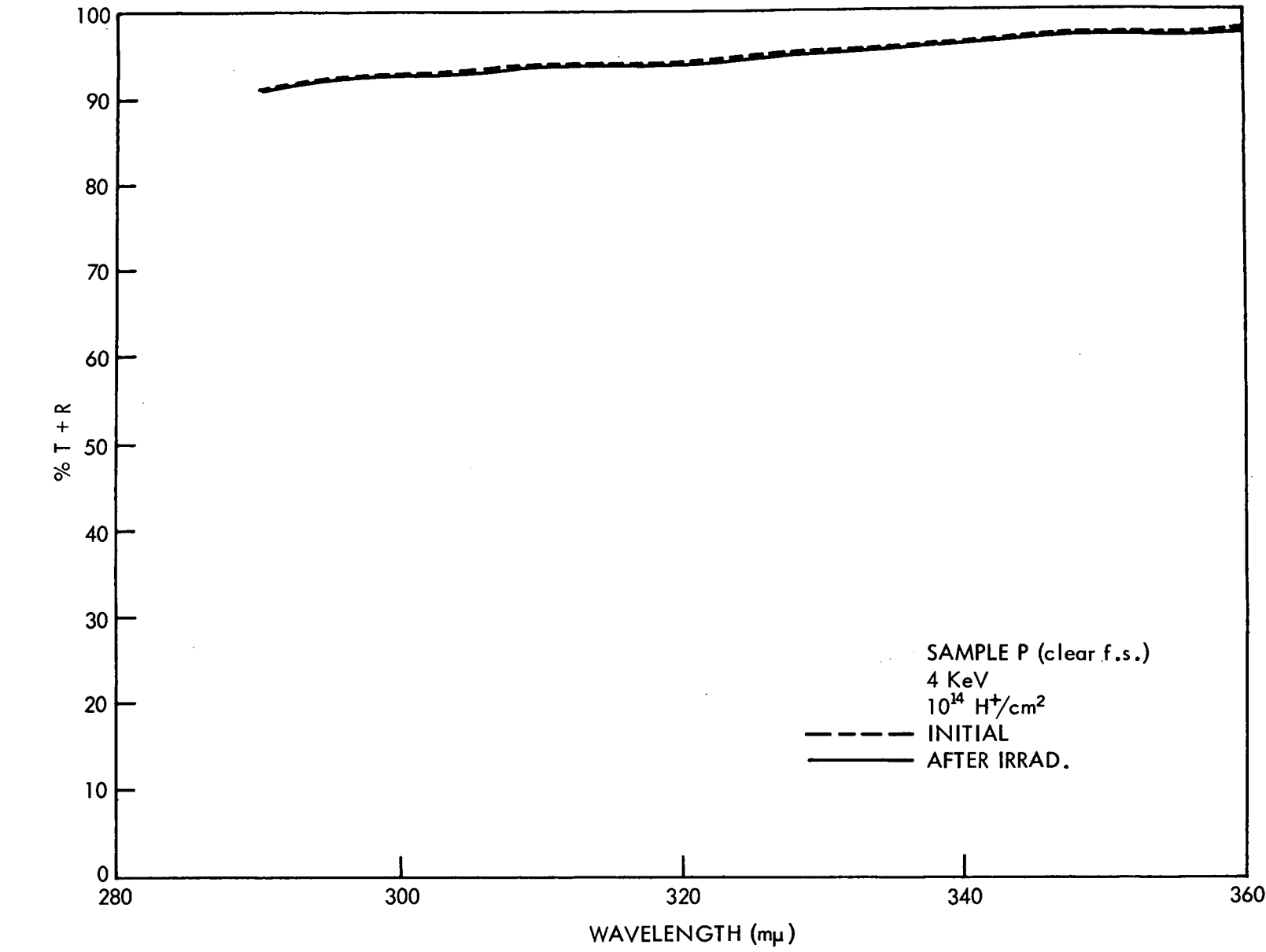


Figure 92.

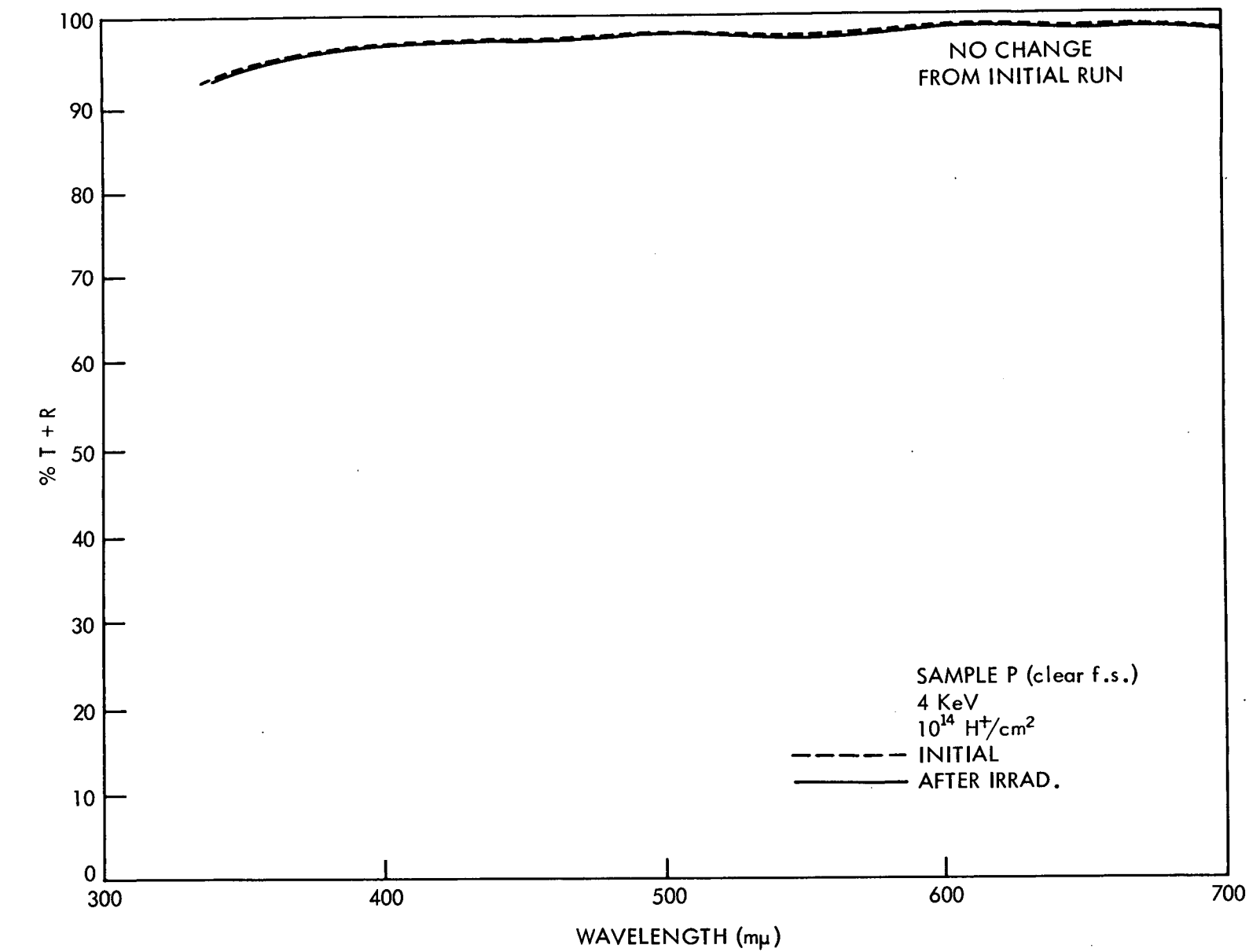


Figure 93.

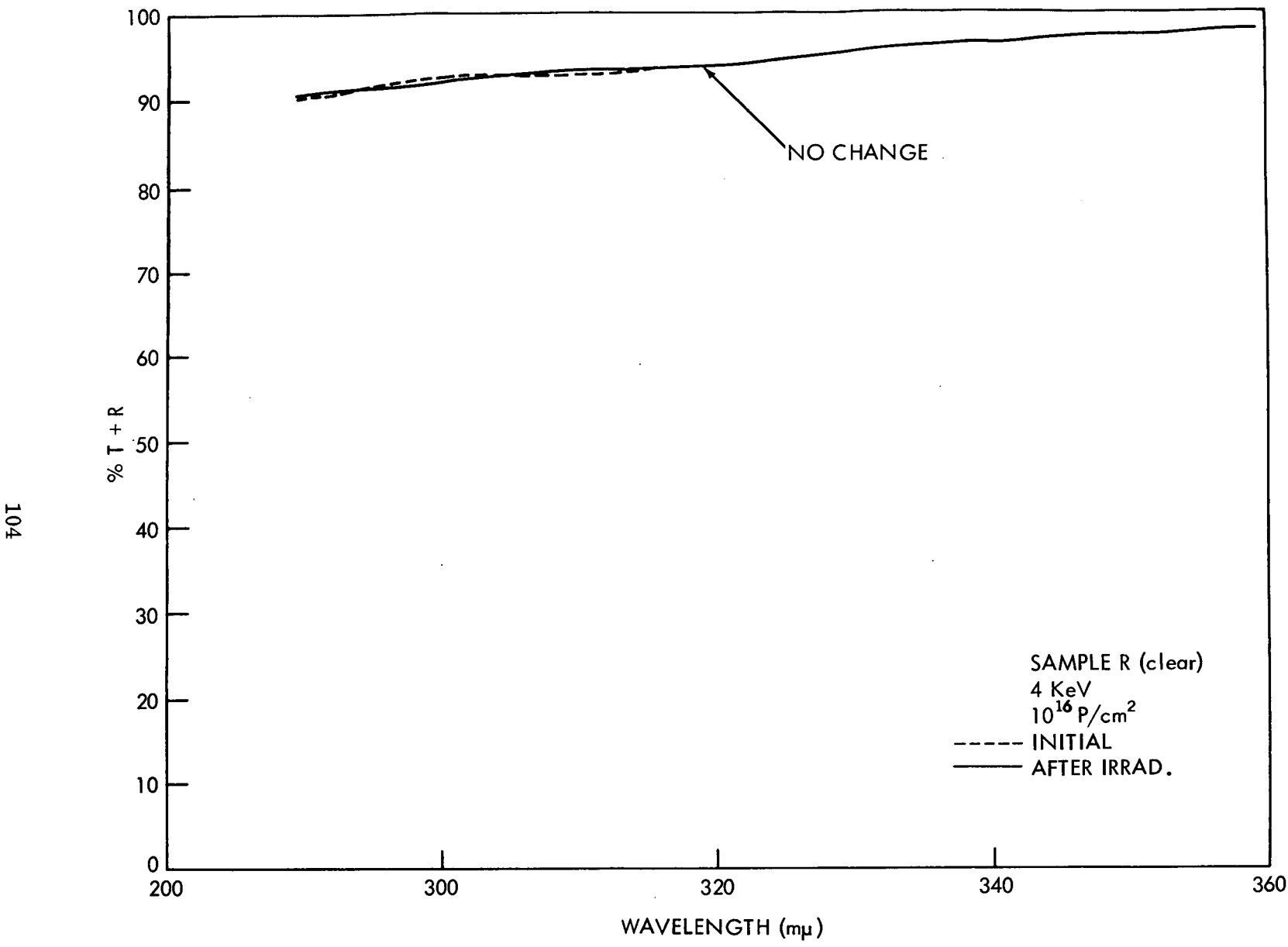


Figure 94.

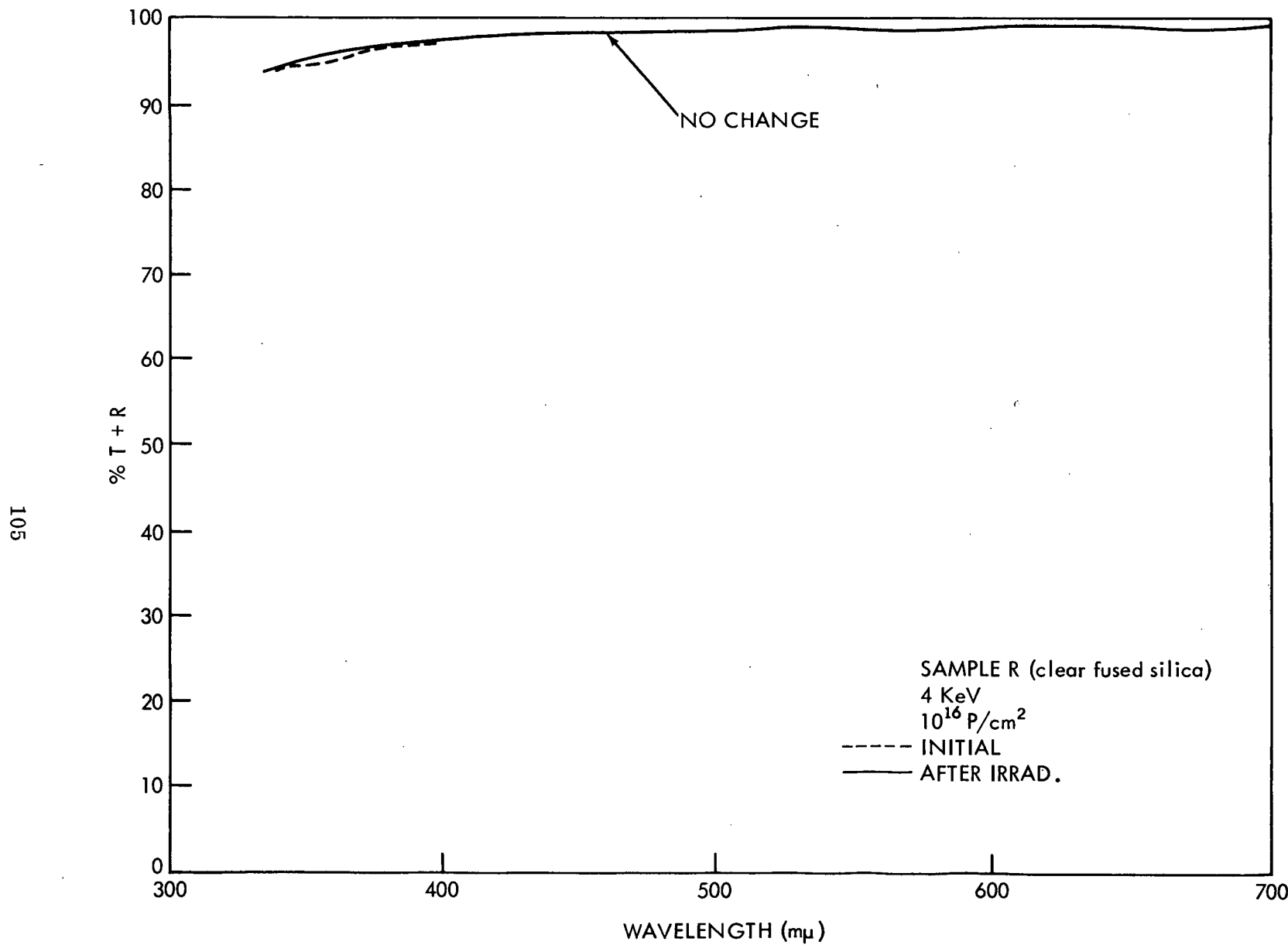


Figure 95.

○ STRING A COVER GLASS ONLY
 □ STRING B COVER GLASS OVER SOLAR CELLS
 ◇ STRING C COVER GLASS ONLY - SHIELDED, CONTROL
 △ STRING D COVER GLASS OVER SOLAR CELLS - SHIELDED, CONTROL
 1 Mev ELECTRONS IN AIR

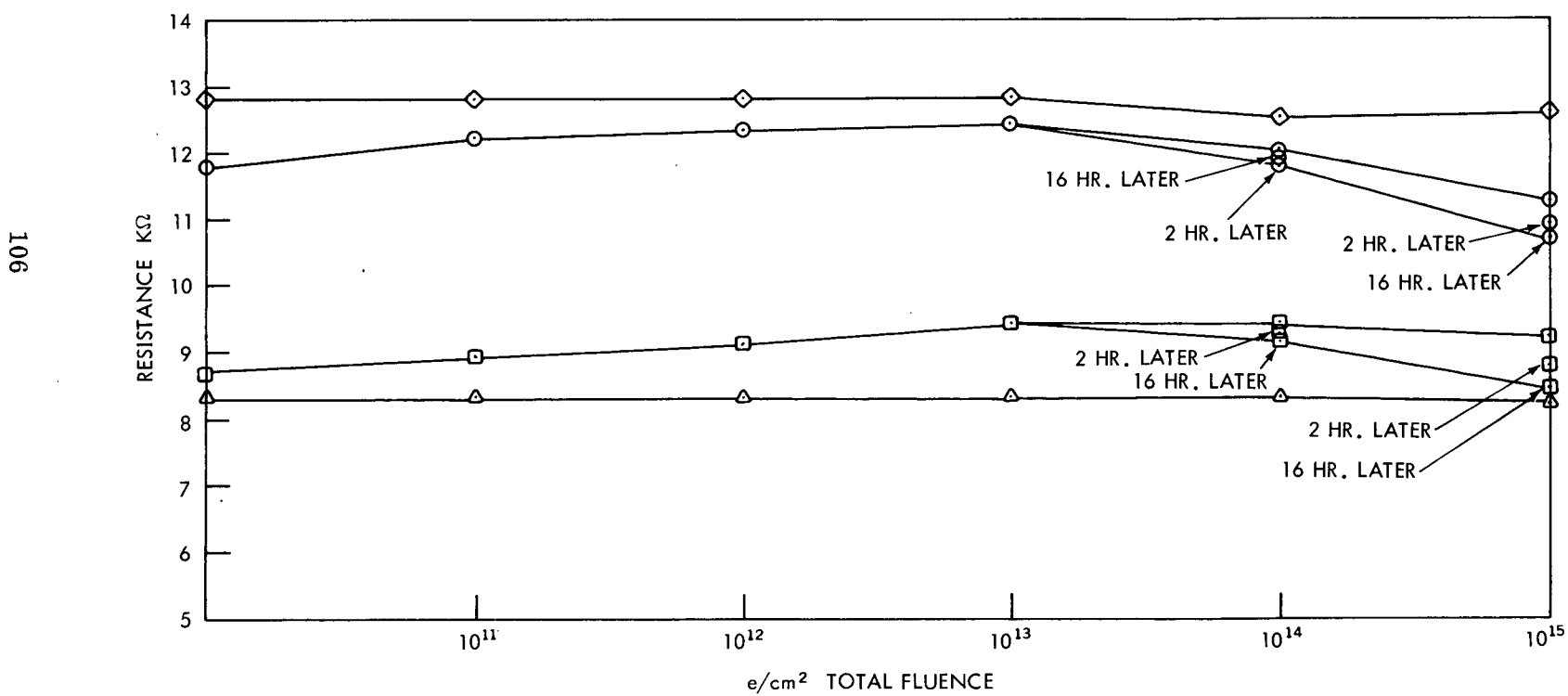


Figure 96.

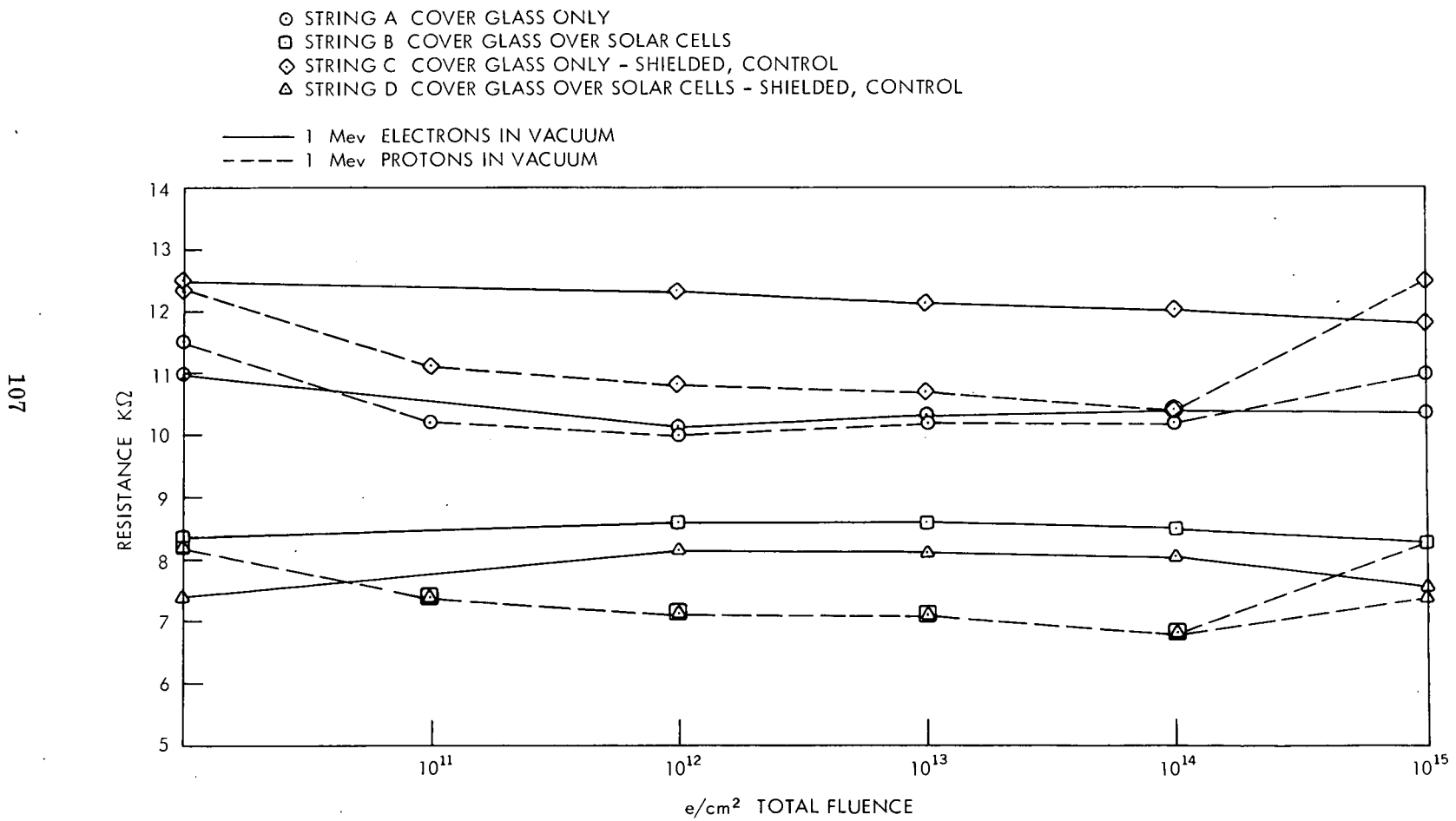


Figure 97.

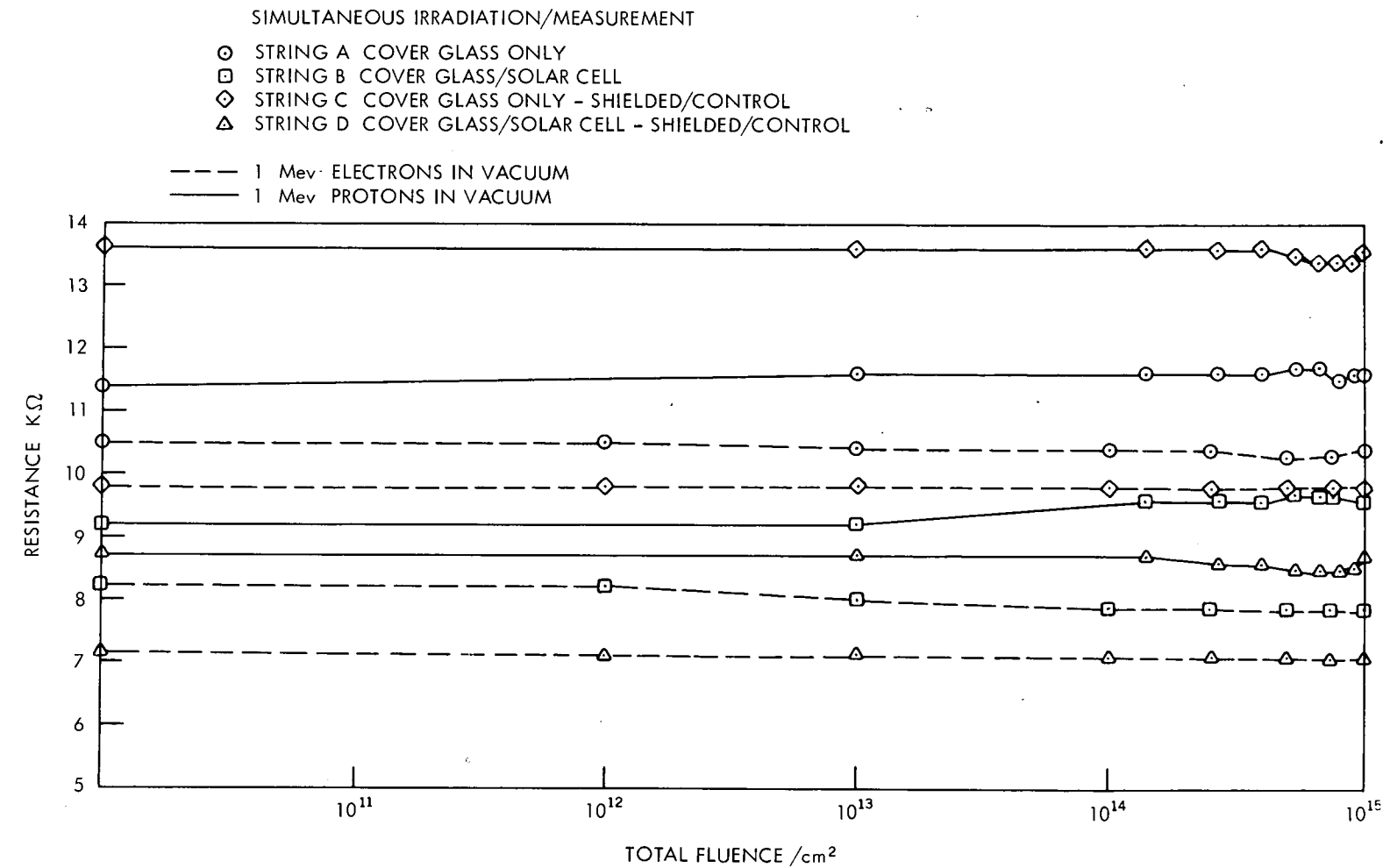


Figure 98.